Stratigraphy, micropalaeontology and stable isotope analysis of Tertiary rocks in the North Canterbury region

---

A thesis submitted in partial fulfilment of the

requirements for the Degree of

Master of Science in Environmental Science

at the University of Canterbury

by Courtney Hutchison

2012

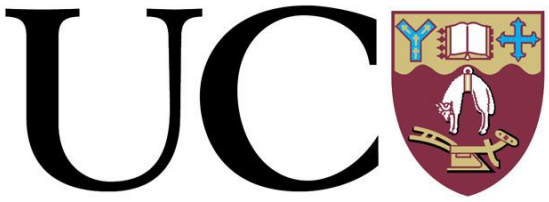

"Rocks are records of events that took place at the time they formed. They are books. They have a different vocabulary, a different alphabet, but you learn how to read them."
-John McPhee

Abstract

Stable isotope, stratigraphic and micropalaeontological studies provide an insight into the preservation of Tertiary global cooling episodes in shelf carbonate rocks from the Mandamus-Pahau District in North Canterbury. Local shelf carbonate isotope analysis ($\delta^{13}C$ and $\delta^{18}O$) shows these shelf rocks have not retained the original sea-water isotopic signature but have been altered during burial diagenesis. The Palaeocene to Late Eocene Coal Creek Formation from this district is a glauconite-rich, inner shelf unit transitioning to a mid-outer shelf environment. Separation of this unit from the Mid-Late Oligocene Cookson Volcanic Group is marked by a ~3-4 Ma hiatus representative of the Marshall Paraconformity. The Marshall Paraconformity is inferred throughout the district due to a distinct break in style and sedimentation from the Late Eocene until the Mid-Late Oligocene. Cookson Volcanic Group tuffaceous beds and pillow basalts represent localised intra-plate volcanism that occurred prior to the deposition of the Late Oligocene Flaxdown Limestone. This Oligocene limestone represents a mid shelf, bryozoan and algal-rich grainstone. Widespread development of this carbonate unit illustrates the absence of tectonically derived sediments prior to the deposition of the Pahau Siltstone Member. The Early Miocene marks the initiation of a new tectonic regime in New Zealand, with the deposition of the inner shelf, quartz-rich Pahau Siltstone Member due to tectonic associated uplift and erosion.

These shelf sediments proved inadequate as a record of global climate excursions, with grainsize and the dominance of burial diagenesis limiting their use in global isotope records. Shelf sediments seen in this study mostly consist of grainstones or sandstones with the coarse grainsize of these units allowing a high flow of pore fluids through sediments. These pore fluids occurred out of equilibrium with bioclasts within these Tertiary units, increasing the alteration potential of bioclasts. This thesis provides strong evidence for problematic global isotopic signatures in local shelf sediments due to grainsize and diagenesis, yet other studies have proved it is possible to reconstruct the global isotope curve from shelf sediment records. Accurate shelf records depend on proxies less prone to diagenetic alteration that act as a reliable gauge of local and global environmental change.

Table of contents

Table of Figures

Chapter 1

Chapter 3

Chapter 7

List of tables

Acknowledgements

Firstly I would like to thank my Supervisor Dr Catherine Reid for her time and advice. Thank you Catherine for always having the time for my interesting interpretations and sometimes imaginative questions. I am also grateful for the time you spent on countless edits and fostering my interest in palaeontology. The knowledge I have gained from you over the length of my thesis is invaluable. I would also like to thank my co-supervisor Dr Travis Horton, for his numerous explanations of geochemical concepts and analysis of my samples at UoC.

There are numerous other members of the staff from the Geological Sciences Department who have helped me throughout the length of my thesis. A big thank you goes to Rob Speirs for the time he spent on my thin section samples and his free sample delivery service at times; Chris Grimshaw for assistance with my lab work and help navigating the sedimentology lab; Kerry Swanson for his help with my SEM images and Sacha for her help with my rock catalogue. Finally I would like to thank Pat and Janet from the Geology Department in my time of need someone was always there to explain the logistics of forms and protocols. Overall I would like to thank the Geology Department for creating a friendly environment it has been a pleasure working with all staff members.

I would like to acknowledge the Mason Trust Fund for the financial support I received enabling me to undertake this thesis. Thank you also to the farm owners in the Culverden region who were kind enough to let me onto their land to undertake my field work.

A huge thank you goes to Louise. I have been so lucky to have someone as kind and caring as you as a friend and flatmate throughout my thesis. You have made home so much more welcoming, days off more relaxing and life in general more exciting. If you didn't help me with field work I don't think roasting marshmallows on the fire and eating a full lamb roast would have been as much fun.

Last but in no respect least I want to thank my whole family for their constant support and love while I have been at University. Mum and dad you have always encouraged me to achieve the best I can, your belief in me has made me who I am today. Sarah and Gus, I can't thank you both enough for the dinners, support and friendship throughout my time at University, I think I at least owe you a nice holiday home. Amie and Jason, your kind words mean so much to me and they are always welcomed. Finally Uncle Philip and Aunty Wyn without your guidance, wisdom and love for travel I would not have taken the chances I have or seen all the beauty the world has to offer. Thanks to the whole family for love, guidance and keeping things in perspective.

-Courtney

1. Introduction

This research thesis covers the stratigraphy, sedimentology and geochemistry of Palaeocene to Miocene rocks in the Mandamus-Pahau District. These rocks reflect tectonic and climatic events at both regional and global scales, as outlined below.

The Mandamus-Pahau District is located within the Culverden Basin to the west of the township of Culverden in the Hurunui district, North Canterbury, New Zealand. Located to the North is Mount Culverden with the Waipara River to the south (figure 1.1). There are four main sites that are studied in this thesis. The Glens of Tekoa section is a site in the region that has been studied relatively recently with Field and Browne (1989) writing a synthesis of the Canterbury region. Sevon (1969) produced a paper on the regional and local geology, with research also previously undertaken by Haast (1871), Hutton (1877), Speight (1918) and Mason (1949). Cascade and Pahau Downs have also been studied previously with Mason (1949) and Andrews (1963; 1968) undertaking detailed sedimentological and palaeontological studies at these sites.

1.1 Regional Geology

The stratigraphy of the North Canterbury region is well known, with various Tertiary lithostratigraphic units overlying Mesozoic basement rocks. The Tertiary units in this region include glauconitic quartzose sandstone deposited prior to the Marshall Paraconformity, local tectonically derived volcanism and Oligocene limestone deposited during the maximum sea-level transgression. The subsequent shallow shelf Pahau Siltstone Member is only confirmed in the Cascade Downs field site although previous studies by Sevon (1969) have speculated this unit occurs within the Glens of Tekoa syncline. The sequence of units throughout the North Canterbury region records sedimentation influenced by uplift and sea-level change linked to Antarctic glaciations.

Late Jurassic-Early Cretaceous

Pahau Terrane rocks make up most of the basement in the Canterbury and Marlborough region, with accumulation of these sediments in the Late Jurassic to Early Cretaceous (Mason, 1949). In the Late Jurassic, a convergent margin had re-establised itself along Gondwanaland, on the Pacific Ocean side of the margin (Rattenbury *et al.,* 2006). The sediments deposited during this time period are from the Pahau Terrane and are mostly

derived from the uplifted Rakaia Terrane. This active margin phase is recorded in sedimentological data, with these units reflecting submarine fan and deep marine deposits (MacKinnon, 1983).The creation of off shore depositional environments is recorded in the Pahau Terrane with interbeds of sandstone and argillite sequences (Sevon, 1969).

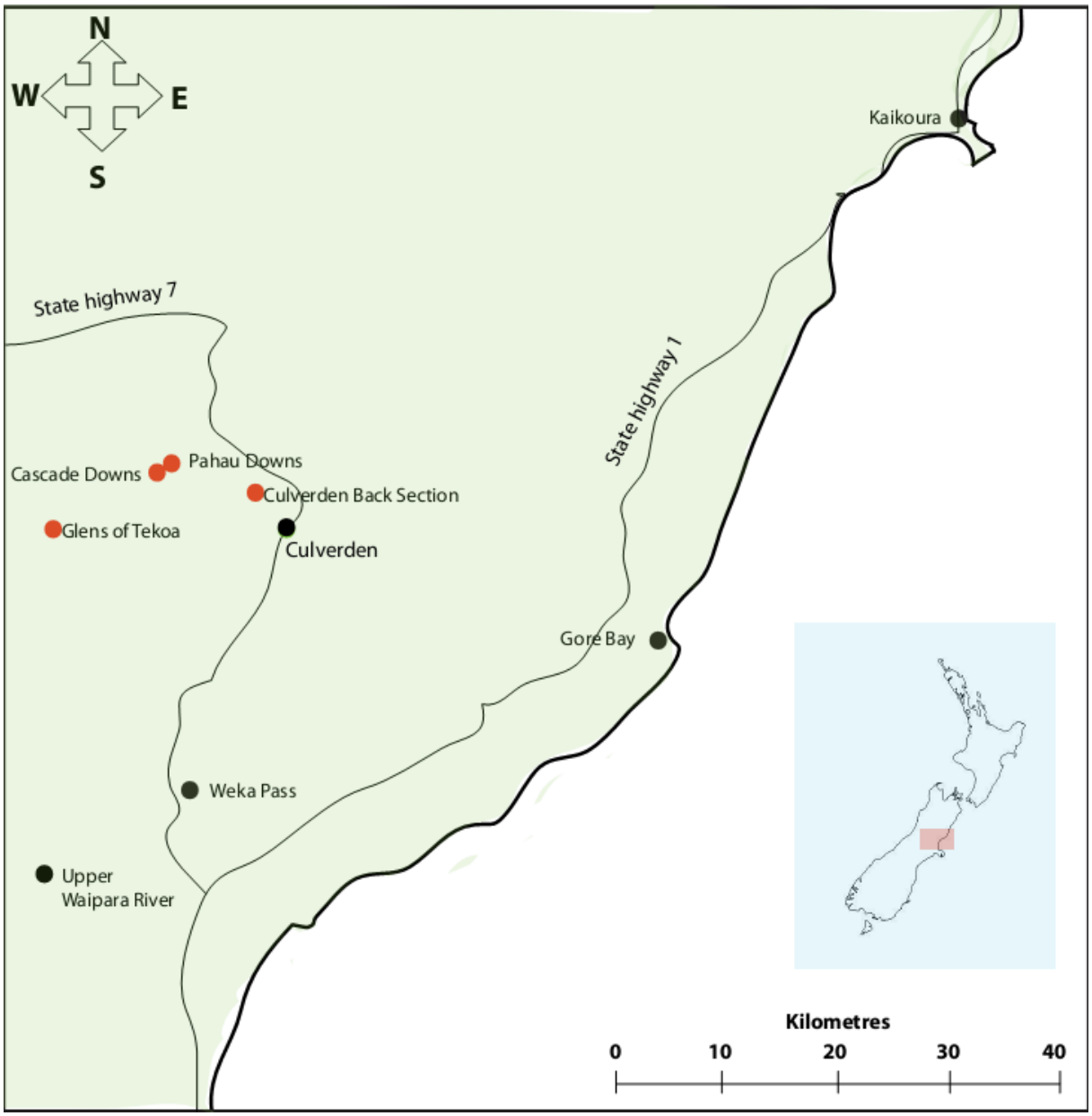

Figure 1.1- Location of the Mandamus-Pahau District and field sites in relation to southern and eastern locations of geological interest.

Late Cretaceous

The Cretaceous tectonic regime changed as a convergent margin was replaced by extensional tectonics (Jongens *et al.,* 2008). Separation of the New Zealand continent from Australia started with the opening of Tasman Sea, dated in the Mid-Late Cretaceous (c.85 Ma) (Jongens *et al.,* 2008). This extensional tectonic setting resulted in development of horst and graben basins in the landmass of Zealandia. These basins were progressively filled through the Late Cretaceous to Early Tertiary (Rattenbury *et al.,* 2006). Fluvial, terrestrial and shallow marine deposits unconformably overlie the Pahau Terrane in numerous locations throughout the Canterbury and Kaikoura regions. These units commonly occur alongside or prior to extensive andesitic and rhyolitic volcanism associated with normal faulting, including the Mandamus Igneous Complex seen in the Mandamus-Pahau District (Rattenbury *et al.,* 2006; Jongens *et al.,* 2008).

Paleocene-Eocene

Tasman Sea opening slowed through the Palaeocene and ceased in the Early Eocene (Jongens *et al.,* 2008). During this period New Zealand experienced a phase of tectonic stability and general subsidence, with widespread marine sedimentation along the eastern side of New Zealand (Rattenbury *et al.,* 2006). In the North Canterbury region Eyre Group marine sediments were being deposited throughout the Palaeocene and into the Late Eocene. This includes Waipara Greensand to the south overlain by glauconitic mudstone, siltstone and sandstone (Rattenbury *et al.,* 2006). The Palaeocene to Eocene in the Madamus-Pahau District is represented by a glauconitic, well-sorted quartzose sandstone from the Coal Creek Formation (Rattenbury *et al.,* 2006). The Eyre Group rocks include shallow marine, relatively high-energy near-shore beach to low energy outer shelf depositional environments (Rattenbury *et al.,* 2006). To the east towards Kaikoura and Gore Bay the Amuri Limestone of the Muzzle Group is the dominant unit consisting of a deep-water micritic limestone (Rattenbury *et al.,* 2006).

Early- Middle Oligocene

In the Late Eocene New Zealand was relatively low-lying, entering into a period of peak marine transgression in the Oligocene (Carter, 1988). Early-Mid Oligocene units are not recorded in the Mandamus-Pahau region, due to the regional Marshall Paraconformity (figure 1.2). The Marshall Paraconformity is seen in shelf successions from the east

continental margin of New Zealand (Fulthorpe *et al.,* 1996). This paraconformity represents a hiatus of 3-4 Ma between ~32-29 Ma, with longer hiatuses signifying erosion during this time (Fulthorpe *et al.,* 1996).

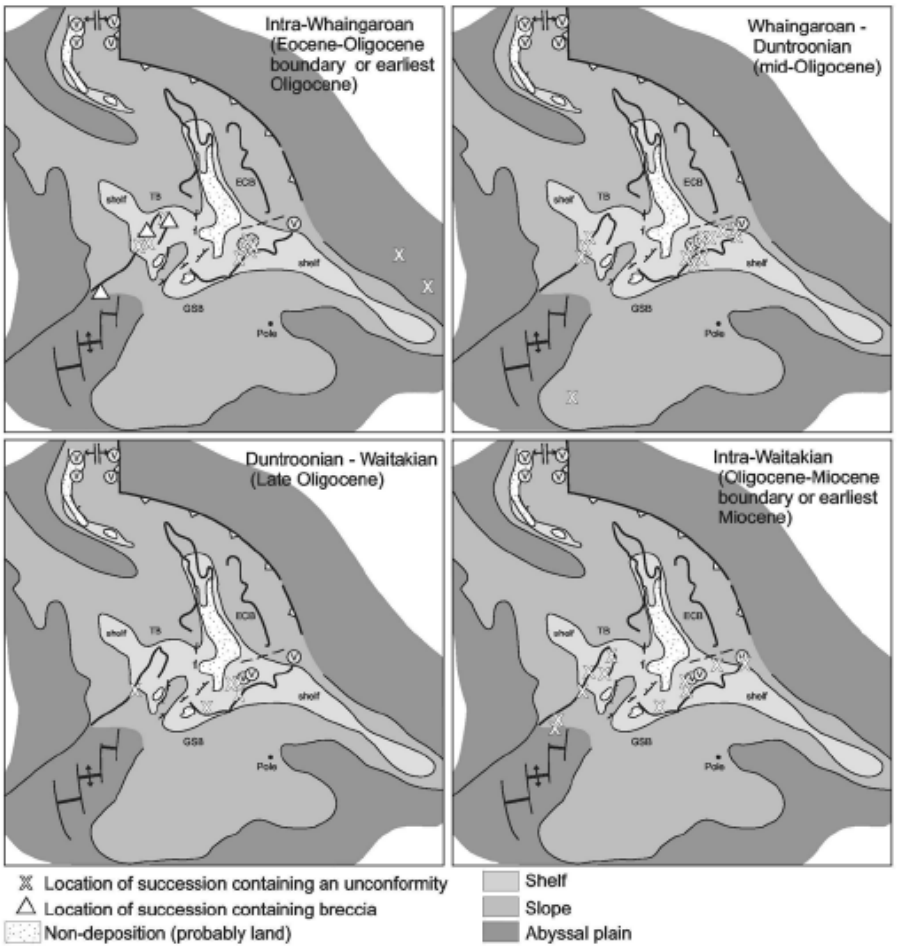

Figure 1.2-Diagrams locating unconformities across the South Island from the Late Eocene to the Early Miocene (Lever, 2007).

There are a number of explanations for the Marshall Paraconformity including sea-level fluctuations, erosive bottom waters associated with the development of the east Antarctic ice-sheet, the Antarctic circum-polar current (ACC) and separation from Australia and Antarctica (Carter, 1985). It is proposed by Fulthorpe *et al.,* (1996) that the Marshall Paraconformity is a record of the Oligocene cooling event. Although erosion occurred, Fulthorpe *et al.,* (1996) determined this 3-4 Ma hiatus is primarily non-depositional, possibly occurring due to lower sea-levels, cooling and increased current intensities. These climatic factors may have limited the deposition of carbonate units during this event (Fulthorpe *et al.,* 1996). A return to deposition following this hiatus first included terrigenous and

glauconitic sediments with this followed by the return to carbonate deposition (Fulthorpe *et al.,* 1996). The North Canterbury Amuri Limestone, Spy Glass Formation, Weka Pass Stone and Flaxdown Limestone (Motunau Group) bound the Marshall Paraconformity (Carter, 1985; Rattenbury *et al.,* 2006). A reduced influx of material during the maximum marine transgression in the Oligocene post Marshall Paraconformity provided a prime setting for the deposition of carbonate units (Lu and Fulthorpe, 2004). A return to carbonate deposition is marked by volcanism related to local instability in the early Late Oligocene in localised regions in North Canterbury.

Late Oligocene

The early Late Oligocene is represented by localised intraplate volcanism. These volcanics from the Mandamus-Pahau District belong to the Cookson Volcanics Group and outcrop extensively throughout the Culverden and Waiau region. The main units from this volcanic group in the district are the Tekoa tuffs interbedded with Oligocene limestones, pillow basalts and breccias (Rattenbury *et al.,* 2006). The volcanic source that produced this group appears to have been from the north-east with the Culverden back section being the most proximal deposit and the Tekoa Tuffs the most distal product (Andrews, 1963).

Following volcanism the Flaxdown Limestone Member was deposited throughout the district**.** Widespread carbonate deposition dominates the eastern South Island in the Late Oligocene. These limestone units conformably overlie or in places are interbedded with the Cookson Volcanics (Rattenbury *et al.,* 2006). This is seen in the Flaxdown Limestone, Weka Pass and Whales Back Limestone (Rattenbury *et al.,* 2006). These limestones consist of shallow to deep water facies, indicative of the continuous carbonate deposition. To the south of the Mandamus-Pahau District the mid to outer shelf Weka Pass Stone was being deposited, with the Spy Glass Formation being deposited in Kaikoura and North Canterbury (Field and Browne, 1989).

Miocene

Miocene deposition reflects a change in both tectonic and sedimentary regimes. Initial inception of the fault at ~23.4 Ma provided horizontal movement along the Alpine Fault (figure 1.3) (Cooper, 2008; Carter and Norris, 1976) The initiation of a compressional regime on the Alpine Fault in the Miocene led to an increase in siliciclastic supply to the shallow

shelf in the North Canterbury region (Lu *et al.,* 2005). This influx of sediment in association with tectonic uplift is seen in Miocene rocks in the North Canterbury region. The siliciclasitc rich rocks from the Miocene include a number of formations; these are the Waikari and Mt Brown Formation (Rattenbury *et al.,* 2006). A switch from carbonate to siliciclastic input is evident in the quartz-rich Pahau Siltstone of the Waikari Formation (Sevon, 1969). It is possible that this unit may relate to molluscan-rich facies of the Miocene Mount Brown Formation in the Waipara area (Field and Browne, 1989).

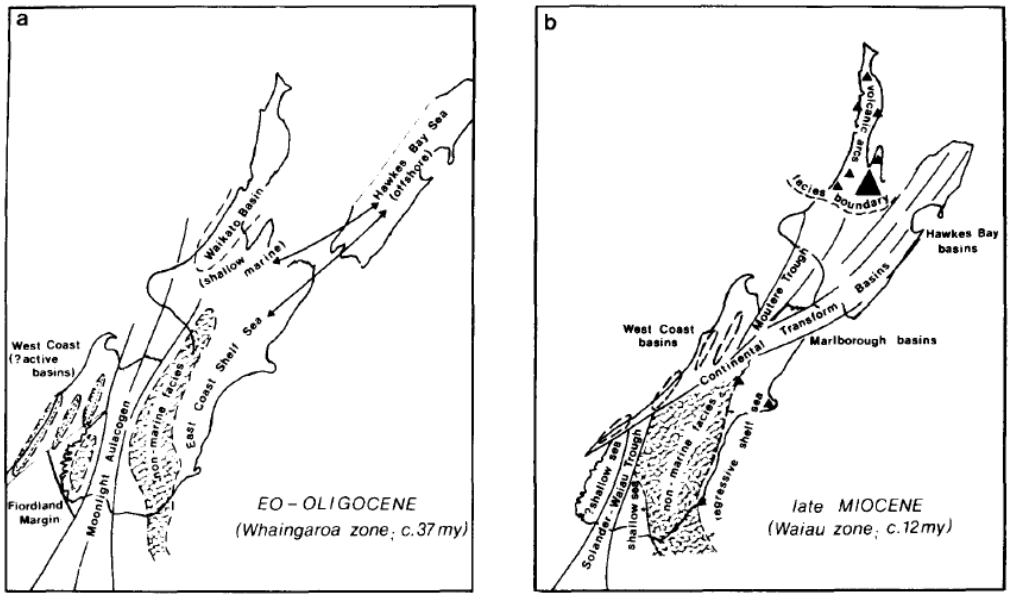

Figure 1.3 - Reconstructions of the New Zealand continent at, a) 37 Ma, Eocene-Oligocene Establishment of the modern Indo-Australian/Pacific plate boundary b) 12 Ma, late Miocene, completion of major transcurrent movement along the Alpine Fault leading to the creation of continental basins (Carter and Norris, 1976).

1.2 Tertiary Climate Events

Earth has experienced continuous change in the climate sector during the past 65 million years with extreme variations from warm cycles with ice free poles, to cold cycles of expansive continental ice sheets and ice capped poles (Zachos *et al.,* 2001). These changes occur in relation to orbitally related rhythms and the Earth's major boundary conditions (Zachos *et al.*, 2001). Several stages of cooling in the Tertiary occurred in response to gradual changes in the geography and location of continents, oceanic gateway and oceanographic controls such as bathmetry (Zachos et al., 2001). Cooling episodes are reflected in sedimentary records throughout the world as global shallowing cycles in tectonically passive basins and margins, although where regional tectonics are active this eustatic signal is lost

(Haq et al., 1987). Two major global climate excursions can be studied with the Oligocene and Mid- Miocene cooling events providing an insight into global climate change. Both of these excursions can be pinned down to climatic or tectonic events that occurred prior to global cooling (Zachos *et al.,* 2001).

Cenozoic climatic and cryospheric developments are largely tied to plate tectonic changes, with the isolation of Antarctica influencing Southern Ocean circulation (Flower and Kennett, 1994). Evidence obtained from the Eocene-Oligocene boundary indicates that it is one of the most important periods of climatic cooling that occurred during the Cenozoic (Kennett *et al.,* 1975). This period of cooling influenced the extent of glaciation on Antarctica due to a major drop in temperature, leading to intensified deep-sea circulation in the Southern Ocean, with enhanced seafloor erosion producing numerous disconformities and highly condensed sequences (Kennett *et al.,* 1975)**.** Following cool climates in the Early Oligocene, a rise in global temperature reached its optimum in the Early Miocene before undergoing cooling during the Middle Miocene (Flower and Kennett, 1994). Middle Miocene cooling is an important step in global climate evolution as it represents the establishment of modern climatic and oceanographic systems (Flower and Kennett, 1994).

1.2.1 Eocene-Oligocene

The Cenozoic trend towards colder deep waters and increased polar ice volumes is recorded in several steps (Flower and Kennett, 1994). The early to early Middle Eocene, recorded as the warmest interval in the Cenozoic was followed by pronounced cooling in the transition from the Eocene to the Oligocene and small scale glaciation occurring in the Late Oligocene (Flower and Kennett, 1994). Cooling observed at the Eocene-Oligocene boundary into the early Oligocene is linked to the widening of the Tasmanian gateway. The Tasmanian gateway had opened earlier in the Eocene, with the opening of the Drake Passage occurring at the Eocene/Oligocene boundary and into the early Oligocene. Opening of the Tasmanian gateway in the Early Eocene, followed by widening of the Tasmanian gateway initiated the flow of cold waters as part of the proto-circum Antarctic current (figure 1.4; 1.5) (Nelson and Cooke, 2001). The opening of the Drake Passage at this time allowed increased circulation. Nelson and Cooke (2001) proposed at this stage circum-Antarctic currents evolved into a more intensified proto-Antarctic Circumpolar Current, affecting the New Zealand sector of

the Southern Ocean (figure 1.5) and possibly even the Atlantic Ocean. The Oligocene epoch also witnessed the strengthening of thermohaline circulation, a glacially induced Antarctic bottom-water system, dominated by cold deep waters (figure 1.5) (Flower and Kennett, 1994). The development of the thermohaline circulation system occurred in the late Oligocene as a response to freezing conditions in high latitudes supplying ventilation to the deepwater circulation system (Wright and Kennett, 1993).

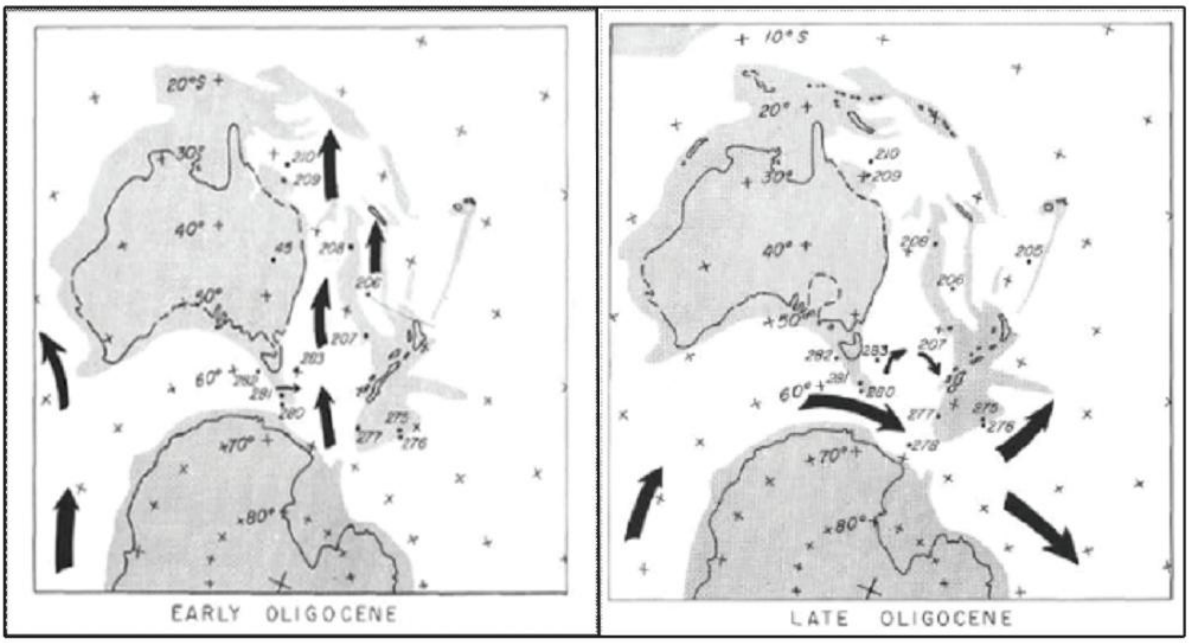

Figure 1.4-Early Oligocene and late Oligocene reconstruction of Australia, Antarctica and New Zealand. The early Oligocene map shows the suggested direction of bottom water prior to bottom water current circulation. The late Oligocene map shows the direction of the ACC from late Oligocene to the present day (Kennett *et al.,* 1975).

1.2.2 Miocene

The next major climate excursion took place after a brief warming in the early Miocene. The climatic transition from the early Miocene to the Mid Miocene is inferred by Flower and Kennett (1993) to have occurred due to a reduction in interaction of warm, saline deep water flows with the Southern Ocean. This decrease in warm, saline deep water flowing into the Southern Ocean may have influenced the meridional heat transfer to the Antarctic, leading to Mid Miocene cooling and an increase in Southern Component Water production (Flower and Kennett, 1993). Following this cooling the Mid Miocene records the development of a major ice cap on East Antarctica (Kennett, 1977; Nelson and Cooke, 2001).

The cooling during the mid-Miocene also facilitated northward extension of ice rafted sediments into the southeast Pacific region (Kennett, 1977).

Flower and Kennett (1994) propose the main climatic and palaeoceanography events that support the Middle Miocene cooling trend. The main events that are relevant to the short term climatic variation in the Middle Miocene are;

1. Plate tectonic development due to :

a. closure of the Tethys Ocean,

b. restriction of the Indonesian seaway.

2. A large global benthic foraminiferal increase, reflecting East Antarctic ice sheet (EAIS) growth and deep water cooling.
3. Middle Miocene high-amplitude sea-level variations (~16-14 Ma), followed by two-step semi permanent fall (~14-12.5 Ma).
4. Increase in oceanographic fronts.
5. Large scale changes in organic carbon deposition compared to carbon sedimentation.
6. Deep water circulation changes.

Global cooling during this epoch (~14.5- 12.7 Ma) represents one of the major phases in the Cenozoic associated with the permanent establishment of an East Antarctic ice sheet (Ennyu and Arthur, 2004). The Middle Miocene was marked by pronounced short-term variations in EAIS volume, sea level and deep ocean circulation (Flower and Kennett, 1994). An increase in the growth of the EAIS is apparent, suggesting the influence of Antarctic ice sheet expansion on global climates due to deep water circulation patterns (Flower and Kennett, 1994). The late Middle –Late Miocene saw the establishment of the subtropical front (STF) and subantarctic front (SAF), alongside renewed ice sheet growth in East Antarctica and the development of a permanent ice sheet on West Antarctica (Nelson and Cooke, 2001).

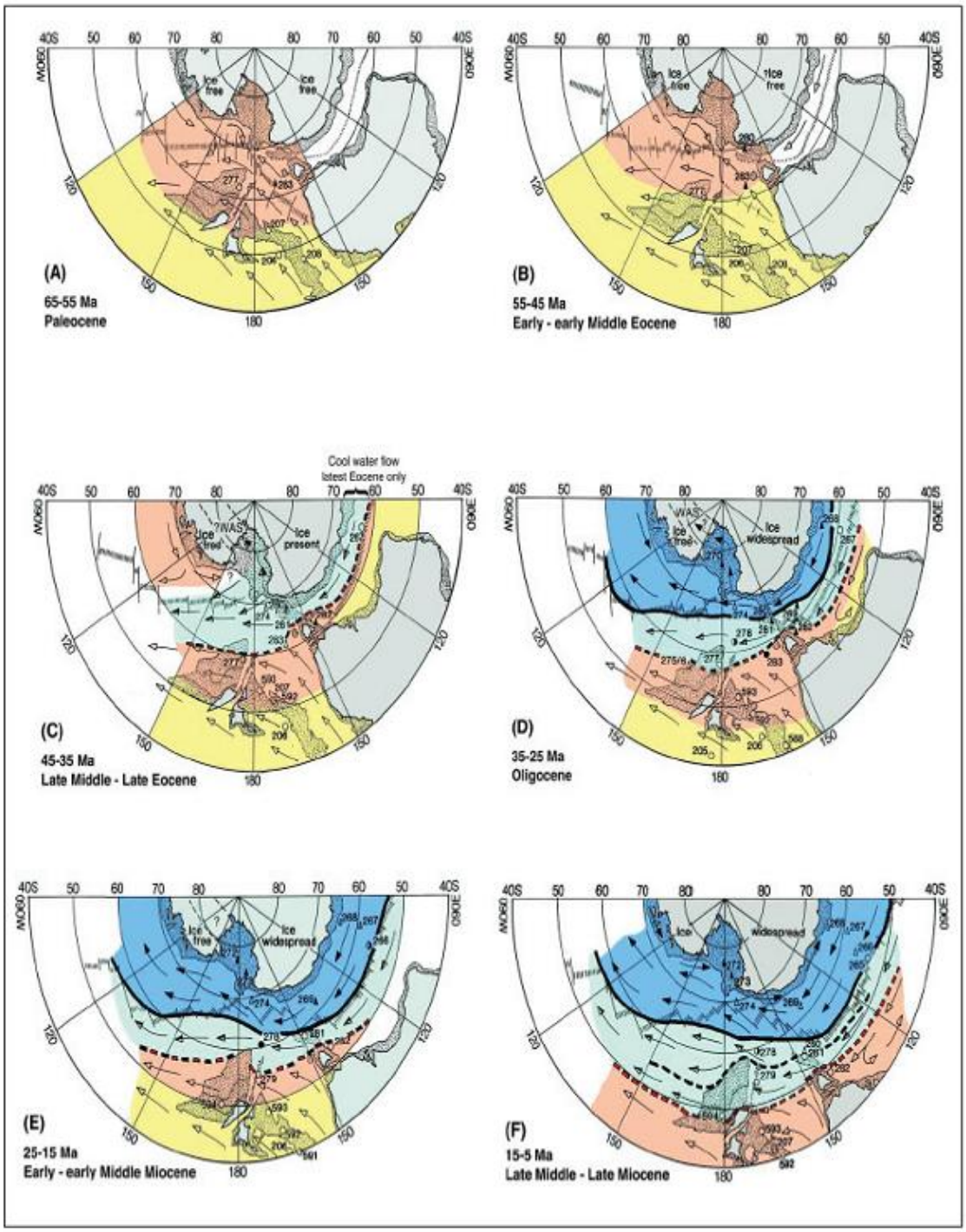

Figure 1.5- Map of the Southern Ocean, showing evolution of the Antarctic Circum-polar current (ACC) and oceanic fronts at ~10 m.y intervals throughout the Cenozoic. These maps display the palaeooceanography for the New Zealand sector of the Southern Ocean(NZSSO). Maps of importance are (b-d) Eocene-Oligocene and (e-f) Early Middle-Late Miocene(from Nelson and Cooke, 2001).

1.2.3 The Global marine isotope curve

Global climate change is reflected in the geochemical record occurring as variations in the Tertiary isotope record (Zachos *et al.,* 2001). These variations appear in both the Oligocene and Miocene isotope records due to the expansion of the Antarctic ice sheet. The deep sea temperatures seen in the oxygen isotope record are derived from the cooling and sinking of water in Antarctica and the Arctic (Zachos *et al*., 2001). Climatic history can be reconstructed by a number of different proxies that are applied to both marine and terrestrial sedimentary data, but the development of high resolution oxygen ($\delta^{18}O$) and carbon ($\delta^{13}C$) has served as the main method of global and regional climate change reconstruction (Zachos *et al.*, 2001). In the case of climate change, oxygen isotope studies provide information on the evolution of deep sea temperature and ice volume on the continents (figure 1.6) (Zachos *et al*., 2001). Oxygen isotope data provides deep-sea temperature and continental ice volume evolution data, as well as high latitude sea surface temperatures (SST), due to the cooling and sinking of polar waters (Zachos *et al.*, 2001). Carbon isotope data on the other hand provides information on global carbon cycle perturbations and changes in circulation patterns in deep sea data influenced by climate change (Zachos *et al*., 2001).

New Zealand has undergone numerous temperature changes over the last 65 million years that can be incorporated in a quantitative temperature based curve (Carter, 2008). There are numerous quantitative curves based on oxygen isotope values that record average past oceanic bottom water temperatures (Carter, 2008). The most commonly used global oxygen isotope-temperature curve was produced by James Zachos and Ian Devereux (2001) and presents information from the K/T boundary through to present day. New Zealand based oxygen isotope curves have been produced from information obtained from deep-sea drilling cores east of New Zealand (ODP leg 181)(Carter, 2008). This data has been used to decipher changes in climate, ocean currents and sediment deposition (Carter, 2008).

Long term trends in $\delta^{18}O$ that occurred over the early-middle Late Eocene and Early Oligocene can be attributed to the combined effect of ice-volume and temperature changes (Zachos *et al.*, 2001). The earliest Oligocene cooling and expansion of the Antarctic continental ice sheets, produced relatively high deep-sea $\delta^{18}O$ values (>2.5‰) indicative of permanent ice sheets and bottom-water temperatures of ~4˚C (Zachos *et al.*, 2001). These

ice sheets occurred until the end of the Late Oligocene (26-27 Ma), with global ice volume dropping and bottom water temperatures increasing from this period up until the Middle Miocene, with several small episodes of glaciations (Zachos *et al.*, 2001). The early Middle Miocene climatic optimum was followed by the reestablishment of ice sheets on Antarctica (Zachos *et al.*, 2001). Compared to the establishment of small-ephemeral ice sheets in the Late Eocene to Early Oligocene, the Middle Miocene ice sheet development was more extensive with development of both the west and east Antarctic ice sheets (Zachos *et al.*, 2001).

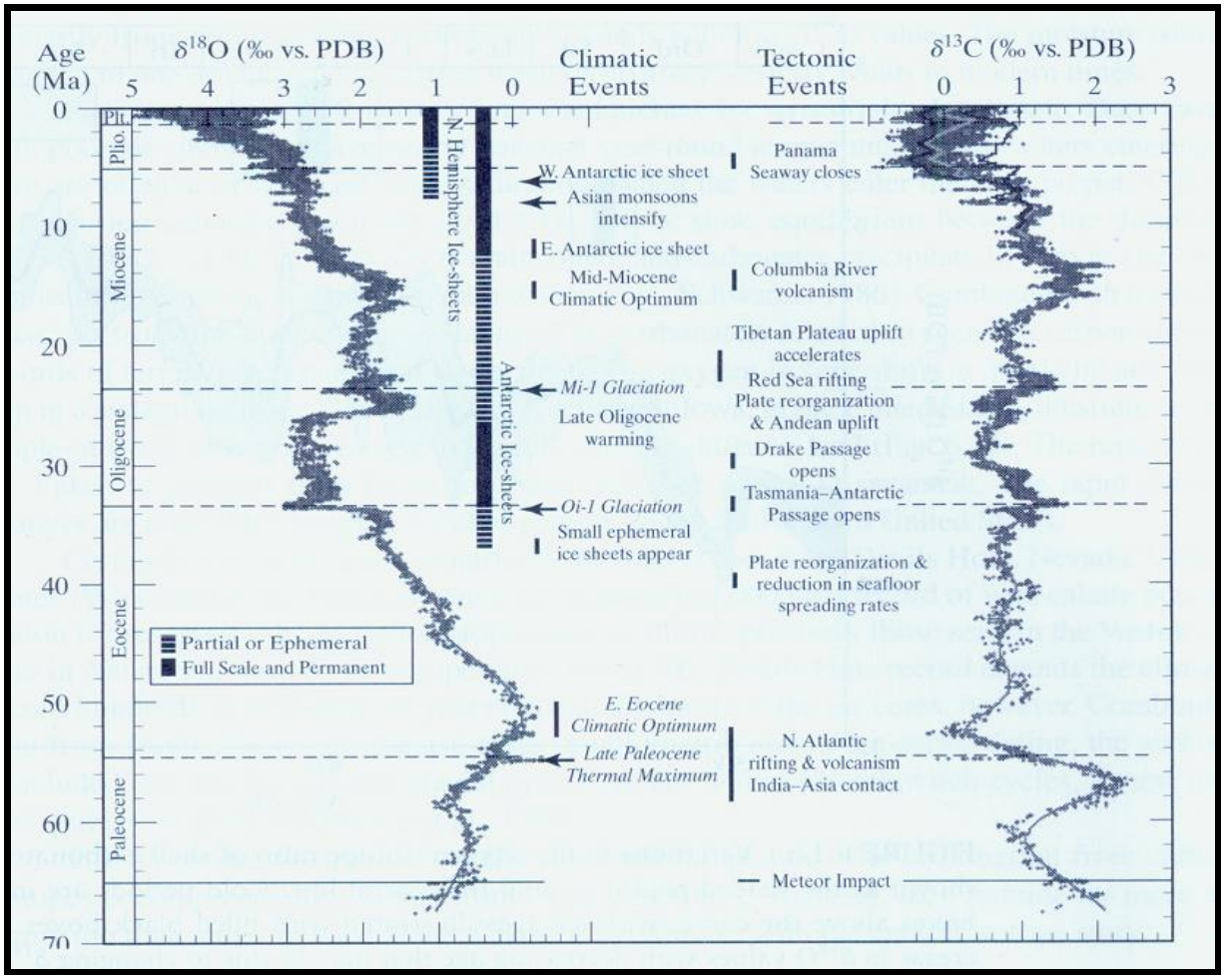

Figure 1.6- Global deep-sea $\delta^{18}O$ and $\delta^{13}C$ records from Zachos *et al.,* (2001).

1.3 Research Aims

This research thesis aims to constrain the age and palaeoenvironments of the Tertiary rocks from the Mandamus-Pahau District in order to link local shelf geochemistry to the Zachos (2001) global deep-sea curves. This will allow for analysis of the preservation potential of shelf sediments from the north Canterbury region to record global climate signals. This will be carried out by describing and interpreting sedimentological features in order to determine depositional environments of the facies within the Tertiary succession. Biostratigraphy will be carried out with the analysis of benthic and planktic foraminifera being used to determine depositional environments and ages for the Mandamus-Pahau facies. Petrographic analysis of sediments is followed up by $\delta^{13}C$ and $\delta^{18}O$ isotopic analysis in order to determine whether the Oligocene and Miocene climate driven excursions appear in these shelf sediments. This analysis will therefore consider whether global isotope stratigraphy is reflected in shelf sediments that may be affected by diagenesis and tectonically induced sediment supply.

1.4 Thesis Structure

The introduction to the thesis, literature review of the regional geology, important New Zealand and Southern Ocean Tertiary geological events and aims have been described in this chapter (chapter 1). Chapter two provides the methodology for this whole thesis. Chapter three looks at the field areas and lithostratigraphy in depth; describing and interpreting sedimentology features that may determine depositional environments. Chapter four describes the biostratigraphy and also includes environmental interpretations based on foraminifera. Chapter five includes diagenetic analysis of units, with paragenesis of unit formation included. Chapter six looks at the geochemical analysis in terms of the stable isotopes involved, ($\delta^{18}O$ and $\delta^{13}C$) global isotope curves and the comparison of shelf sediments to the Zachos (2001) deep-sea curve. The two final chapters discuss the results reviewed in the five previous chapters (chapter 7) and then conclude this thesis (chapter 8).

2. Methodology

The majority of sites used in this research project were chosen from literature reviews and a GNS geological map of the Kaikoura region before the field work was undertaken. Sites of importance were also identified in the field. After analysis of these sites was complete, appropriate sites were then chosen for stratigraphic columns.

All sections of stratigraphic importance were measured in the field with representative rocks from these sections collected. Sedimentological structures were noted and beds and sections were measured wherever this was possible. At the University of Canterbury the samples and data were used for thin section analysis, foraminiferal processing, SEM imaging, staining and geochemical analysis.

2.1 Stratigraphic columns

Stratigraphic sections were measured in the field where the applicable units outcropped and where sections were accessible. The sections were measured with an 8 metre tape measure and were generally rounded to the nearest 10mm.

The stratigraphic columns will be correlated between locations based on lithostratigraphy, biostratigraphy, sedimentological and palaeontological data used to interpret depositional environments. The main units of interest in these sections are: Coal Creek Formation (Palaeocene-Eocene), Cookson Group Volcanics (early-mid Oligocene) Flaxdown Limestone Member (late Oligocene), Pahau Siltstone Member (Miocene). The data from the stratigraphic columns is incorporated into topographic data to produce geological maps of the different sections visited. The stratigraphic columns were created using Adobe illustrator (14.0.0).

2.2 Foraminiferal sample preparation and picking

Samples used in this study are all from the Mandamus-Pahau district of North Canterbury. A subset of 30 samples from 149 samples were considered for foraminiferal processing and picking due to stratigraphic location and quality.

The processing of rocks in order to obtain foraminiferal species occurs in a number of steps. As all of the samples used for this thesis were rock samples and not loose sediment samples the same procedure was followed for all samples. The rocks were first manually crushed with a mechanical press so that no single piece exceeded 1cm in size. After the rocks were crushed they were then placed in the oven at 59˚C (under 60˚C in order to avoid any alteration that would affect the geochemical analysis) to dry. Once the samples had dried out they were placed in the fume cupboard and covered in 2-3 cm of 10% H_2O_2 and left for at least an hour to disaggregate. Disaggregated samples were then sieved through a 63µm sieve. The slurry obtained from the sieving of disaggregated samples was then transferred into another container and put in the oven at 59˚C. These samples were then bagged and labelled for picking. At all steps in this process the mechanical press, sample pots and sieves were rinsed in methylene blue, a stain that will colour and identify contaminated $CaCO_3$ particles from earlier samples.

In order to avoid a bias form of picking in this thesis the picking tray was separated out into 23 squares of similar sizing and a random number generator (www.random.org) was used in order to determine which squares foraminifera would be picked from. In each tray half of the squares were collected from. A single-grain layer of sediment was spread over the picking tray and foraminifera that fell within the randomly generated squares were picked until a minimum of 100 specimens were collected for biostratigraphic and palaeoenvironmental analysis. A Meiji binocular microscope was used for analysis and a wet brush was used for picking the specimens. Initially specimen were sorted into broad groups with one group per square on a 50 square micro-slide, and subsequently sorted into one species per square as identification progressed.

2.2.1 SEM imaging

SEM images of both benthic and planktic foraminifera were produced for detailed imaging of significant taxa. Specimens were mounted on standard 12.5mm grooved slug stubs using carbon tape and then coated with gold/palladium. Images were produced using a JEOL 7000F FE SEM set at 5.0kV and a working distance on 9-12mm.

2.3 Thin section analysis

Rock samples were collected from 149 locations throughout the stratigraphic sections measured around the Mandamus-Pahau district in North Canterbury. These samples were taken for biostratigraphic, geochemical and thin section analysis.

Seventeen thin sections were later cut at the University of Canterbury for petrographic description and to obtain additional environmental data for limestone samples that were too well cemented to be broken down for foraminiferal analysis. These samples were also used for representative descriptions of the variations within units by percentage estimations, general thin section descriptions (carbonate, sandstone and volcanic) and classification within the Folk and Dunham scale. The chosen samples were mounted on slides and covered by a thin glass slide.

2.3.1 Alizarin red-s staining

Ten of the petrographic samples were re-sectioned as uncovered thin sections in order for alizarin red-s staining to be undertaken using Dickson's (1965, 1966) method. The purpose of this staining was to identify ferroan vs non-ferroan calcite cements. This method consists of:

1. Immersing the uncovered thin section (for 10-15 seconds) in an etching solution of 15ml of 36% HCl that has been dissolved in a solution of 1500ml distilled water.
2. This immersed specimen is then dipped (for 30-45 seconds) in the staining solution consisting of:
   a) 2g alizarin red-S dissolved in 100ml 1.5% HCl solution.
   b) 2g potassium ferricyanide crystals dissolved in 100ml 1.5% HCl solution.
   c) Both these parts are then mixed to the ratio 3:2 (alizarin to ferricyanide).
3. The thin sections are then washed with distilled water and then air dried under a low temperature heat lamp.

2.4 Carbonate Stable Isotope Analyses

Carbonate oxygen and carbon isotope analyses were undertaken in the Stable Isotope Laboratory at the University of Canterbury. Bulk geochemical and foraminiferal samples were used for these analyses. The bulk geochemical samples were obtained by crushing whole rock samples in order to create a carbonate powder. These bulk samples provided a broad overview of the carbonate geochemistry, where foraminifera could be picked from

samples. Five to ten foraminifera were picked from samples previously sieved for biostratigraphy. Both bulk and foraminiferal samples were added to 100 percent phosphoric acid in sealed reaction vessels that had been flushed with helium gas and reacted at 70 °C (Horton *et al.,* 2004). A Finnigan Delta and XL mass spectrometer were used to measure isotopic ratios. Repeated analyses of NBS-18 and NBS-19 carbonate standards were used for both the carbon and oxygen isotope ratios (Horton *et al.,* 2004). Carbonate isotope data was measured to a precision of ~0.2 permil (Horton *et al.,* 2004).

3. Lithostratigraphy

The facies associations present in the Palaeocene to Miocene stratigraphy in the Mandamus-Pahau District are described in this chapter, with designation depending on sedimentological and biological components. The facies defined in this chapter are used to interpret the depositional environments of each stratigraphic unit. In this thesis 8 facies were identified and interpreted from the Early to Middle Eocene to the Middle Miocene (table 3.1). The facies descriptions in this chapter are followed by interpretations of the depositional processes, environments and site based mapping and stratigraphy.

3.1 Stratigraphic overview

The stratigraphy of this thesis covers the Coal Creek Formation (Eyre Group), Cookson Volcanic Group, Flaxdown Limestone Member (Motunau Group) and Pahau Siltstone Member (Motunau Group, Waikari Formation). The Eyre Group is separated from the overlying Motunau Group by the Marshall Paraconformity. The Marshall Paraconformity is an erosional surface on the top of the Coal Creek Formation is represented by a break in time from the late Eocene to the mid-late Oligocene in this field area.

Coal Creek Formation

The Coal Creek Formation is a quartz and glauconite rich unit. This unit spans a large range in terms of time and space, varying from a Palaeocene cross-bedded glauconite rich unit to a well cemented phosphatized quartz and glauconite rich unit.

Cookson Volcanics Group

This volcanic group unconformably overlies the Coal Creek Formation. This unit ranges in thickness and volcanic product throughout the Mandamus-Pahau District depending on proximity to the volcanic source. Volcanic material from the Cookson Volcanic Group in the field area consists of Tekoa Tuffs and pillow basalts.

Flaxdown Limestone Member

This unit includes reworked volcanic material from the Cookson Volcanics, grading from a calcareous volcanic unit to a volcaniclastic limestone at the base of this unit grading into a relatively pure limestone at the top of the unit. The Flaxdown limestone is a thick limestone unit forming syncline ridges at the Glens of Tekoa .

Pahau Siltstone Member

Following widespread carbonate depositon that led to the production of the Flaxdown Limestone, sedimentation converted to siliciclastic deposition producing the Pahau Siltstone. The siliciclastic component in this unit consists solely of quartz.

3.2 Lithofacies descriptions

Eight lithofacies were identified from the Tertiary rocks from the Mandamus-Pahau District. These lithofacies include: 1. Cross-bedded Quartz and Glauconite-rich Sandstone, 2. Glauconite and Quartz-rich Sandstone, 3. Pillow Basalt, 4. Volcanic Tuff, 5. Molluscan-rich Grainstone, 6. Bryozoan and Algal-rich Grainstone, 7. Fossiliferous Sandstone, 8. Quartz-rich Sandstone.

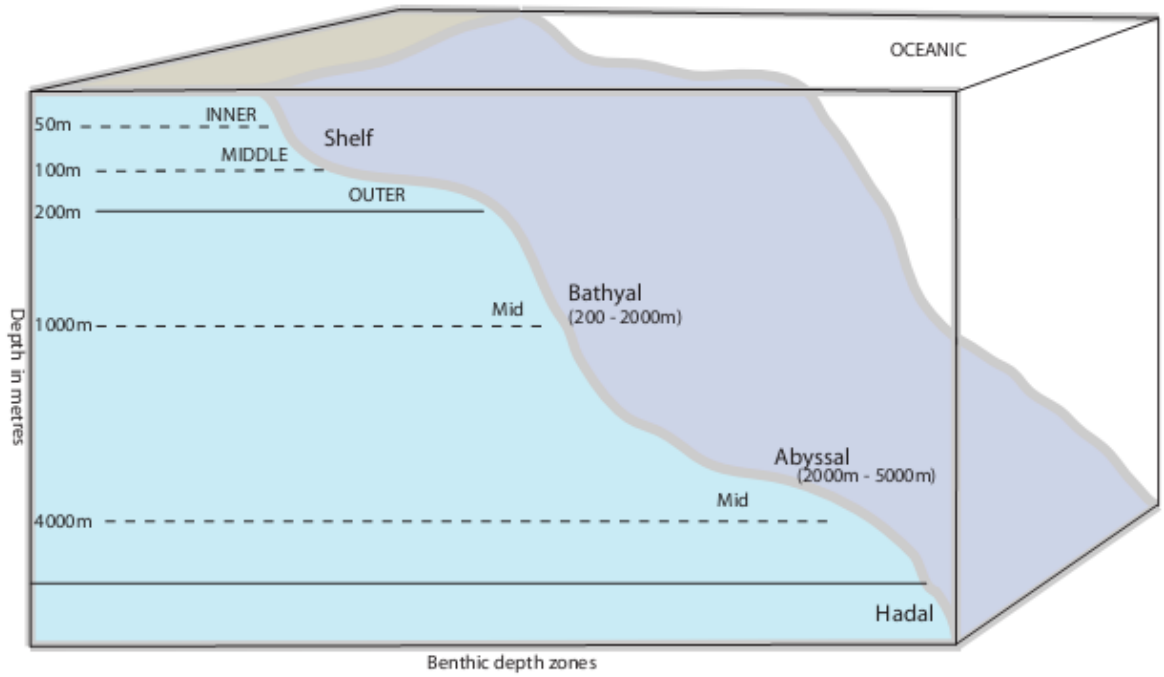

Figure 3.1- Box diagram of the terminology for benthic depth zones as indicators for paleodepth. Explanations for depositional interpretations in table 3.1. Modified from Hayward *et al.,* 2010.

Lithofacies	Samples	Components	Depositional Setting	Depositional Interpretation
Cross-bedded Glauconite-rich Sandstone	13,12	Glauconite Quartz Siltstone layer	High energy environment Unidirectional sedimentation	Inner Shelf
Massive Glauconite-rich Sandstone	3,12; 4,10; 5,2a;	Glauconite Quartz Foraminifera	moderate energy reworking of glauconite	Mid-Outer Shelf
Pillow Basalt	9,20; 14,11	Plagioclase Pyroxene Olivine	Proximal volcanism- Intraplate volcanism	Mid Shelf
Volcanic Tuff		Volcanic lithics Fine ash Calcareous layers	Distal Volcanism eruptive pulses	Mid Shelf
Molluscan-rich Grainstone	10,1 (10); 14,12	Mollusca Barnacles Foraminifera Bryozoan Echinoderm Volcanic lithics	Current swept carbonate shelf	Mid Shelf
Bryozoan and Algal-rich Grainstone	4,3 ; 4,4; 4,5; 4,9(12); 9,3; 11,4; 11,3m	Hematite Bryozoan Coralline red algae Mollusca Echinoderm Foraminifera	Current swept carbonate shelf	Mid Shelf
Fossiliferous Sandstone	12,4	Quartz Foraminifera Mollusca	Low to Moderate energy and sedimentation	Subtidal Inner Shelf
Quartz-rich Sandstone	5,5a; 5,6g; 12,2 2.4m	Quartz Glauconite Foraminifera Mollusca	Moderate to high energy and sedimentation	Subtidal Inner Shelf

Table 3.1- Lithofacies interpretation of Tertiary strata in the Mandamus-Pahau District North Canterbury.

3.2.1 Cross-bedded Glauconite-rich Sandstone Facies

Description:

This facies is characterised by a medium to coarse, moderately sorted cross-bedded sandstone. The thickness of the Cross-bedded Glauconite-rich Sandstone Facies ranges from 7 to 9 metres. The main sedimentary structures evident in this facies are cross-bedding defined by glauconite and quartz content cut by 10-20cm beds of dark grey siltstone (figure 3.2a). The cross-beds seen in this facies appear to be trough cross-bedding not tabular (average dip of 24°). The trough-like appearance of these cross-beds is indicated by the curve in the bottom surfaces of some beds. It appears troughs have been created and then been filled with low angle cross laminations (3.2b). The upper and lower contacts within the sandstone and between the siltstone and sandstone are sharp and show no gradational features.

Glauconite and quartz content varies throughout this facies with quartz-rich layers occurring in 5-10 centimetre laminations up to 1-2 metre beds in places. Sharp basal contacts define quartz and glauconite rich beds. Glauconite-rich layers (~15-20% glauconite) occur to a lesser extent in beds of 0.8 centimetres up to 10 centimetres. Glauconite content decreases towards the top in laminations. These glauconite-rich laminations then grade into quartz rich layers showing higher percentages of glauconite (~15-20%) at the base decreasing towards the top of the bed (~2-3%). The colour of this facies varies depending on the quartz or glauconite concentrations. Upper contacts with the glauconite and quartz-rich facies are not visible.

Occurrence:

This facies is limited to Coal Creek located to the south west of the Glens of Tekoa site and only occurs in the Coal Creek Formation.

Figure 3.2a- Cross-bedded Glauconite Sandstone Facies, cut by a thin 10-20cm dark grey bed of siltstone. Location: Coal Creek, Glens of Tekoa.

Figure 3.2b- Cross-beds showing foresets marked by layering of beds of high glauconite concentrations. Location: Coal Creek, Glens of Tekoa.

Figure 3.2c- Image displaying the scale of cross-beds within the Cross-bedded Glauconite-rich Sandstone Facies. Location: Coal Creek, Glens of Tekoa.

Interpretation:

The trough cross-beds observed in this facies are due to migration of current ripples. The formation of ripple cross-beds depends on a high quantity of sediment, including suspended sediments quickly covering and preserving the ripples (Boggs, 2006). These cross-beds are indicative of an environment of high energy and sedimentation rate. The normal graded bedding seen in the cross-bedded facies can be attributed to waning currents. This grading occurs due to the difference in the rate of settling between the glauconite and quartz grains because of the variation in density of these minerals (Boggs, 2006). The thin repetitious successions of glauconite and quartz rich beds seen in this cross-bedded facies are indicative of rhythmic bedding within beds (Boggs, 2006).

The inclusion of glauconite within this cross-bedded facies is indicative of remobilised and reworked glauconite (Amorosi, 1997). Generally high percentages of glauconite is linked to low sedimentation rates in marine environments, yet the cross-beds in this facies suggest a high energy environment. It is likely that the glauconite is a parautochthonous form that has been remobilised and moved from place of origin (Amorosi, 1997). Reasons for mobilisation and reworking of this glauconite may have been due to storm surges and gravity flow processes (Amorosi, 1997). Glauconite that has undergone transport due to storm, tidal and turbidity currents (as indicated by trough cross-beds) indicates substantial movement and redistribution of glauconite on the seafloor (Amorosi, 1997).

The combination of trough cross-bedding, graded bedding and high abundance of parauthochthonous glauconite indicates an environment dominated by high energy and sedimentation levels. As these characteristics are common in the shallow marine environment it is likely this unit was deposited on the inner shelf.

3.2.2 Massive glauconite-rich Sandstone Facies

Description:

The previous cross-bedded facies gives way to a Massive Glauconite-rich Sandstone Facies. Grainsize and sorting in this facies are not consistant with grainsize varying from fine to coarse sand and sorting ranging from poorly sorted to well sorted. The thickness of this facies ranges from 1 to 50 metres. The variations in this facies consist of as low as 2-3%

glauconite up to 30% glauconite with most exposures averaging ~10% glauconite (3,3a,b). Quartz contributes a high proportion of the remainder of the facies with ~65% quartz in the majority of the samples from this facies, (figure 3.3) although some samples contain as little as 5% quartz. The majority of quartz grains are distributed in the range of 1-10 cm thick beds with quartz grains of fine sand to fine pebble (6 mm) size. Grains are sub-angular to sub-rounded with the finer quartz grains appearing to be more rounded than the larger pebble sized grains. A mud matrix or sparite cement makes up the remainder of most samples of this facies consisting of ~12-20%.This facies appears to grade into a more quartz rich version at the top 30cm of the facies, but these outcrops are difficult to access.

Phosphate nodules occur throughout the majority of the exposures of this facies, with nodule size varying from 1 mm through to 5-10 cm (figure 3.4). The phosphate nodules appear to occur in the less calcareous fine sands. These nodules are local in situ phosphatic nodules.

Trace fossils are more abundant in this facies than body fossils. These glauconite-rich sands consist of two forms of trace fossils, with the less bioturbated section characterised by *Ophiomorpha* traces and the more intense bioturbations are *Planolites* tubes that contain quartz-rich sediment. The most commonly seen body fossil in this facies is *Ostrea* shell fragments that are very infrequent and only appear in a small isolated section at the back north-west side of the Glens of Tekoa syncline. Foraminifera are moderately abundant in this facies and these will be described in chapter 4. Thin section analysis of this glauconitic sandstone showed most foraminifera are planktic forms (figure 3.3a, b), however processed rock samples showed only 28% of foraminifera to be planktic.

Occurrence:

This facies is abundant throughout the Mandamus-Pahau District occurring at 3 separate locations in the field area including along the Mandamus River and Syncline at the Glens of Tekoa, Cascade Downs and Culverden back section. This facies only occurs in the Coal Creek Formation.

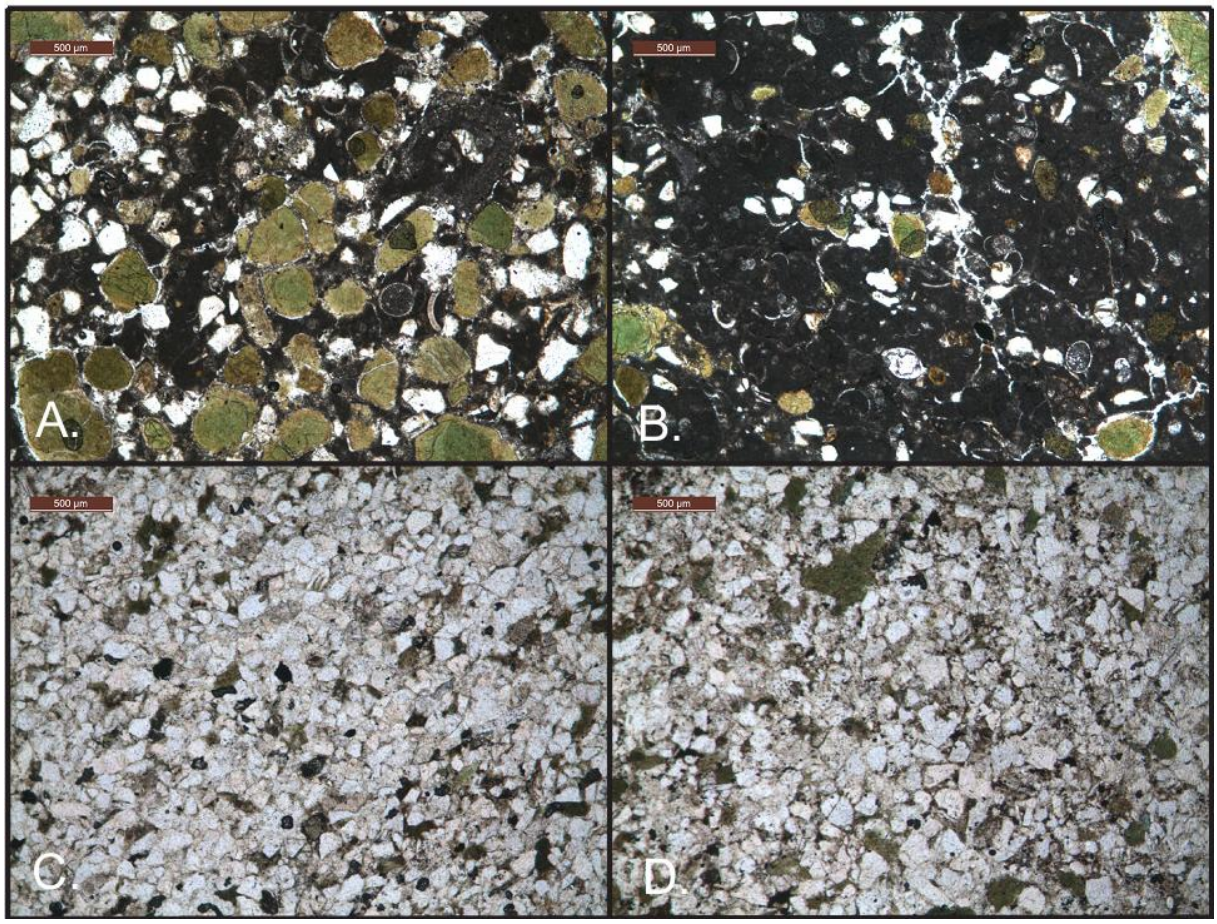

Figure 3.3- Thin sections showing the Massive Glauconite-rich Sandstone Facies. (A,B) Highest glauconite percentage at 30%. Sample 3,12 from Cascade Downs (C, D) portray the range in grainsize and glauconite content. Sample 4,10.3 from Glens of Tekoa (Scale bar: 500µm).

Figure 3.4- Phosphate nodules in the Massive Glauconite Sandstone Facies exposed at Cascade Downs.

Interpretation:

Phosphate nodules occur frequently in this facies (figure 3.3) and it is likely that these nodules have been precipitated at the seafloor. In modern environments the production of phosphate nodules is linked to water depths of 40-300m, generally in regions of low sedimentation rates (Prothero and Schwab, 2004). Phosphate is produced when organic matter is microbially degraded by redox reactions on the sea-floor (Pufahl, 2010). These phosphate nodules may be linked to the upwelling of cold, nutrient-rich ocean waters into regions of warm shelf waters (Prothero and Schwab, 2004). The rapid influx of nutrients onto the continental shelf leads to high productivity and the creation of large amounts of organic material (Prothero and Schwab, 1996). The formation of this phosphate may also indicate nutrient fed settings with a supply of organic material to seafloor sediments (Pufahl, 2010). Phosphate development could also be favoured by marine transgression and the increased upwelling of nutrients on the continental shelf (Selley, 2000). This indicates that pore fluids in the sediment pile must have been reducing over a regional scale at the time of phosphate

production. Sedimentation rates were probably low and the depth of this facies is limited to a shelf environment.

The occurrence of *Ophiomorphia* and *Planolites* trace fossils in this facies indicate a marine shelf environment (Boggs, 2006). These trace fossils belong to the *Skolithos* and *Cruiziana* ichnofacies that are common in the sandy shore and sublittoral zone (MacEachern *et al.,* 2010). The *Skolithos* (containing *Ophiomorphia*) ichnofacies is common in shifting particulate substrates in marine waters (MacEachern *et al.,* 2010). Whereas the *Cruziana* (*Planolites*) ichnofacies indicates an environment with lower energy and more cohesive substrates (MacEachern *et al.,* 2010). The higher abundance of *Planolites* trace fossils compared to *Ophiomorphia* indicates dominance of the *Cruziana* ichnofacies. It is therefore likely that this facies occurs in a similar setting to *Cruziana* ichnofacies common on the shelf, from the subtidal zone into deeper, quieter shelf waters (MacEachern *et al.,* 2010).

High percentages of planktic forams (28% in sieved samples) in this facies indicate mid to outer shelf depths (Hayward, 1999). The occurrence of glauconite, phosphate nodules and planktic foraminifera confirm a marine environment.

3.2.3 Volcanic Facies

A. Pillow Basalt Facies

Description:

The Pillow Basalt facies is a volcanic facies associated with the Cookson Group Volcanics. Thickness of this facies is at least 2.4m. Mineral variations occur in the two samples collected from this facies (14,11; 9,20). The main minerals in this basalt are plagioclase and pyroxene and they make up the highest proportion of this facies; with 55-60% plagioclase and 10-40% pyroxene (figure 3.5). This facies varies from a medium to very coarsely crystalline basalt. Characteristic textures visible in this facies include porphyritic textures in pyroxene, and microlites in plagioclase.

Dominant features of this Pillow Basalt facies include baked glassy margins, cracks and vesicules filled with microcrystalline calcite crystals. Upper contacts are gradational into the Volcaniclastic Tuffaceous facies (figure 3.6). Lower contacts with the Glauconite and Quartz-

rich facies are poorly exposed but regionally the Marshall Paraconformity occurs between the two.

Occurrence:

This facies is located at Cascade Downs, Pahau Downs and the Culverden back section. This facies occurs in the Cookson Group Volcanics.

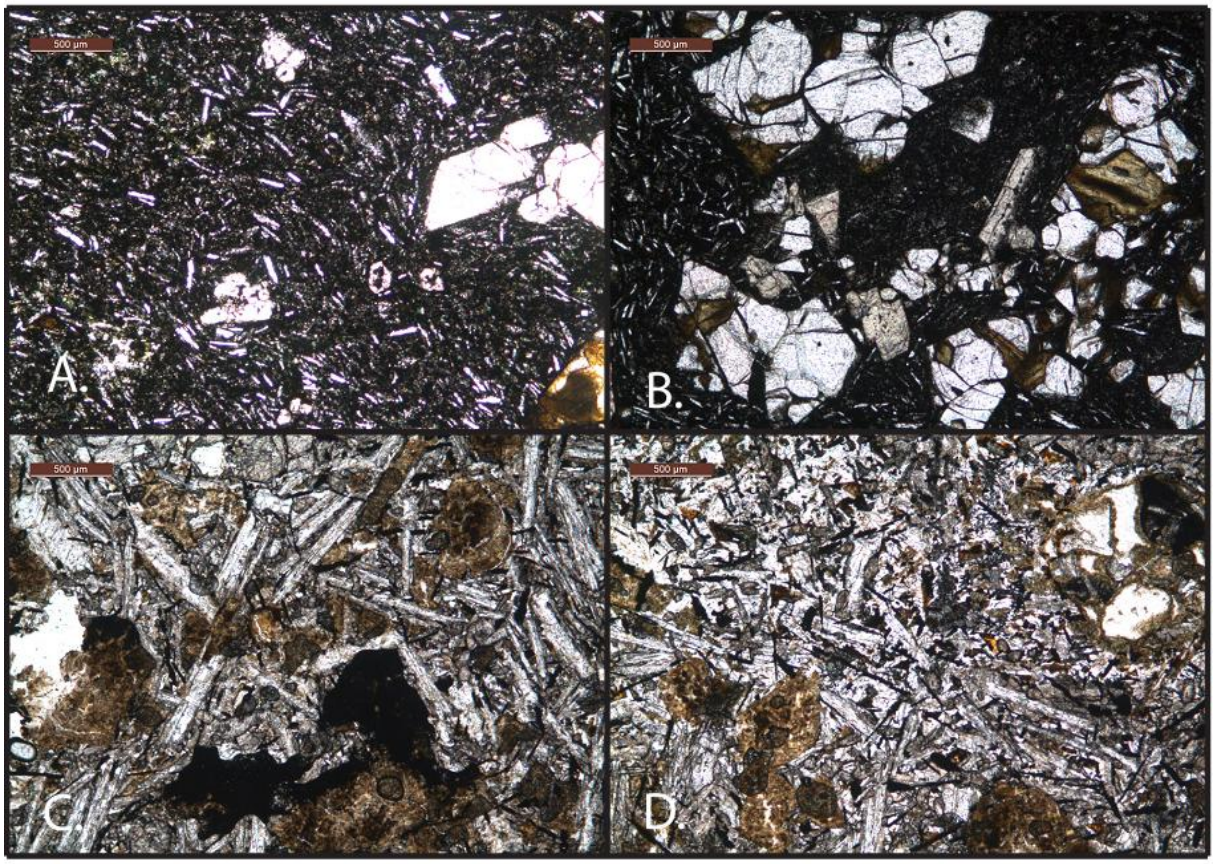

Figure 3.5- Thin sections showing features in pillow basalt. A, B) Fine to medium crystalline basalt . Sample 14,11 from Culverden back section. C, D) Very coarse crystalline basalt. Sample 9,20 from Pahau Downs (Scale bar: 500µm).

Figure 3.6- Pillow basalt with tuffaceous material and calcareous cement. Location: Culverden back section.

Interpretation:

This Pillow Basalt facies represents a basaltic eruption. It is difficult to define in terms of depth as pillow lavas form in shallow to deep water environments, depending on volatile content. The depth of the pillow basalt within this facies is constrained by the overlying bryozoan and algal-rich facies and molluscan-rich facies, which are described in section 3.2.4 and 3.2.5.

There appears to have been a submarine source for this volcanic activity, which can be determined from the pillow morphology and the interaction of this facies with the overlying volcanic tuff facies. Sea level fall could also provide evidence for the deposition of this facies in a mid shelf environment (Field and Browne, 1989).

B. Volcaniclastic Tuffaceous Facies

Description:

This tuffaceous facies is up to 2.4 m thick and includes a reddy-brown tuff interspersed with thin beds of calcareous material (figure 3.7). Glauconite is visible but content is very low at ~1%. Individual beds of tuffaceous material are ~7-10cm thick interspersed with very fine calcareous beds. Volcanic lithics are 1 to 3 millimetres in size and consist of minerals such as

biotite, plagioclase and olivine. Quartz lithics are also visible, but are not the dominant lithic type. This volcaniclastic tuffaceous facies grades into the bryozoans and algal-rich grainstone facies above incorporating volcanic lithics within the grainstone facies.

Occurrence:

This facies is located at the Glens of Tekoa in the most western field site and this facies occurs in the Cookson Group Volcanics.

Figure 3.7- Volcaniclastic Tuffaceous Facies interbedded with calcareous layers. Location; Syncline, Glens of Tekoa

Interpretation:

This facies is only located in the field site furthest to the west of the field area. It is likely this facies is more of a distal product of volcanism than the Pillow Basalt facies**.** The same volcanic source that produced the pillow lava is likely to have produced the tuffaceous material. This volcaniclastic tuffaceous facies is also likely to have been reworked and deposited as interbeds between calcareous layers. Grading of this tuff into calcareous beds suggests a reworked deposit. It is likely pulses in eruption occurred and then the tuff was

reworked shortly after. As this facies is occurring at the same time and in the same location as the Pillow Basalt facies the depositional environment can be interpreted from the overlying overlying bryozoan and algal-rich facies and molluscan-rich facies inferring a mid shelf environment.

3.2.4 Molluscan-rich Grainstone facies

Description:

This Molluscan-rich Grainstone Facies forms outcrops of creamy-white bioclastic limestone. Texturally this facies is a coarse grainstone grading into a coarse rudstone with intermittent layers of shelly packstone (>50cm). Thickness of this facies ranges from 2.5 to 8.5m. This facies overlies the basaltic pillow lava facies (figure 3.8). Upper contacts are gradational into the bryozoans and algal-rich grainstone facies.

Mollusca form 60-78% of the bioclasts in this facies (figure 3.9). Most commonly molluscs in this facies are bivalves. Bioclasts that are common aside from molluscs include foraminifera (benthic), echinoid fragments, brachiopods, barnacles and fenestrate and branching bryozoan. Whole fossils are rare and include bivalves and brachiopods (14, 12).

Occurrence:

The Molluscan-rich Grainstone facies is located at the Culverden back section and Pahau Downs. This facies only occurs in the Flaxdown Limestone Member.

Figure 3.8- Molluscan-rich Grainstone Facies overlying the Volcaniclastic Tuffaceous Facies. Location: Pahau Downs

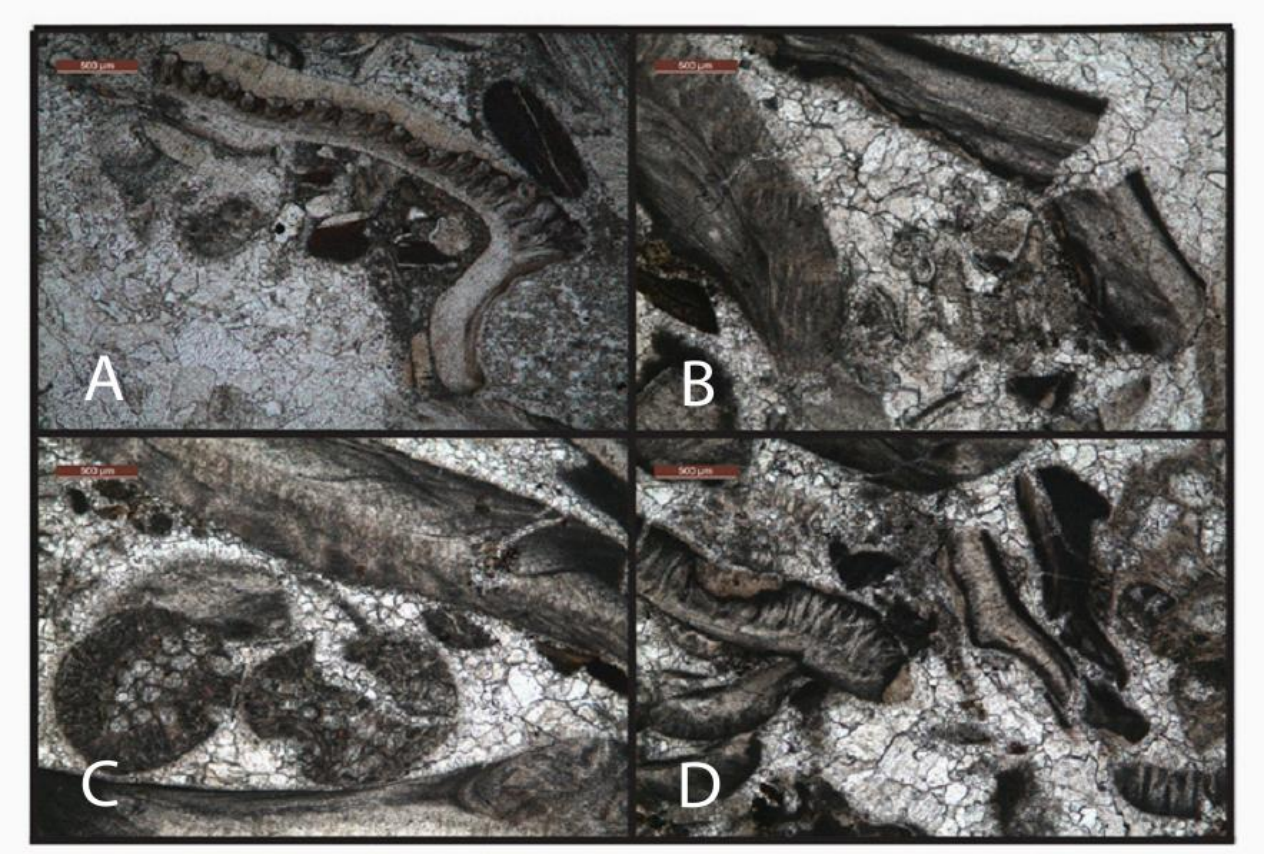

Figure 3.9- Thin section images of the Molluscan-rich Grainstone Facies. A) Large mollusc valve. B,C,D) High concentration of mollusc fragments surrounded by calcite overgrowth.(Scale bars: 500µm)

Interpretation:

This Molluscan-rich Grainstone Facies consists of a matrix of both calcite cement and mud indicating variations in sedimentation rate and energy (Boggs, 2006). The main changes within this facies are from grainstone to a hydrothermally altered rudstone with layers of a shelly packstone. Variations from grainstone into beds of shelly packstone indicate fluctuations in energy with deposition of a lime-mud matrix within the molluscan-rich limestone.

Branching bryozoans and echinoderm fragments are the other abundant bioclasts in this facies. The optimal shelf setting for this group of delicate branching bryozoan is quite broad with a mid to outer shelf depth of 50-200 metres (Smith, 1995). The inclusion of a small concentration of tuffaceous material at the bottom of this unit and its similarities to the bryozoan and algal-rich facies (excluding the algae) indicates that this unit is mid shelf. This

environment is also indicated by the absence of mud (in grainstone sections), describing a current swept environment in which mud has been removed. This absence of mud in combination with bioclast composition indicates a mid shelf environment.

3.2.5 Bryozoan and Algal-rich Grainstone Facies

Description:

The Bryozoan and Algal-rich Grainstone Facies consists of a creamy-white, moderately sorted fine to medium packstone to medium to coarse grainstone facies. Thickness of this facies ranges from 1 to 9.8 m. The lower contact with the volcanic tuff facies is sharp, with possible post depositional dissolution between these facies. In the Tekoa and Culverden back section contacts are gradational from the molluscan-rich grainstone. Upper contacts into the Pahau Siltstone Member were not identified in the field.

Bryozoan and coralline red algae are the two most abundant bioclasts in this facies. Bryozoans in this facies range from ~10% to 78% (figure 3.13) and include both fenestrate and branching forms. Coralline red algae range from abundance of ~10% to 55% (figure 3.11) and consist of the branching and encrusting forms. Bioclasts that are common aside from bryozoans and coralline red algae include foraminifera (benthic) echinoid fragments, crinoids and mollusc fragments. Fossils are more fragmented in the packstones. Whole macrofossil fragments of this grainstone facies include brachiopods and bivalves.

Basaltic lithics (< 2mm) and post depositional hematite staining occur at the base at in the Pahau Downs outcrop (figure 3.14). Stylotilisation is consistant throughout the bottom of this facies and decreases upwards. This diagenetic feature is visible in bands of 1.5 to 2cm decreasing to weakly developed bands of 2 to 3 cms (figure 3.12).

Occurrence:

The Bryozoan and Algal-rich Grainstone Facies is located at the syncline at the Glens of Tekoa, Pahau Downs, Cascade Downs and the Culverden back section. This facies only occurs in the Flaxdown Limestone Member.

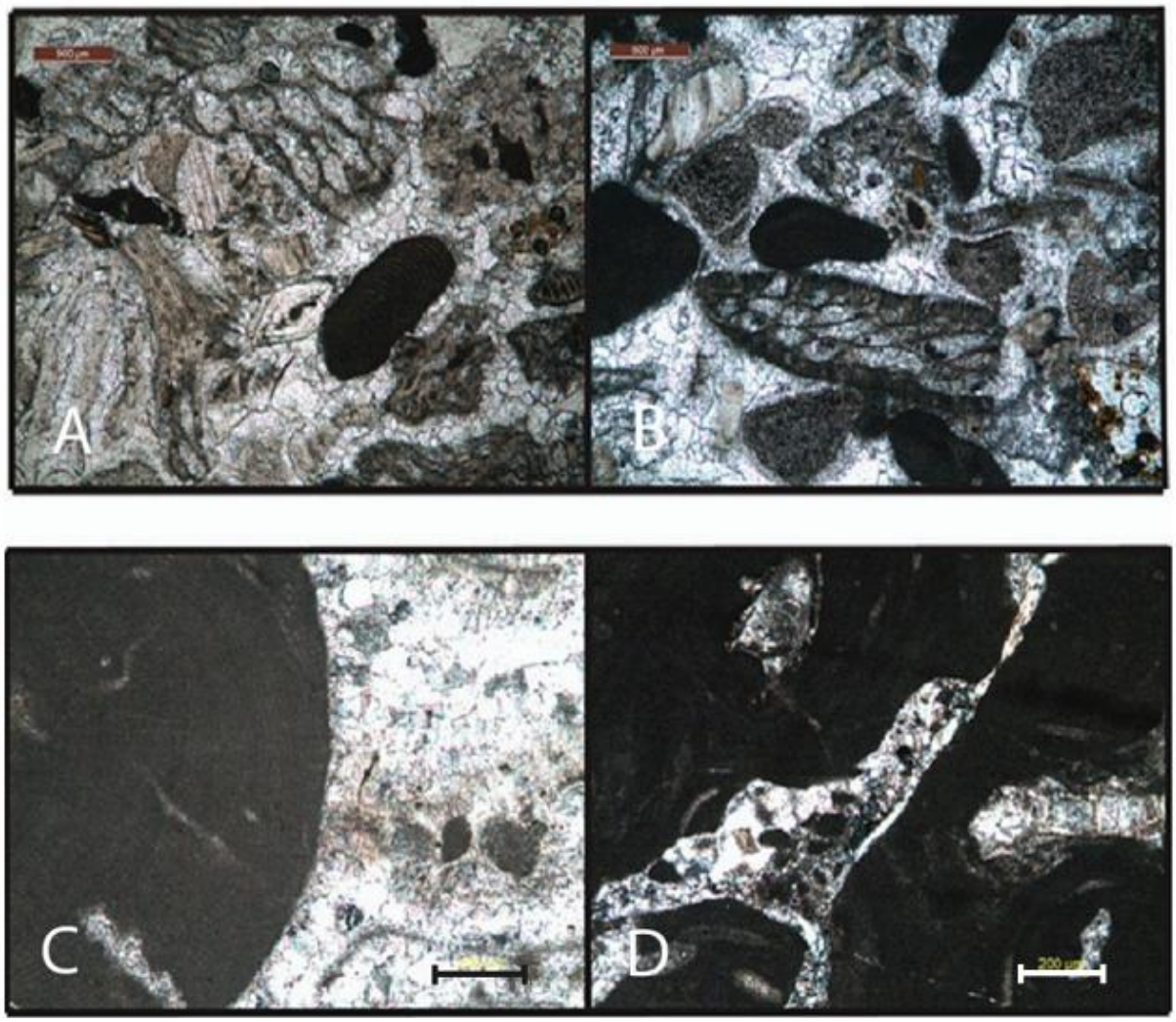

Figure 3.11- Thin sections of the Bryozoan and Algal-rich Grainstone Facies. A ,B) show small broken fragments of algae alongside bryozoan. (Scale bar: 500µm). C, D) algal-rich limestone facies showing large portions of algae (Scale bar:200 µm). Samples 4,3 and 4,5 from Glens of Tekoa.

Figure 3.12- Styolitization in the Bryozoan and Algal-rich Grainstone facies. Stylolites become more weakly developed up the section. At the bottom of this picture they are 1.5-2 cm apart decreasing to 2-3cm apart half way up the outcrop. Location: Glens of Tekoa.

Interpretation:

Algae

The environment of this facies can be determined from the abundance of red coralline algae (22-55%)**.** Controlling factors that determine coralline algal growth sites consist of depth, light and energy (Wray, 1977)**.** These branching and encrusting forms of algae suggest relatively shallow water depths with the optimum depth of coralline algae genera covering a broad range from 0-90 metres, although these algae occur in higher abundance at the shallower end of this range (Perrin *et al.,* 1995; Wray, 1977).

Bryozoans

Bryozoans are the abundant fossil type in this facies with this unit consisting of percentages of bryozoan as high as 85%. The most abundant bryozoan colonial growth form in this facies is a delicate form of branching bryozoan. Due to the delicate nature of these bryozoans it is limited to shelf environments of low energy and sedimentation (Smith, 1995). The optimal shelf setting for this group of delicate branching bryozoans is quite broad with a mid to outer shelf depth of 50-200 metres (Smith, 1995). Overall bryozoan abundance peaks at ~40-90 metres on the shelf (in respect to all bryozoan forms), with deeper waters providing an environment for abundant branching forms (up to 50%) (Smith, 1995).

This facies varies from a packstone to grainstone in at the Culverden back section. The relative energy and sedimentation regime in consideration to the bryozoan indicates a mid to outer shelf environment, with the inclusion of high abundances of coralline algae in most samples suggesting a mid shelf environment. The classification of this facies as a grainstone, suggests deposition in a current swept setting in which mud was removed (Selley, 2000). This facies therefore formed in a relatively high energy mid shelf environment with periods of waning energy, allowing packstone deposition.

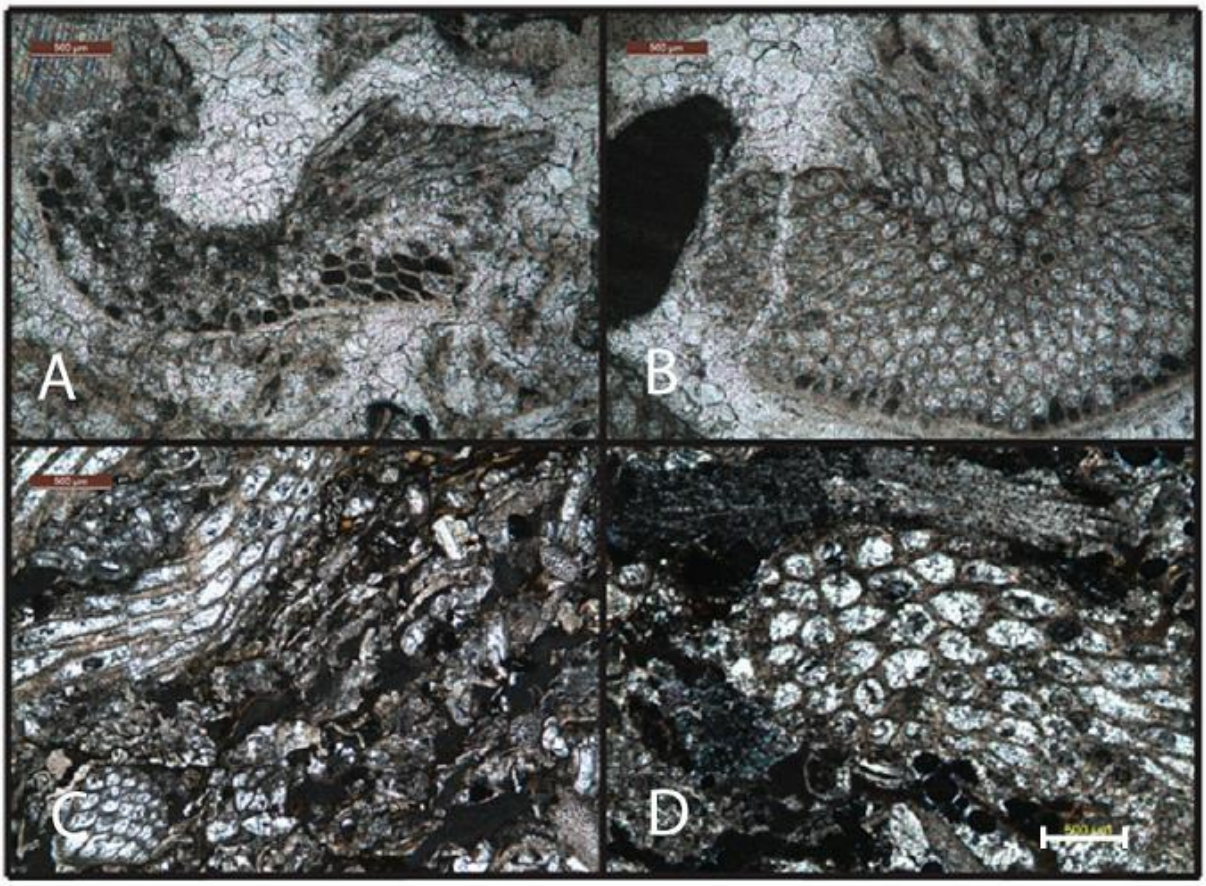

Figure 3.13- Thin section showing branching bryozoans in the Bryozoan and Algal-rich Grainstone Facies. Samples A) 4,5 B) 4,9(12) from Glens of Tekoa C & D) 11,4 from Culverden back section. (Scale bars: 500µm)

Figure 3.14- Bryozoan and Algal-rich Grainstone Facies. Location: Pahau Downs

3.2.6 Fossiliferous Sandstone Facies

Description:

This Fossiliferous Sandstone Facies consists of a grey fine to medium sandstone with beds of molluscan fossils. Sorting is consistent with a poorly sorted sand. Thickness of this facies ranges from 1.4 to approximately 3.7 metres. The thickness of this facies can be further separated into varying amounts of fossiliferous material. Beds are distinguishable when they are separate by shell beds, but are indistinguishable in other sections. Layers of well indurated fossiliferous beds 1-10 centimetres in thickness are interbedded with layers of well lithified fossiliferous beds with concretionary horizons. Quartz is the dominating mineral in this facies; consisting of 78% sub-rounded to sub-angular quartz grains, with the remainder of this facies consisting of a terrigenous mud matrix (figure 3.16). Glauconite content ranges from 1-4%, remaining relatively low. Upper contacts of this facies into the quartz-rich sandstone facies are sharp.

Mollusca are the most common fossil type in this facies with 55% of the bioclast count consisting of mollusc fragments. The fossiliferous beds in this facies consist of common whole and fragmented molluscs. Gastropods, bivalves and brachiopods are the main fossils found in this facies. The most common Mollusca include *Glycymeris* and *Polinices,* identified specimen include *G. huttoni* and *P. huttoni.* Trace fossils were not identified in this facies.

Post depositional features observed in this facies include well indurated concretionary beds (figure 3.15). These features occur in beds rich in fossiliferous material, with a concentration of calcium carbonate. Large concretions of 5-10 centimetres are visible in these beds.

Occurrence:

This facies is located in Cascade Stream at Cascade Downs. This facies only occurs in the Pahau Siltstone Member.

Figure 3.15- Fossiliferous Sandstone Facies, with concretionary horizons. Location: Cascade Stream, Cascade Downs.

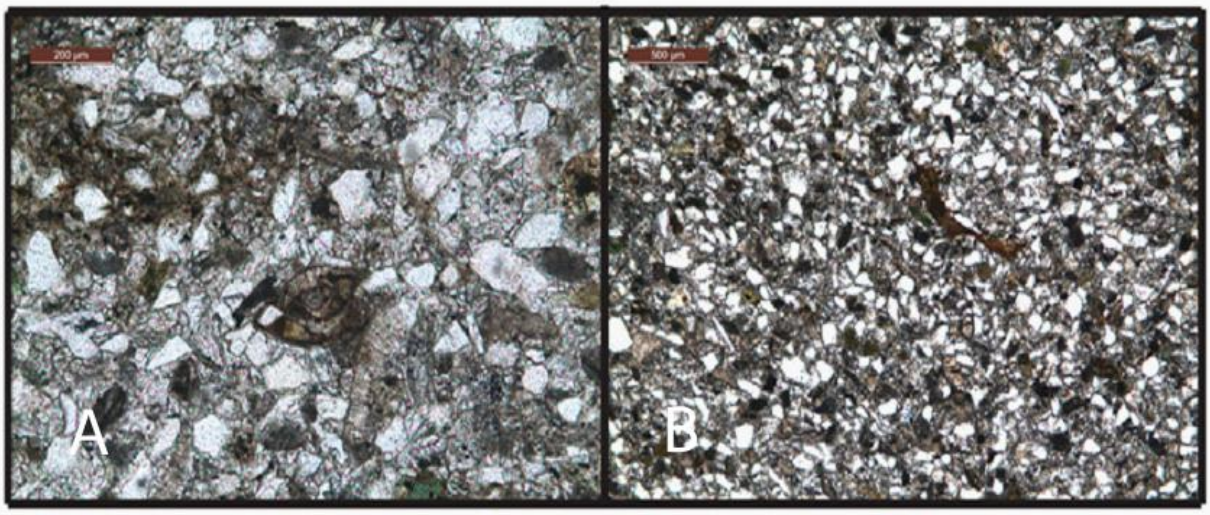

Figure 3.16- Thin section images showing, A) Higher magnification (Scale bar:200 µm) foraminifera and mollusc fragments in a Fossiliferous Sandstone Facies. B) Overview of sandstone facies (Scale bar 500 µm). Sample 12,4 from Cascade Downs.

Interpretation:

Mollusca are the abundant fossil type in this facies with a number of fauna being identified. Re-occuring species of *Glycymeris* and *Polinicies* indicate a reasonably shallow environment. *Polinicies* (*P .huttoni)* are found shallow tidal zones, such as intertidal sand flats or in the subtidal zone (Beu and Maxwell, 1990). *Glycymeris* can be found in this facies in a Miocene

form *G. huttoni.* This species is a younger version of *G. manaiaensis,* which is common in shallow-water, near shore beds (Beu and Maxwell, 1990). The presence of these forms indicates an inner shelf environment typical of a sheltered subtidal zone.

3.2.7 Quartz-rich Sandstone facies

Description:

This quartz-rich facies consists of a browny grey, very fine to medium sandstone. Sorting is consistent with a moderately to moderately well sorted sand. Thickness of this facies ranges from 0.9 to 8 m. Beds of quartz-rich material are separated by molluscan-rich beds. Colour is relatively consistent throughout this facies with slight variations in the well indurated concretionary horizons. Quartz is the dominant clast type in this sandstone with the quartz percentages varying between very well indurated concretionary layers and the well indurated concretionary beds (figure 3.17). In the concretionary beds quartz percentages range from 42-47%. In the less well indurated beds sub-rounded to sub-angular quartz percentages are as high as 86%, with a terrigenous mud making up the matrix. Glauconite content is low with a maximum of 1%. Upper contacts are not visible. Lower contacts are sharp from the molluscan-rich facies.

Macrofossils are not as common as the previous facies with as little as 2% bivalves in the bioclast count of thin sections. Foraminifera make up 98-100% of the bioclast count (figure 3.17), with no other fossils, or trace fossils visible. Post depositional features include concretions, in concretionary horizons occurring every 1-2 metres with concretion sizes of 5-10 centimetres. Weathering is visible in this facies.

Occurrence:

This facies is located in Cascade Stream at Cascade Downs. This facies only occurs in the Pahau Siltstone Member.

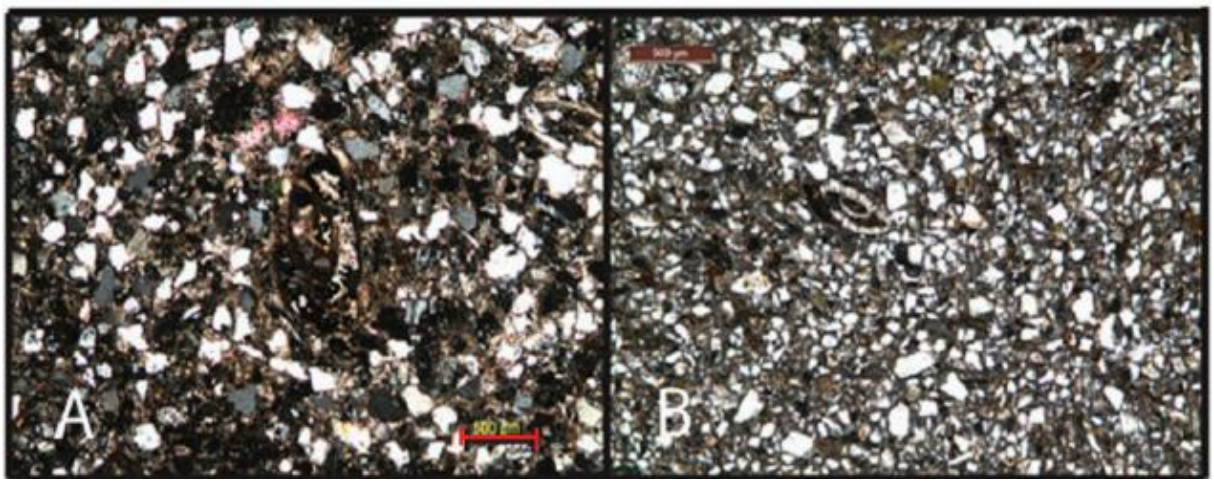

Figure 3.17- Thin section images showing a quartz-rich sandstone facies with foraminifera present. A. sample 5,5a in cross polarised light, B. 12,2.2.4m . Location: Cascade Downs (Scale bars: 500µm).

Interpretation:

In the rare molluscan rich beds, similar to the previous facies, fragmented molluscan material is visible in low percentages. It appears that quartz-rich beds with rare mollusca still show a shallow environment. The increase in quartz compared with the last facies suggests a small change in environment, with a moderate energy and relatively high sedimentation setting.

The lower abundance of fossiliferous material and higher mud content in this quartz-rich facies compared to the Fossiliferous Sandstone Facies suggests variation between the two. It is likely the Fossiliferous Sandstone Facies records a more current swept environment with winnowing of mud occurring and the concentration of molluscs. Whereas it appears this Quartz-rich Sandstone Facies reflects periods of lower energy with the deposition of high percentages of quartz and a mud matrix.

3.3 Measured sections

Following on from sedimentology in this thesis, this section incorporates the lithofacies and Tertiary units into stratigraphic sections. Geological maps of the locations and extent of units at the field sites have been included in Appendix D. Figures 3.18 and 3.19 provide a broad overview of the Stratigraphy of the district and are followed by representative stratigraphic sections and maps of each field site. Figure 3.20 locates the field sites and provides overview of the stratigraphy of each site in relation to other important North Canterbury locations.

Legend

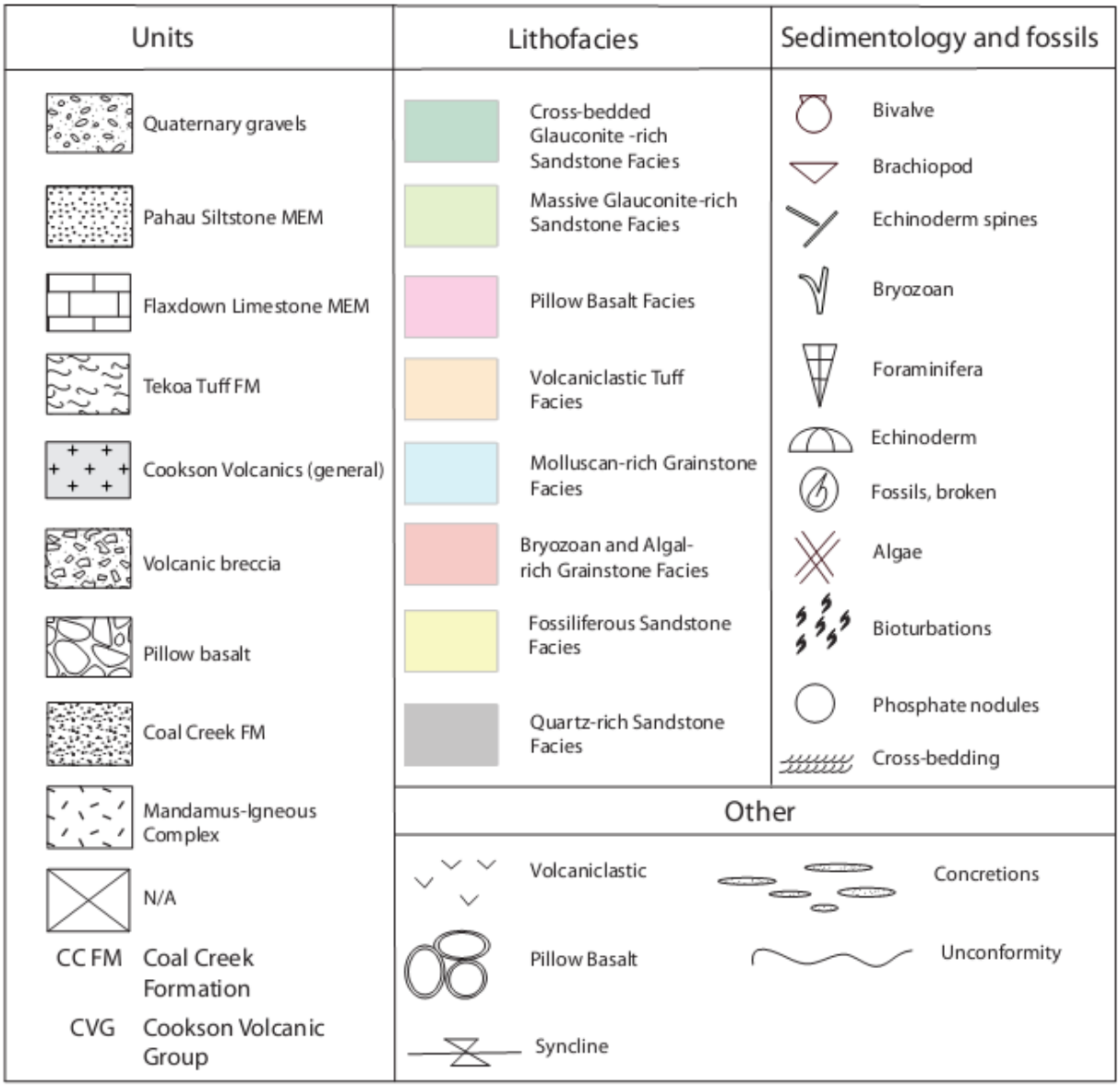

Figure 3.18- Legend of symbols used in the stratigraphic columns and maps.

The Mandamus-Pahau District

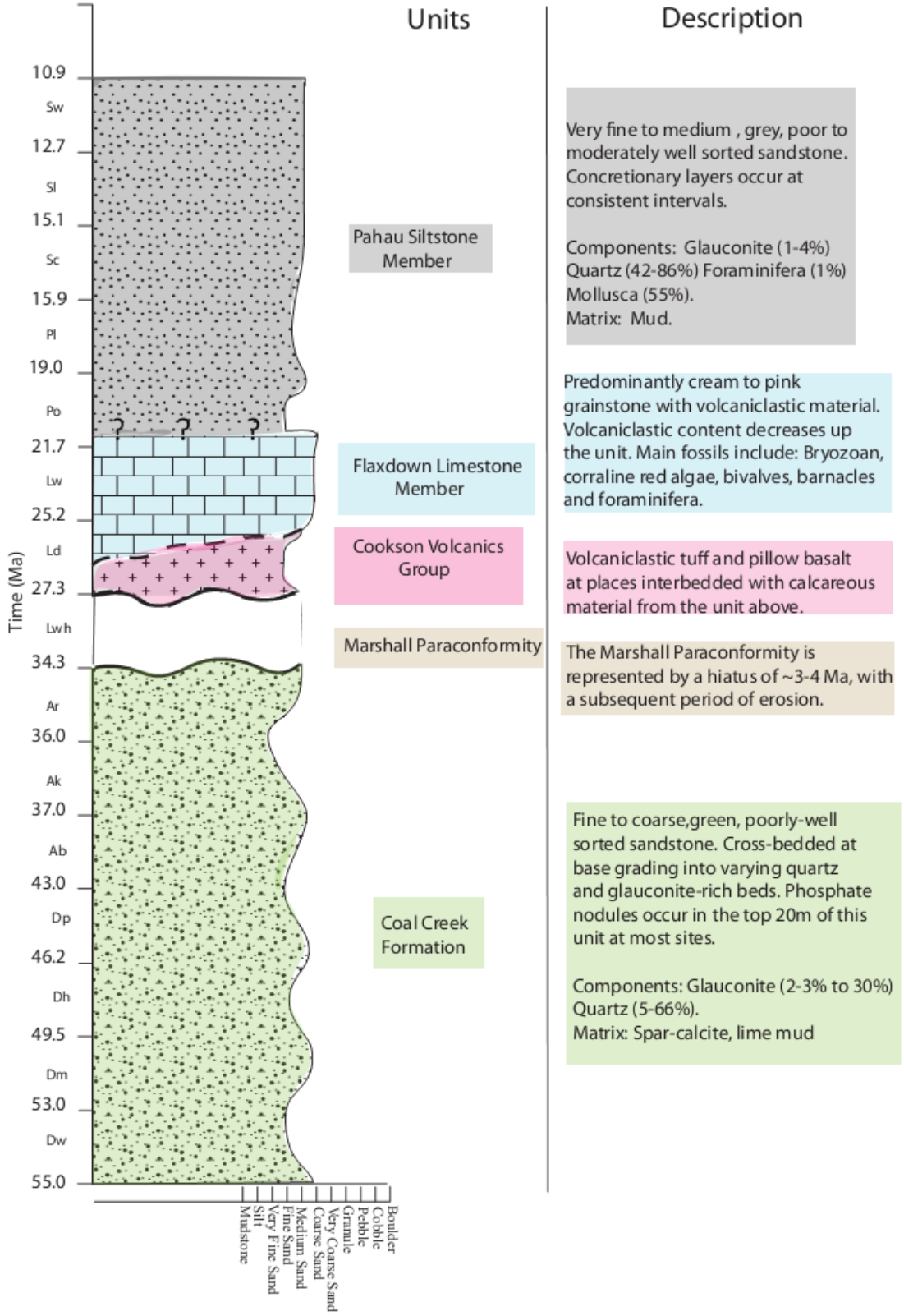

Figure 3.21- Stratigraphic column of the Glens of Tekoa field area showing stratigraphic location of samples, matrix type and percentages (see figure 3.18 for key).

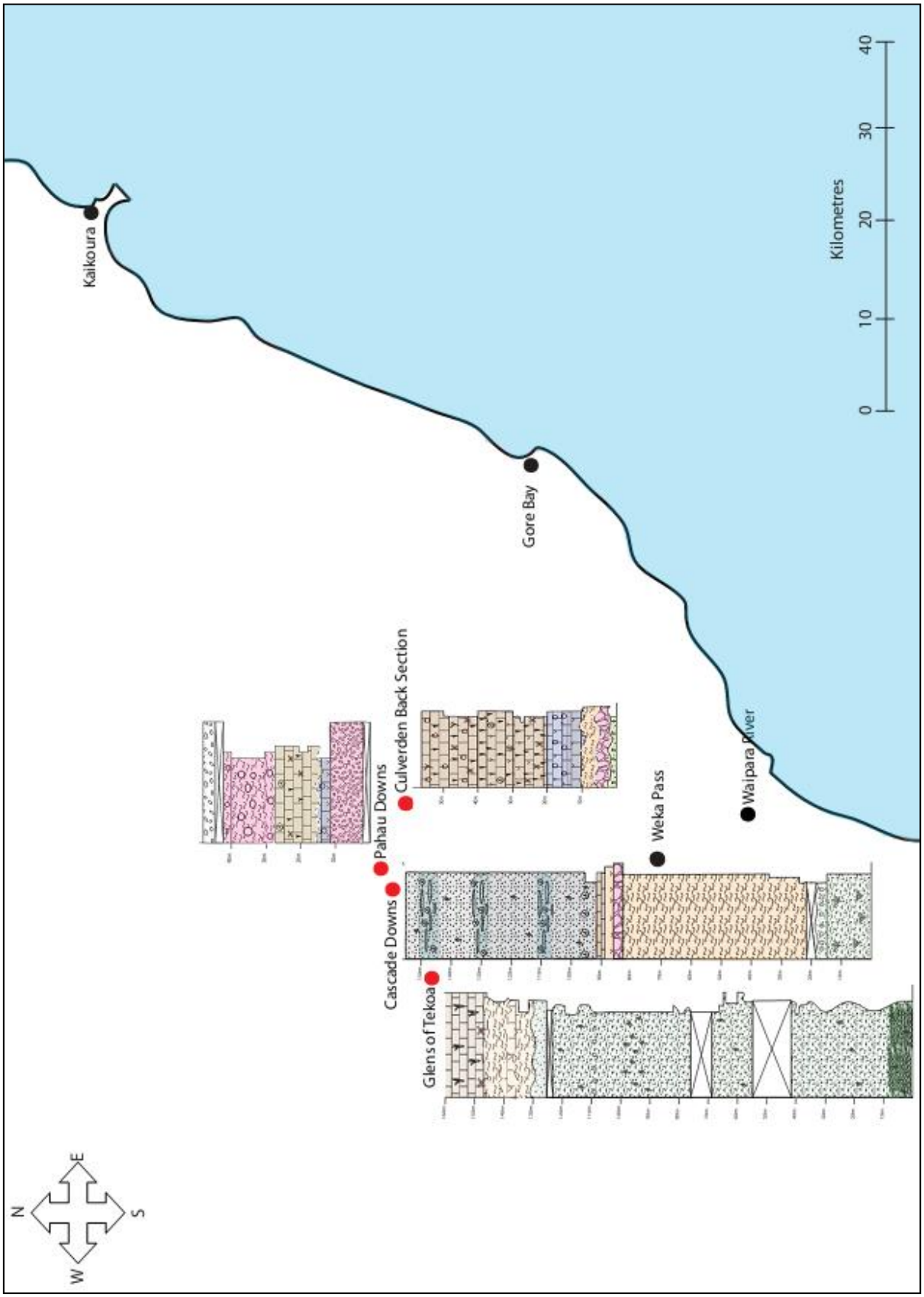

Figure 3.20- An overview of the stratigraphy of field sites in correlation to one another.

3.3.1 Glens of Tekoa

Glens of Tekoa is the western most field site (figure 3.20) from the Mandamus-Pahau District. At the Glens of Tekoa the Coal Creek Formation includes the Cross-bedded Glauconite-rich Sandstone Facies and the Massive Glauconite-rich Sandstone Facies before the occurrence of the Marshall Paraconformity. The overlying Cookson Volcanics Group includes the Volcaniclastic Tuff facies unique to the Tekoa Tuffs. The Flaxdown Limestone also occurs at the Glens of Tekoa site with only the Bryozoan and Algal-rich Grainstone facies located at this site (figure 3.21).

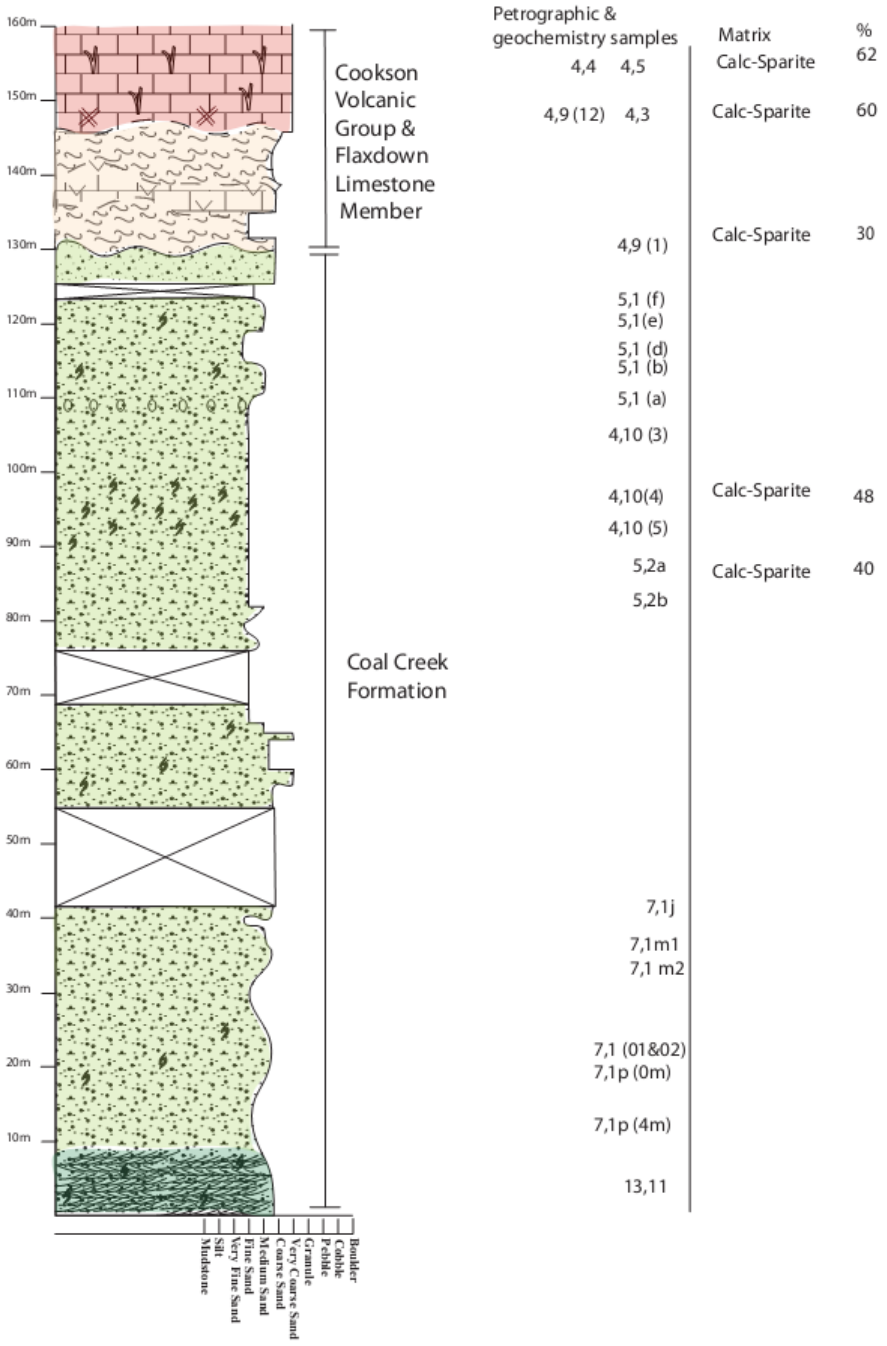

Figure 3.21- Stratigraphic column displaying the Tertiary units of the Mandamus Pahau District and brief descriptions. (See figure 3.18 for key).

3.3.2 Cascade Downs

Cascade Downs is located between Glens of Tekoa to the west and Pahau Downs across the Pahau River to the east (figure 3.23). At this site the Coal Creek Formation includes the Massive Glauconite-rich Sandstone facies before the occurrence of the Marshall Paraconformity. The overlying Cookson Volcanics Group includes the Volcaniclastic Tuffaceous facies unique to the Tekoa Tuffs and the Pillow Basalt facies. The Flaxdown Limestone occurs at the Cascade Downs site with only the Bryozoan and Algal-rich Facies located at this site (figure 3.22).

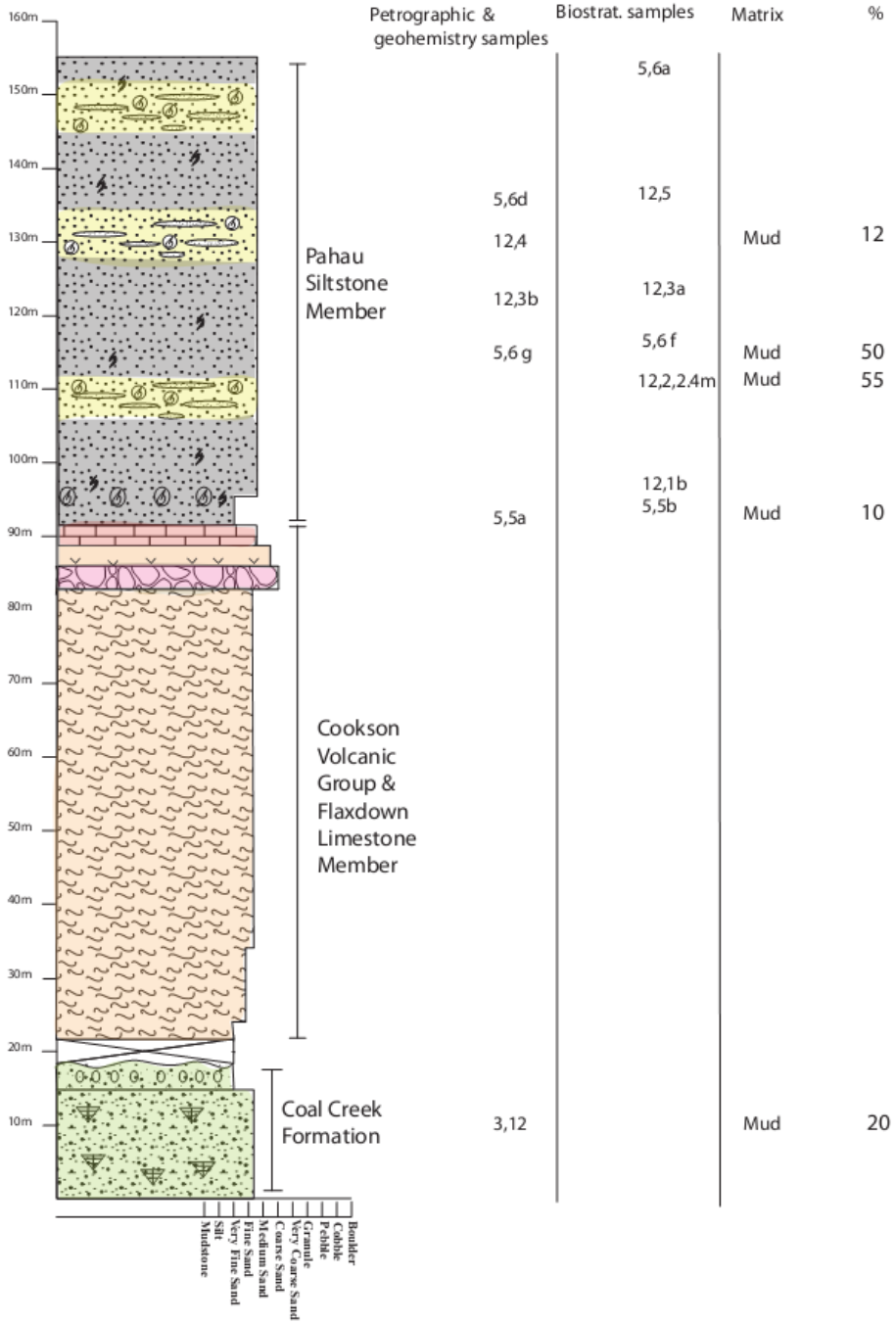

Figure 3.22- Stratigraphic column of the Cascade Downs field area showing stratigraphic location of samples, matrix type and percentages (see figure 3.18 for key).

3.3.3 Pahau Downs

The Pahau Downs site is located on beside Cascade Downs to the east, with the Pahau River located ~2metres from this site. At this site Coal Creek Formation is not seen. The Cookson Volcanics Group is the oldest unit at this site. The volcanic at this site include the Volcaniclastic Tuffaceous facies and the Pillow Basalt, with these facies occurring together throughout the majority of this stratigraphic section. The Flaxdown Limestones occurrence at this location is different to other sites in that it is located between the Cookson Volcanics Group. The Pillow Basalt Facies outcrops on either side of the Flaxdown Limestone with tuffaceous sections occurring throughout the pillow basalt sections, before river Quaternary gravels outcrop (figure 3.23).

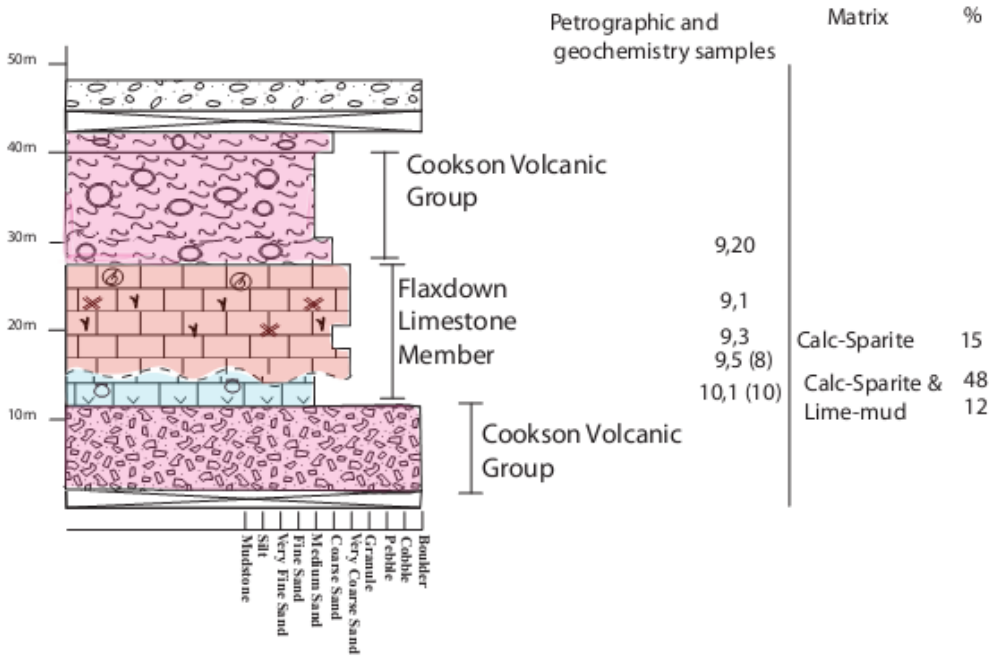

Figure 3.23- Stratigraphic column of the Pahau Downs field area showing stratigraphic location of samples, matrix type and percentages (see figure 3.18 for key).

3.3.4 Culverden Back section

This most eastern site is located ~5km north west from the Culverden township. The Coal Creek Formation, (Massive Glauconite-rich Sandstone Facies) occurs as a thin layer at this site. The overlying Cookson Volcanic Group occurs at this site with Pillow Basalt facies being the dominant volcanic facies at this site. The Flaxdown Limestone is the main unit at this site, covering a considerable area. This unit shows large variations in grainsize (both packstones and grainstones occur at this site) with both the Molluscan-rich Grainstone and Bryozoan and algal-rich facies occurring at this site (figure 3.24).

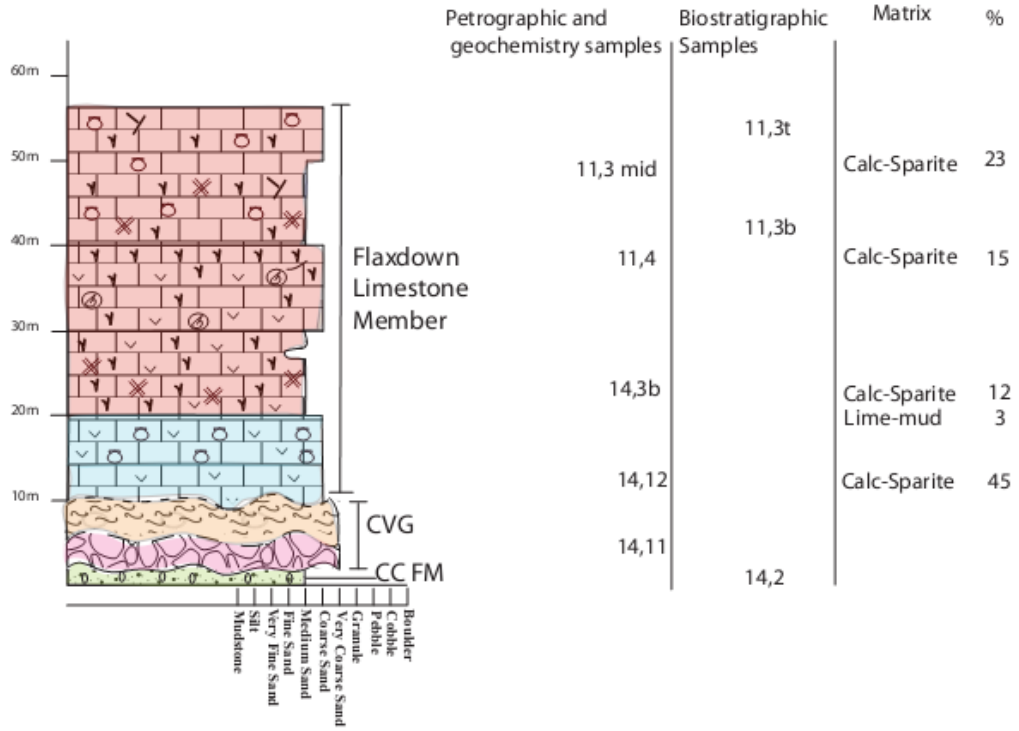

Figure 3.24- Stratigraphic column of the Culverden back section field area showing stratigraphic location of samples, matrix type and percentages (see figure 3.18 for key).

Summary

In this chapter 8 lithofacies were outlined, these are: Cross-bedded Glauconite-rich Sandstone, Massive Glauconite-rich Sandstone, Pillow Basalt, Volcanic Tuff, Molluscan-rich Grainstone, Bryozoan and Algal-rich Grainstone, Fossiliferous Sandstone and Quartz-rich Sandstone. The Coal Creek Formation consists of two lithofacies the Cross-bedded Glauconite and Quartz-rich Sandstone facies and the Glauconite and Quartz-rich Sandstone facies, with these forming the base of all stratigraphic columns but Pahau Downs. At all

locations (excluding Pahau Downs) the Marshall Paraconformity is present with a break in time from the Coal Creek Formation to the Cookson Volcanics Group. Post Marshall Paraconformity a return to carbonate sedimentation is seen with the deposition of the Flaxdown Limestone. This carbonate deposition is then replaced by the occurrence of siliciclastic sandstone units higher in the stratigraphy.

In summary the Coal Creek Formation (Cross-bedded Glauconite-rich Sandstone Facies and Massive Glauconite-rich Sandstone Facies) is deposited in an inner shelf environment deepening to a mid-outer shelf setting. The Cookson Volcanic Group (Pillow Basalt Facies and Volcaniclastic Facies) is deposited in a mid shelf environment, constrained by the overlying Flaxdown Limestone. The Flaxdown Limestone Member (Molluscan-rich Grainstone Facies and Bryozoan and Algal-rich Grainstone Facies) is deposited in a mid shelf setting. The final unit the Pahau Siltstone Member (Fossiliferous Sandstone Facies and Quartz-rich Sandstone Facies) is deposited in an inner shelf environment.

4. Micropalaeontology

In this chapter foraminiferal assemblages are described and applied to determine biostratigraphy of Late Eocene to Mid Miocene (figure 4.1) rocks from the Mandamus-Pahau District and provide evidence for environmental interpretations. Foraminifera are identified down to the species level where possible. A number of texts were used to identify foraminifera, the main texts used were *Manual of New Zealand Permian to Pleistocene Foraminiferal Biostratigraphy* (Hornibrook *et al.,* 1989), *Tertiary Foraminifera from Oamaru District (N.Z)* (Hornibrook , 1961), *Recent Elphidiidae of the South–West Pacific and Fossil Elphidiidae of New Zealand* (Hayward *et al.,* 1997) and *New Zealand Eocene and Oligocene Benthic Foraminifera of the Family Notorotaliidae* (Hornibrook, 1996).

4.1 Introduction

4.1.1 Biostratigraphy

The age of samples were determined by species age ranges and the overlap between age distributions within each sample. Thirty samples were processed for foraminifera in order to undertake age and palaeoenvironmental analysis. Of these thirty samples only ten contained a sufficient quantity of foraminifera for analyses to proceed. Preservation varies within all samples and therefore some samples were not able to be identified down to species level. Planktic and benthic foraminifera were also poorly preserved, a number of specimens were not resolved to species level, but were included within the planktic:benthic ratio. In this analysis the majority of samples could not be resolved to stage level due to the wide age distribution of preserved foraminiferal species, although both long ranging and short ranging species have been included in this biostratigraphy.

Samples from the Coal Creek Formation, Flaxdown Limestone Member and Pahau Siltstone Member are described and correlated to the lithofacies from the chapter 3. The relation of the abundant foraminifera in each unit, in association with the minor (<10%) species provide interpretations of the environment in which they were deposited. Dominant species from each unit have been identified in order to infer environments. The dominant species in these units include benthic foraminifera genera: *Cibicides, Elphidium, Notorotalia* and *Zeaflorilus.*

Planktic foraminifera of importance in these samples are limited to the Coal Creek Formation and include *Globigerina* and *Globorotalia*.

4.1.2 Palaeoenvironments

Distribution of foraminifera

Deep-water fossil foraminifera are a proxy for assessing large scale changes in palaeoceanographic changes including upwelling, nutrient supply, climate related surface water mass circulation, variation of bottom-water oxygen and carbonate concentrations (Hayward *et al.,* 2010). Fossil foraminifera in shallower environments can record a number of other variations including palaeosalinity, palaeoenvironment and palaeo-sea level and climate related sea level change (Hayward *et al.,* 2010). Fossil benthic foraminifera from both shallow and deep-water environments are useful in determining water depth and the paleoenvironment in which sediments have accumulated (Hayward *et al.,* 2010). Individual foraminifera do not tell us much about the depositional environment, instead it is foraminiferal assemblages that are good indicators of paleodepth (Hayward, 2004). The utilisation of dominant benthic taxa, in combination with planktic foraminiferal percentage and benthic species diversity provide conventional techniques used to determine palaeodepth (Hayward, 2004).

The dominance, abundance and assemblages of benthic foraminifera have long played a role in the interpretation of paleodepth. The recognition of the correlation between increased abundance of planktic foraminifera and increasing water depth was first applied by Grimsdale and Van Morkhoven in a 1955 study (van der Zwaan *et al.*, 1990). This study also looked at the reason for this correlation, including a decrease in turbidity away from the coast, leading to an increase in primary production (van der Zwaan *et al.*, 1990). Benthic foraminifera generally followed a pattern of increasing abundance from the near shore to the outer continental shelf, followed by a drastic decrease at greater depths (van der Zwaan *et al.*, 1990). It is likely this change is due to benthic foraminiferal abundance being linked to the distribution of organic carbon within sediment, which reaches its highest levels in shelf sediments and towards the outer shelf (van der Zwaan *et al.*, 1990). Therefore benthic/planktic ratios are a reliable estimate of paleodepth and ocean productivity. The only problem with this concept is that benthic foraminiferal abundance can be unpredictable

at times, with environments such as anoxic basins recording high benthic foraminiferal abundance (van der Zwaan *et al.*, 1990).

The use of foraminifera as palaeodepth indicators is developed with the general notion that benthic and planktic foraminifera occur along a depth gradient, but there are a number of problems that may prevent the accuracy of this concept according to van der Zwaan *et al.*, (1990). These problems include:

a. The factors that control the bathymetric distribution of benthic species are not well understood.
b. Foraminiferal distribution varies from location to location, depending on factors that are not well defined or understood. Distribution being influenced by both local and global factors.
c. It is unknown whether species retain the same palaeodepth or if this changes over time. This is reiterated by the redistribution of *Osangularia* from near shore to deep sea environments during the Cenozoic (Hornibrook *et al.,* 1989).
d. The reconstruction of life assemblages from fossil data may not be reliable due to the redistribution of shallow water species into greater depths (Hornibrook *et al.,* 1989). The comparison of Miocene fauna with recent and present day assemblages may be more valid (Hornibrook *et al.,* 1989).

Geological application in New Zealand

Modern bathymetry of the world oceans consists of a well defined break between the shelf and slope due to Pleistocene sea levels and may have only existed at periods of low sea level in past climates (Hornibrook *et al.,* 1989). Marine climates fluctuated during the Cenozoic, with the northward movement of New Zealand away from a high latitude position affecting this (Hornibrook *et al.,* 1989). The early Oligocene saw the onset of the circum-Antarctic current producing cold bottom waters in deeper ocean settings, allowing deep ocean species to move to shallower environments and an environment for new species to colonise (Douglas and Woodruff, 1981; Murphy and Kennett, 1986). This transition to modern ocean conditions most likely occurred about the early Middle Miocene, due to the increase of polar cooling (Douglas and Woodruff, 1981).

This brief history of the use of foraminifera as paleodepth indicators highlights the problems associated with reconstructing paleodepth and bathymetry from fossil records (Hornibrook *et al.,* 1989). Even though there are a number of problems with paleodepth analysis, factors affecting shallow water and deep-water sediments can be interpreted to provide a more concise analysis. The interpretation of sedimentological characteristics of units can also be combined with foraminiferal data to interpret general depositional environments. Both foraminiferal and sedimentary analyses were used to determine the palaeoenvironments of 8 facies from 4 separate units from the Mandamus-Pahau District.

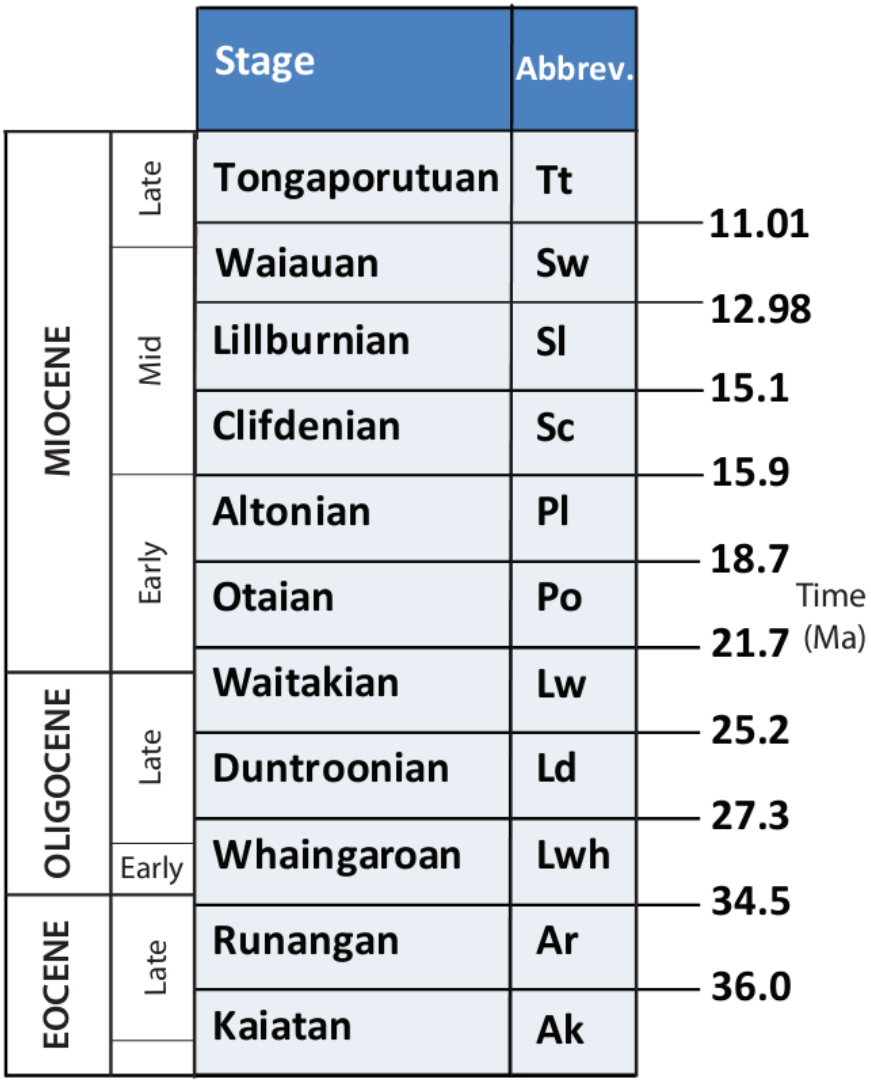

Figure 4.1- Geological timescale of the Late Eocene to Late Miocene in New Zealand (Irvine, 2012, modified from Hollis *et al.,* 2010).

4.2 Sample descriptions

4.2.1 Coal Creek Formation

There is only one sample from the Coal Creek Formation that was used for biostratigraphy (sample 14,2). This sample was collected from the Culverden back section site, 2m up the stratigraphic section (figure 3.24), in the Massive Glauconite-rich Facies. Approximately 20 other samples of the Coal Creek Formation from the Glens of Tekoa site were processed but did not contain any foraminifera. This means that the foraminifera used for environmental and age analyses were limited to sample 14,2 from the Culverden back section. Foraminifera identified from this sample are poorly preserved with fragmented chambers and weathered tests. Data collected from foraminifera of the Culverden back section only considers the Massive Glauconite-rich Facies, a stratigraphically younger section of the Coal Creek Formation. Due to a lack of biological material/foraminifera within the cross-bedded facies from the Glens of Tekoa, the age and environment of this facies could not be determined.

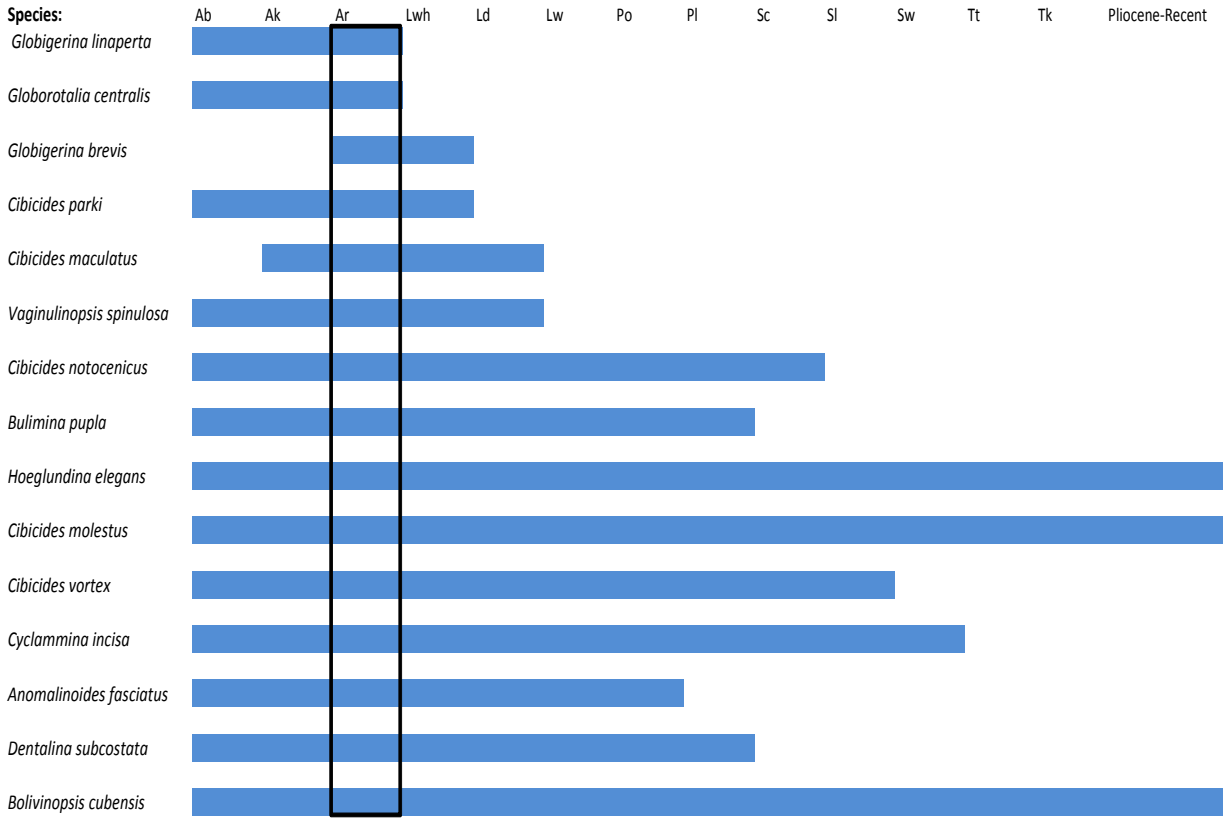

Table 4.1- Table constraining the age range of benthic and planktic foraminifera from sample 14,2. Location: Culverden back section (figure 3.24). Raw data is shown in Appendix B.

There were 12 benthic and 3 planktic species identified to species level (table 4.1). Sample 14,2 contains 28% planktic foraminifera and 72% benthic foraminifera. The most common benthic taxa are *Cibicides* (5 species, 50% of the sample) with the dominant species consisting of *Cibicides parki* (29%) (figure 4.2) and *Cibicides maculatus.* Planktic foraminifera include *Globigerina linaperta* (17%) *Globorotalia centralis* (11%) and *Globgerina brevis* (1%)(figure 4.3).

Observed age range:

The Coal Creek Formation is constrained to the Runangan stage (36-34.3 Ma) of the Late Eocene (table 4.1). The age of this sample is restricted to the Runangan stage by planktic foraminifera *Globigerina linaperta* (Heretaungan-Runangan), *Globorotalia centralis* (Bortanian-Runangan), and *Globigerina brevis* (Runangan-Whaingaroan) (Hornibrook *et al.,* 1989). As well as the co-occurrence of longer ranging Eocene to Oligocene taxa such as *Cibicides maculatus, Cibicides parki* and *Bulimina pupula*.

Environmental indicators:

The main benthic species indicative of this mid-outer shelf environment include *Cibicides maculatus* (15%) and *Cibicides parki* (29%) (Hornibrook *et al.,* 1989). Planktic and benthic foraminiferal percentages (28 planktic: 72 benthic) within this sample indicate a mid to outer shelf setting (Hayward *et al.,* 1999). Hayward *et al.,* (1999) states that planktic percentages of ~10-30% describes a mid shelf environment and ~30-65% planktic foraminifera is indicative of mid-outer shelf depths of 50-200 metres. The proximity of these planktic percentages to the mid-outer shelf environment and key species previously described indicate a deep shelf environment. It is therefore likely that this planktic foraminifera percentage represents a mid to outer shelf environment.

The Coal Creek Formation indicates a similar age to the Amuri Limestone that was being deposited to the east. The depositional environment of the Amuri Limestone has been determined to be a basin setting indicating a slope environment. Dominance of *Cibicides sp.* and the inclusion of low concentrations of *Bolivina pupula* (2%) indicate a shallower environment than the Amuri Limestone. Trace fossil and grain size analysis of this facies

indicates a mid-outer shelf setting, as indicated by the species and benthic/planktic ratio in this chapter. This correlates with the mid-outer shelf interpretation of the glauconite and quartz-rich sandstone facies of the Coal Creek Formation in chapter 3.

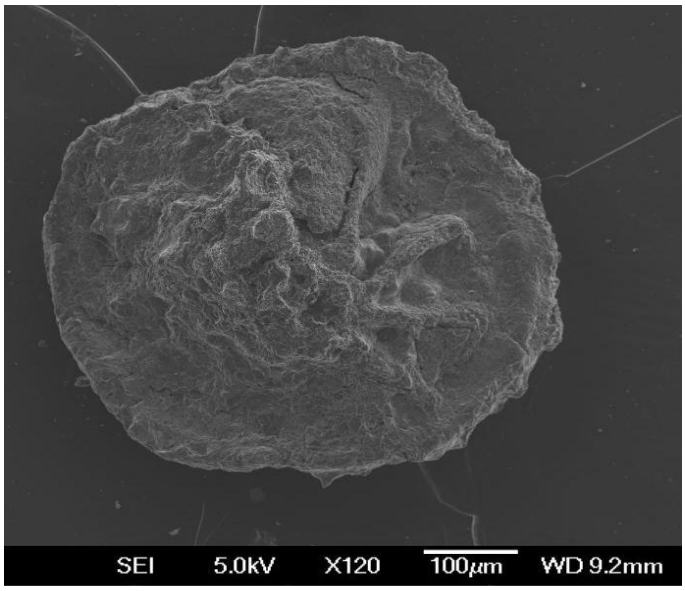

Figure 4.2- SEM image of *Cibicides parki,* from the Coal Creek Formation. Sample: 14,2 from Culverden back section.

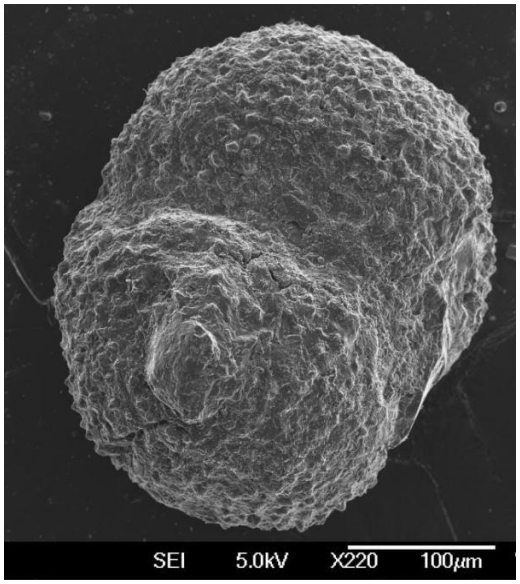

Figure 4.3- SEM image of *Globorotalia centralis,* from the Coal Creek Formation. Sample: 14,2 from Culverden back section.

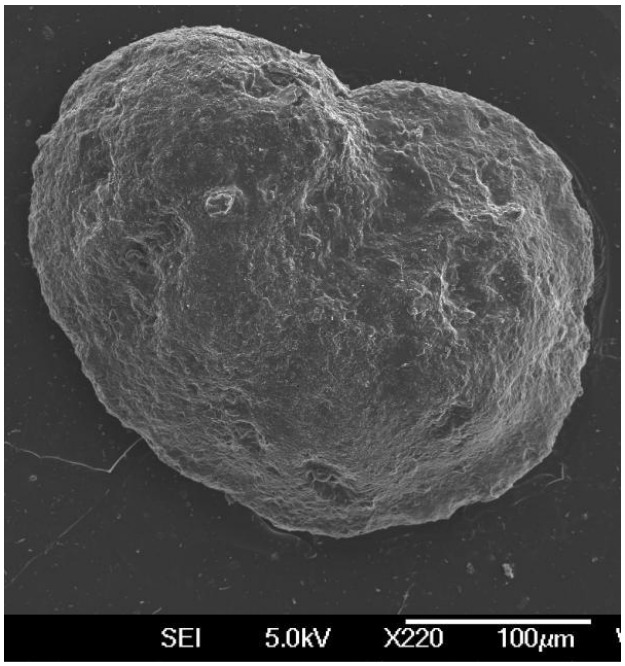

Figure 4.4- SEM image of *Cibicides vortex,* from the Coal Creek Formation. Sample: 14,2 from Culverden back section.

4.2.2 Flaxdown Limestone Member

The Flaxdown Limestone Member is a relatively well cemented, resistant unit. Only two samples (11,3b and 11,3t) from this unit were able to be processed for biostratigraphic purposes. The foraminifera obtained from these samples were of poor preservation with broken chambers and weathered tests. The two samples used for biostratigraphic analyses in this chapter are both from the Culverden backsection site (figure 3.24).

Sample 11,3b

This sample was collected 42 m from the base of the Culverden back section stratigraphic column (figure 3.24), from the Bryozoan and Algal-rich Grainstone facies. The assemblage from this sample consists entirely of benthic foraminifera. Of the foraminifera collected from this sample only 7% were not able to be identified down to species level. There were 7 benthic species identified to species level (table 4.2) in this sample. The most common benthic taxa identified are *Cibicides* (4 species, 67% of the sample) with the predominant species consisting of *Cibicides perforatus* (37%) and *Cibicides temperata* (23%). The other genera of high abundance is *Elphidium* (2 species, 24% of the sample), with both *Elphidium advenum* (21%) and *Elphidium charlottense* (3%) occurring in this sample.

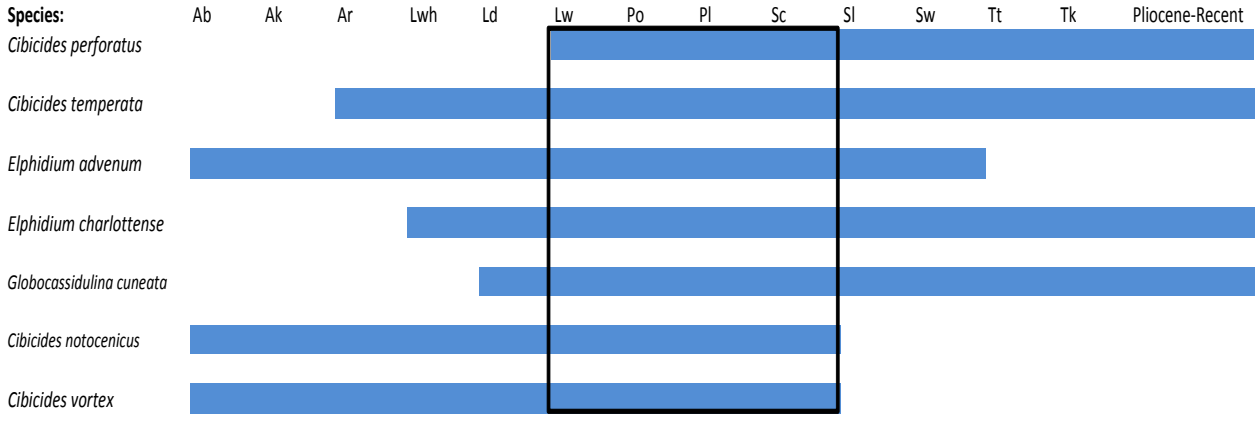

Table 4.2- Table constraining the age range of benthic foraminifera from sample 11,3b of the Flaxdown Limestone Member. Location: Culverden back section (figure 3.24). Raw data is shown in Appendix B.

Observed age range:

This samples age is constrained to *Waitakian* to *Clifdenian* stage (table 4.2) as it includes *Cibicides perforatus (Waitakian-Opoitian), Elphidium advenum* and *Cibicides notocenicus*

(Bortonian-Clifdenian) (Hornibrook *et al.,* 1989). This gives sample 11,3b an age range of 25.2-15.1 Ma.

Environmental indicators:

Sample 11,3b from the Bryozoan and Algal-rich Grainstone facies is defined by species *Cibicides perforatus* (37%) (figure 4.7), *Cibicides temperata* (23%) (figure 4.5), *Elphidium advenum* (21%)(figure 4.6) and *Elphidium charlottense* (3%). The combination of high percentages of *Cibicides* and *Elphidium* and the lack of planktic foraminifera (100% benthic sample) indicate a shallow shelf environment (Hayward *et al.,* 1999). *Elphidium* species present in this sample, *E. advenum* and *E. charlottense,* are found in shallow sheltered or exposed inner shelf environments. Although the occurrence of *C. temperata* suggests a deeper environment as this species commonly occurs in environments of mid to outer shelf (50-200 metres) (Hayward, 2004). The relative of abundance of both *C. temperata* and *E. advenum,* makes an exact environmental interpretation difficult. An environmental interpretation of inner to mid shelf depth could be identified when taking both *Elphidium* and *Cibicides* into consideration. A comparison of the environmental indicators in this chapter to the sedimentological and palaeontological features identified in chapter 3, indicate this sample may be slightly deeper than inner-mid shelf. A more suitable depth is mid shelf. It is possible that this sample is from a mid shelf environment and *Elphidium* specimen may have washed into the mid shelf. This correlates with the shelf interpretation of the Bryozoan and Algal-rich Grainstone facies that comprises the Flaxdown Limestone Member

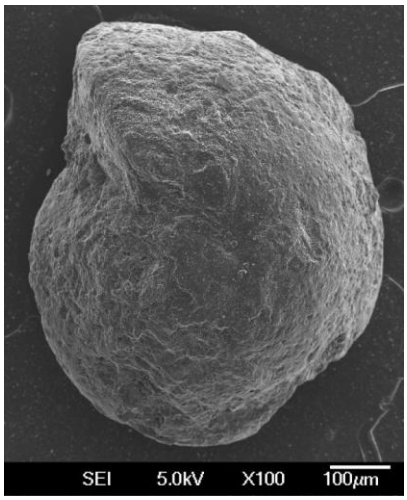

Figure 4.5- SEM image of *Cibicides temperata,* from the Flaxdown Limestone. Sample: 11,3b from Culverden back section.

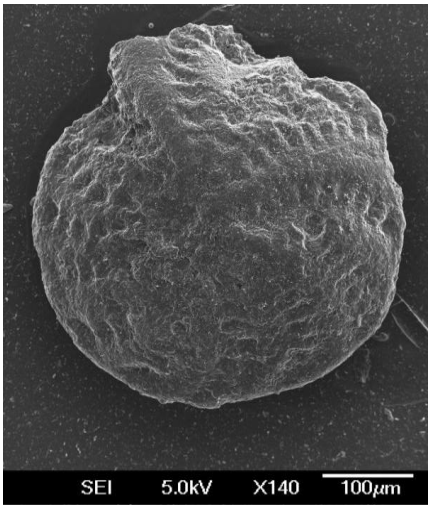

Figure 4.6- SEM image of *Elphidium advenum* from the Flaxdown Limestone. Sample: 11,3b from Culverden back section.

Sample 11,3t

This sample was collected 55 m from the base of the Culverden back section stratigraphic column (figure 3.24), from the Bryozoan and Algal-rich Grainstone facies. The assemblage from this sample consists entirely of benthic foraminifera. Of the foraminifera collected from this sample only 5% were not identified down to species level. There were 6 benthic species identified to species level (table 4.3) in this sample. The most common benthic taxa identified are *Cibicides* (4 species, 85% of the sample) with the predominant species consisting of *Cibicides temperata* (62%) and the occurrence of *Cibicides perforatus* (17%). The other genera of high abundance is *Elphidium* (1 species, 9% of the sample), with *Elphidium advenum* (9%) occurring in this sample.

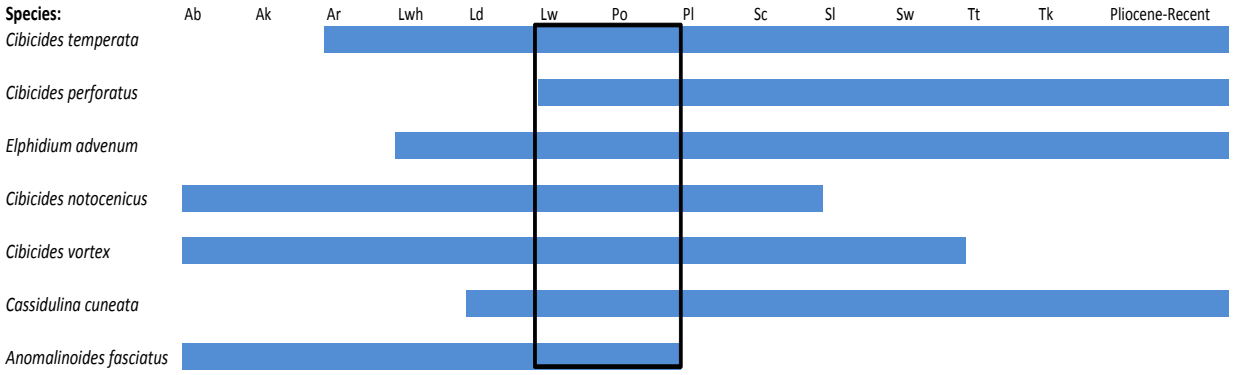

Table 4.3- Table constraining the age range of benthic foraminifera from sample 11,3t of the Flaxdown Limestone Member. Location: Culverden back section (figure 3.24). Raw data is shown in Appendix B.

Observed age range:

This samples age is constrained to the Waitakian to Otaian stage (table 4.3). The main foraminifera providing this unit with an age of Waitakian to Otaian stage include *Cibicides perforatus* (Waitakian-Opoitian), *Cassidulina cuneata, Cibicides notocenicus* and *Anomalinoides fasciatus* (Bortonian-Otaian) (Hornibrook *et al.,* 1989). This gives sample 11,3t an age range of 25.2-19 Ma.

Environmental indicators:

Sample 11,3t from the Bryozoan and Algal-rich Grainstone facies can be distinguished from 11,3b by a higher abundance of *Cibicides temperata* (62%). In contrast *Cibicides perforatus* (17%) is present in this sample in considerably lower abundance than sample 11,3b (table 4.3). The high abundance of *Cibicides temperata* in this sample and a lack of high *Elphidium*

percentages indicate a deeper shelf environment. This is reaffirmed by the fact that *C. temperata* commonly occurs in environments of mid to outer shelf (50-200 metres) (Hayward, 2004). *Elphidium advenum* (9%), *Cibicides vortex* (2%) and *Anomalinoides fasciatus* (1%) are typically inner shelf species, with their low abundance in this sample in association with high *C. temperata* occurrence suggesting a mid shelf environment**.** This mid shelf environment is reinforced by the lack of planktic foraminifera, suggesting a shallower environment than the outer shelf. A comparison of the environmental indicators interpreted in this chapter to the sedimentological features identified in chapter 3 correlate with a mid shelf environment.

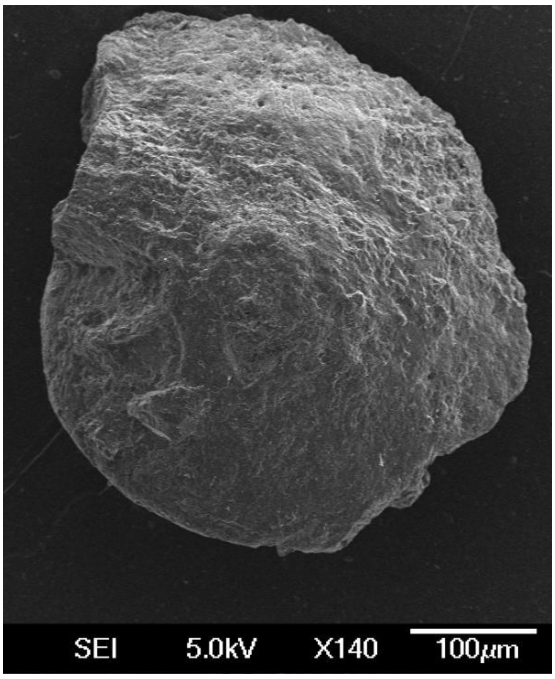

Figure 4.7- SEM image of *Cibicides perforatus,* from the Flaxdown Limestone. Sample: 11,3t from Culverden back section

4.2.3 Pahau Siltstone Member

The Pahau Siltstone Member provided the best foraminifera samples out of all of the units collected. These samples provided an abundance of foraminifera, but the preservation of these foraminifera was low. All Pahau Siltstone Member samples that were processed provided foraminifera. All of the foraminifera used to distinguish the environment and age of the Pahau Siltstone Member are from Cascade Downs (figure 3.22), as this was the only site where this unit was identified.

Sample 5,5b

This sample was collected at Cascade Downs, (see figure 1.1) 94 m from the base of the stratigraphic section (figure 3.22), within the Fossiliferous Sandstone facies. This assemblage consists solely of benthic foraminifera. Of the foraminifera collected 4 species were identified to species level, with only 3% of foraminifera not being identified to species level. The most common benthic species in this sample are *Notorotalia spinosa* (75%) and *Cibicides perforatus* (16%) (table 4.4).

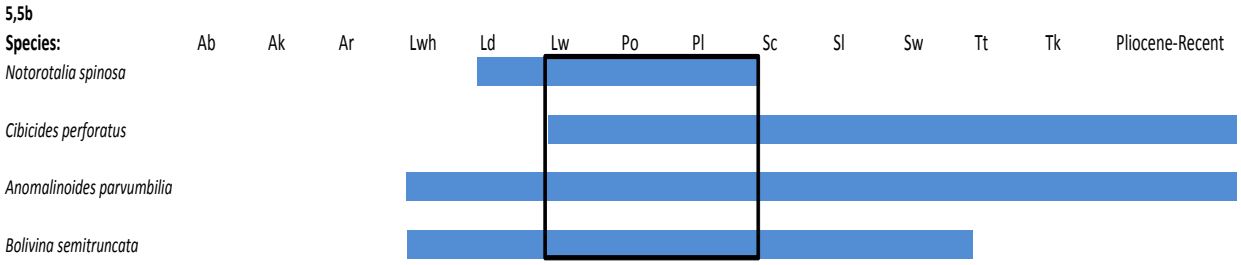

Table 4.4- Table constraining the age range of benthic foraminifera from sample 5,5b of the Pahau Siltstone Member. Location: Cascade Downs (figure 3.22). Raw data is shown in Appendix B.

Observed age range:

This samples age is constrained to the Waitakian to Altonian stage (table 4.4), based on the occurrence of *Cibicides perforatus* (Waitakian-Opoitian), and *Notorotalia spinosa* (Duntroonian-Altonian) (Hornibrook *et al.,* 1989). This gives sample 5,5b an age range of 25.2-15.9 Ma. When compared stratigraphically to the other Pahau Siltstone samples this age can be constrained to Waitakian to Otaian.

Environmental Indicators:

High abundances of *N. spinosa* are common in shelf environments and in combination with low abundance of *C. perforatus* possibly indicates a shelf environment as shallow as the the inner shelf (Hornibrook *et al.,* 1989). The correlation of foraminiferal indicator species and sedimentology and palaeontological studies undertaken in chapter 3 reinforce an inner shelf environment. Although the lack of high abundance of other inner shelf species such as *Zeaflorilus stachei* and *E. advenum* suggests this sample may be deeper than other samples.

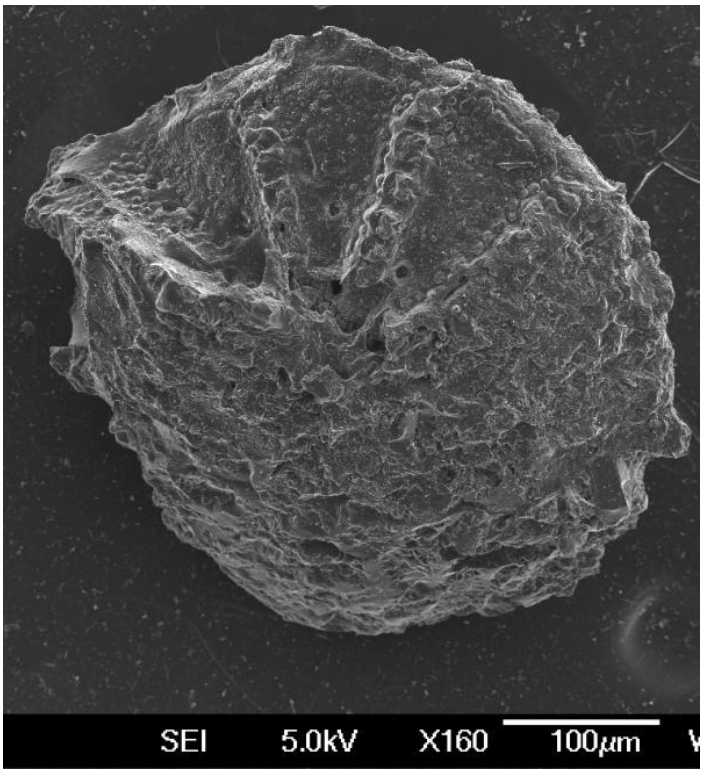

Figure 4.8- SEM image of *Notorotalia spinosa* from the Pahau Siltstone. Sample: 5,5b from Cascade Downs.

Sample 12,1b

This sample was collected at Cascade Downs, 99 m from the base of the stratigraphic section (figure 3.22), within the Fossiliferous Sandstone facies**.** This assemblage consists solely of benthic foraminifera**.** Of the foraminifera collected 4 species were identified to species level, with 21% of these foraminifera identified to genus level and 40% identified as benthic foraminifera. The most common benthic species in this sample is *Elphidium crispum* (32%) (table 4.5). Unidentified *Cibicides* (17%) specimens were also abundant. The remaining species only occurred in small abundances (<6%).

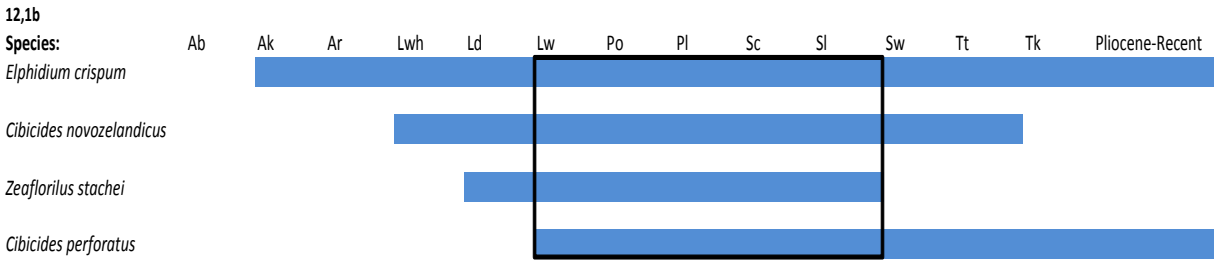

Table 4.5- Table constraining the age range of benthic foraminifera from sample 12,1b of the Pahau Siltstone Member. Location: Cascade Downs (figure 3.22). Raw data is shown in Appendix B.

Observed age range:

This samples age is constrained to the Waitakian to Lillburnian stage (table 4.5), based on the occurrence of *Cibicides perforatus* (Waitakian-Opoitian), *Cibicides novozelandicus* and *Zeaflorilus stachei* (Duntroonian-Lillburnian) (Hornibrook *et al.,* 1989). This gives sample 12,1b an age range of 25.2-12.7 Ma. When compared stratigraphically to the other Pahau Siltstone samples this age can be constrained to Waitakian to Otaian.

Environmental Indicators:

The high abundance of *Elphidium crispum* in this sample compared to any other species indicates a relatively shallow inner shelf environment, as *Elphidium crispum* is abundant in subtidal environments of 0-20 metres (Hayward *et al.,* 1997). This is reinforced by the combination of *C. perforatus, C. novozelandicus* and *Z. stachei,* which also indicate an inner shelf environment (Hornibrook *et al.,* 1989). A lower percentage of *Z. stachei* in these samples and its inclusion with deeper shelf genus *Cibicides* eliminates a depositional environment as shallow as the intertidal zone. The correlation of foraminiferal indicator species, the lack of planktic foraminifera, sedimentology and palaeontological studies undertaken in chapter 3 reinforce an inner shelf environment.

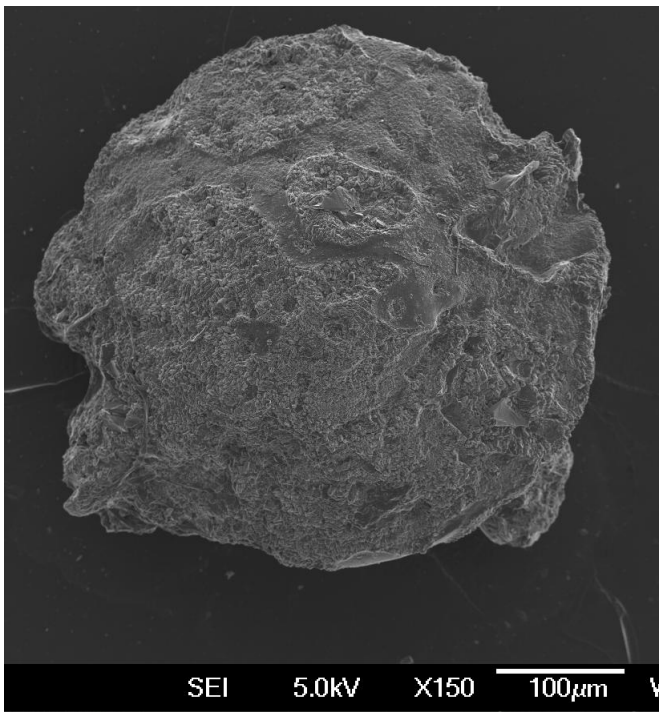

Figure 4.9- SEM image of *Elphidium crispum* from the Pahau Siltstone. Sample: 12,1b from Cascade Downs.

Sample 12,2,2.4m

This sample was collected at Cascade Downs, 112 m from the base of the stratigraphic section (figure 3.22) from the Quartz-rich Sandstone facies. The assemblage consists solely of benthic foraminifera. Of the foraminifera collected 7 species were identified to species level, with only 6% of foraminifera not being identified to species level, with 5% of these foraminifera identified to genus level and 1% identified as benthic foraminifera**.** The most common benthic taxa identified are *Cibicides* (2 species, 84% of the sample) with the predominant species being *Cibicides perforatus* (77%) (table 4.6). The remaining species only occurred in small abundances (<5%).

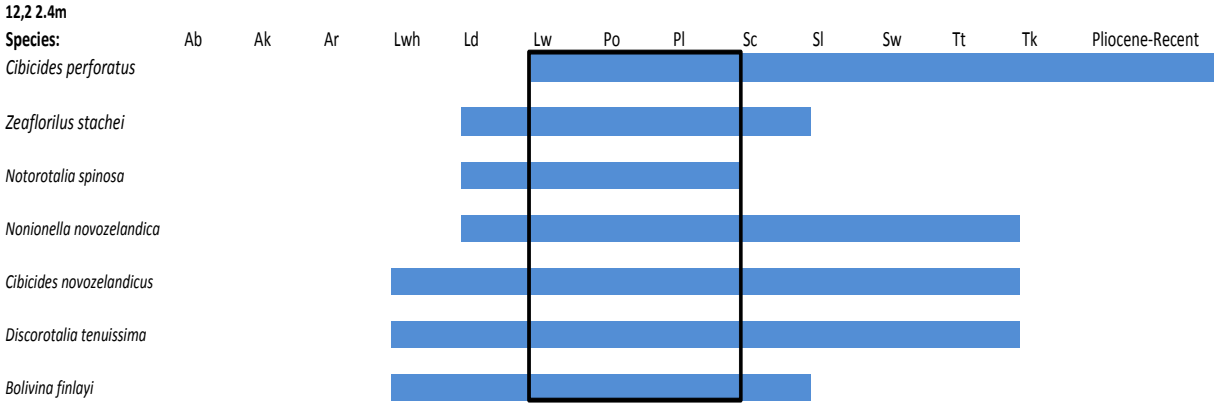

Table 4.6- Table constraining the age range of benthic foraminifera from sample 12,2 2.4m of the Pahau Siltstone Member. Location: Cascade Downs (figure 3.22). Raw data is shown in Appendix B.

Observed age range:

This samples age is constrained to the Waitakian to Altonian stage (table 4.6), based on the occurrence of *Cibicides perforatus* (Waitakian-Opoitian) and *Notorotalia spinosa* (Duntroonian-Altonian) along with *Z. stachei* and *B. finlayi* (Hornibrook *et al.,* 1989). This gives sample 12,2 2.4m an age range of 25.2-15.9Ma. When compared stratigraphically to the other Pahau Siltstone samples this age can be constrained to Waitakian to Otaian.

Environmental Indicators:

High abundances of *N.spinosa* and *Z.stachei* are most common in the inner shelf, with the combination of *C. perforatus, C. novozelandicus* and *Z. stachei* reinforcing an inner shelf environment (Hornibrook *et al.,* 1989). This sample is located in the inner shelf. The correlation of foraminiferal indicator species, the lack of planktic foraminifera,

sedimentology and palaeontological studies undertaken in chapter 3 reinforce an inner shelf environment.

Sample 5,6f

This sample was collected from Cascade Downs, 118 m from the base of the stratigraphic section (figure 3.22) within the Quartz-rich Sandstone facies**.** This assemblage consists solely of benthic foraminifera**.** Of the foraminifera collected 8 species were identified to species level, with 24% of foraminifera not being identified to species level (21% of these foraminifera identified to genus level and 3% identified as benthic foraminifera)**.** The most common benthic taxa identified are *Cibicides* (4 species, 58% of the sample) with the predominant species being *Cibicides novozelandicus* (23%), *Cibicides vortex* (13%) and *Cibicides temperata* (12%) (table 4.7). The remaining species only occurred in small abundances (<7%).

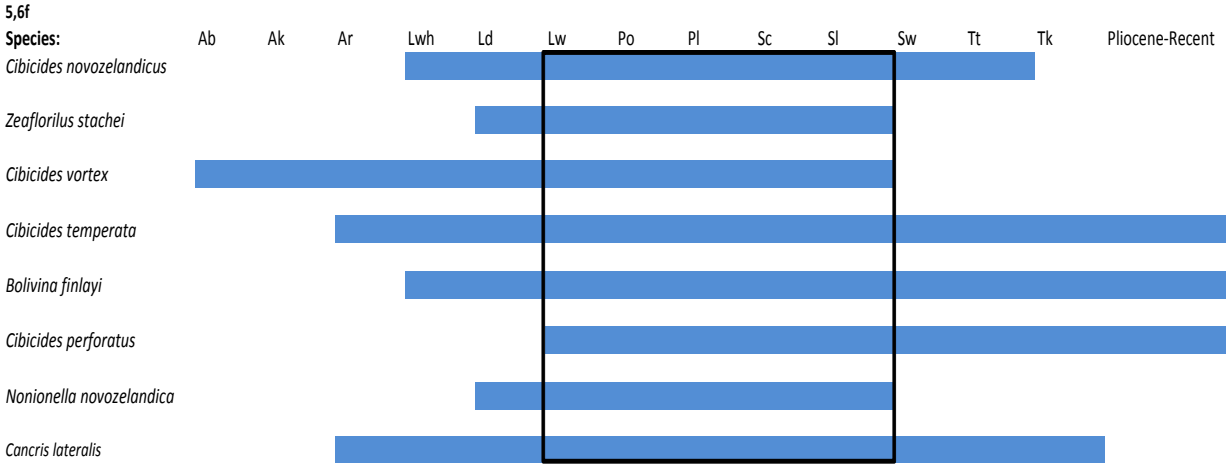

Table 4.7- Table constraining the age range of benthic foraminifera from sample 5,6f of the Pahau Siltstone Member. Location: Cascade Downs (figure 3.22). Raw data is shown in Appendix B.

Observed age range:

This samples age is constrained to the Waitakian to Lilliburnian stage (table 4.3) based on the occurrence of *Cibicides perforatus* (Waitakian-Opoitian), *Cibicides vortex* (Bortonian-Lillburnian), *Z. stachei* and *N. novozelandica* (Hornibrook *et al.,* 1989). This gives sample 5,6f an age range of 25.2-12.7 Ma. When compared stratigraphically to the other Pahau Siltstone samples this age can be constrained to Waitakian to Otaian (see figure 4.11).

Environmental Indicators:

The combination of *C. perforatus, C. novozelandicus* and *Z. stachei* in this sample indicate an inner shelf environment (Hornibrook *et al.,* 1989). Low abundances (<7%) of other inner shelf species are present in this sample including *Cibicides vortex* (13%) common at 5-50 metres depth (Hornibrook *et al.,* 1989). The correlation of foraminiferal indicator species, the lack of planktic foraminifera, sedimentology and palaeontological studies undertaken in chapter 3 reinforce an inner shelf environment.

Sample 12,3b

This sample was collected at Cascade Downs, 122 m from the base of the stratigraphic section (figure 3.22) within the Fossiliferous Sandstone facies. This assemblage consists solely of benthic foraminifera. Of the foraminifera collected 11 species were identified to species level, with only 8% of foraminifera not being identified to species level, with 4% of these foraminifera identified to genus level and 4% identified as benthic foraminifera**.** The most common benthic species identified is *Notorotalia spinosa* (39%), *Zeaflorilus stachei* (15%) and *Cibicides perforatus* (12%) (table 4.8). The remaining species only occurred in small abundances (<6%)**.**

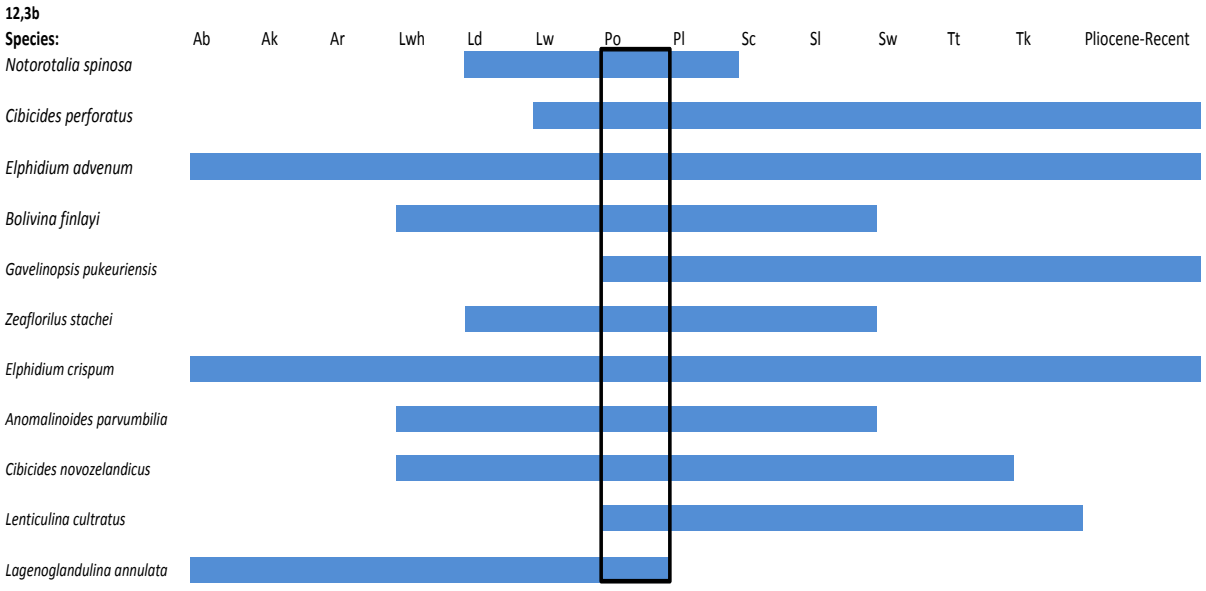

Table 4.8- Table constraining the age range of benthic foraminifera from sample 12,3b of the Pahau Siltstone Member. Location: Cascade Downs (figure 3.22). Raw data is shown in Appendix B.

Observed age range:

This samples age is constrained to the Otaian stage (table 4.8) based on the occurrence of *Gavelinopsis pukeuriensis* (Otaian-Recent), *Lenticulina cultratus, Z. stachei, N. spinosa* and *Lagenoglandulina annulata* (Bortonian-Otaian) (Hornibrook *et al.,* 1989). This gives sample 12,3b an age range of 21.7-19 Ma.

Environmental Indicators:

The high abundances of *N. spinosa* and *Z. stachei* seen in this sample are common in inner shelf environments (Hornibrook *et al.,* 1989). The combination of *C. perforatus, C. novozelandicus* and *Z. stachei* also suggest this sample is from an inner shelf environment, although a lower percentage of *Z. stachei* in these samples and its occurrence with deeper marine *Cibicides* eliminates an inner shelf depositional environment as shallow as the intertidal zone (Hornibrook *et al.,* 1989). The correlation of foraminiferal indicator species, the lack of planktic foraminifera, sedimentology and palaeontological studies undertaken in chapter 3 reinforce an inner shelf environment.

Sample 12,5

This sample was collected at Cascade downs, 139 m from the base of the stratigraphic section (figure 3.22) within the Fossiliferous Sandstone facies. This assemblage consists solely of benthic foraminifera. Of the foraminifera collected all 9 were identified to species level. The most common benthic species in this sample are *Zeaflorilus stachei* (68%), *Notorotalia spinosa* and *Cibicides perforatus* (9%) (table 4.9). The remaining species only occurred in small abundances (<4%).

Table 4.9- Table constraining the age range of benthic foraminifera from sample 12,5 of the Pahau Siltstone Member. Location: Cascade Downs (figure 3.22). Raw data is shown in Appendix B.

Observed age range:

This samples age is constrained to the Waitakian to Otaian stage, (table 4.9) based occurrence of *Cibicides perforatus* (Waitakian-Opoitian), *Bulimina senta, Notorotalia spinosa* and *Glandulina symmetrica* (Bortonian-Otaian) (Hornibrook *et al.,* 1989). This gives sample 12,5 an age range of 25.2-19 Ma**.** When compared stratigraphically to the other Pahau Siltstone samples this age can be constrained to the Otaian.

Environmental Indicators:

As with sample 12.3b the high abundances of *N. spinosa* and *Z. stachei* seen in this sample are common in the inner shelf. The combination of inner shelf assemblages *C. perforatus* and *Z. stachei* are also seen in this Pahau Siltstone sample (Hornibrook *et al.,* 1989). The correlation of foraminiferal indicator species, the lack of planktic foraminifera, sedimentology and palaeontological studies undertaken in chapter 3 reinforce an inner shelf environment.

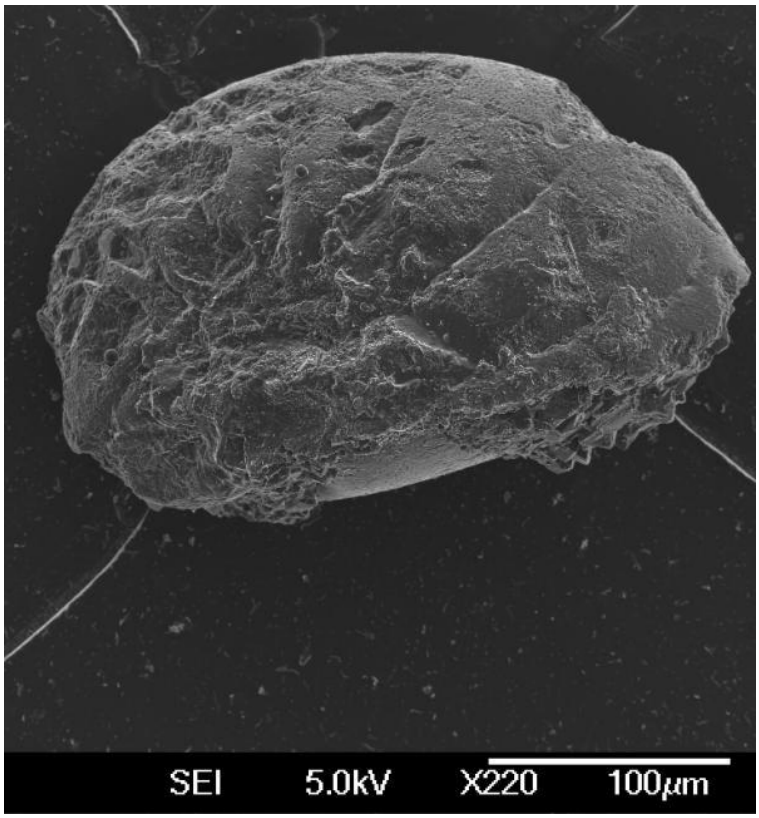

Figure 4.10- SEM image of *Zeaflorilus stachei* from the Pahau Siltstone. Sample: 12,5 from Cascade Downs.

Sample 5,6a

This sample was collected at Cascade Downs, 156 m from the base of the stratigraphic section (figure 3.22) within the Quartz-rich Sandstone facies. This assemblage consists solely of benthic foraminifera. Of the foraminifera collected 5 species were identified to species level, with 14% of foraminifera not being identified to species level, with 6% of these foraminifera identified to genus level and 8% identified as benthic foraminifera. The most common benthic taxa identified are *Cibicides* (4 species, 85% of the sample) with the predominant species being *Cibicides perforatus* (43%) and *Cibicides temperata* (35%) (table 4.10). The remaining species only occurred in small abundances (<6%).

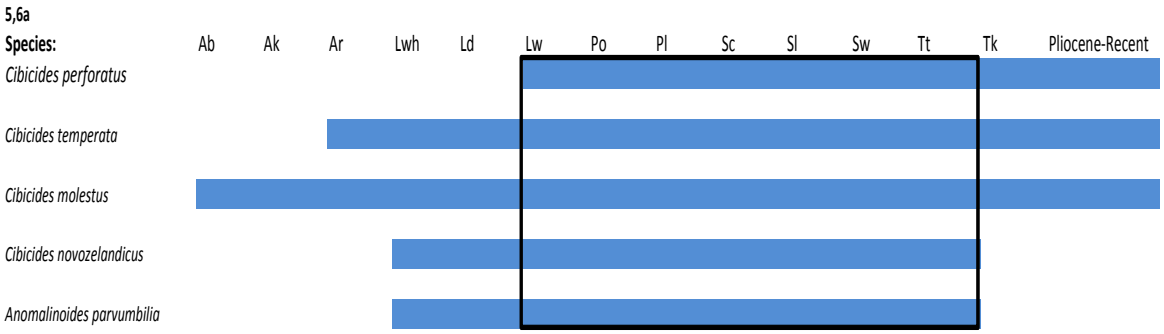

Table 4.10- Table constraining the age range of benthic foraminifera from sample 5,6a of the Pahau Siltstone Member. Location: Cascade Downs (figure 3.22). Raw data is shown in Appendix B.

Observed age range:

This samples age is constrained to the Waitakian to Tongaporutuan stage (table 4.10) based on the occurrence of *Cibicides perforatus* (Waitakian-Opoitian), *Cibicides novozelandicus* (Whaingaroan-Tongaporutuan) and *Anomalinoides parvumbilia* (Whaingaroan-Tongaporutuan) (Hornibrook *et al.,* 1989). This gives sample 5,6a an age range of 25.2-6.5Ma. Due to the fact that this sample is stratigraphically the youngest sample, the age can only be constrained to Otaian to Tongaporutuan.

Environmental indicators:

This sample contains slightly different foraminiferal assemblages to the previous six Pahau Silstone samples. The occurrence of *C. temperata* suggests a deeper environment as this species commonly occurs in environments of mid to outer shelf (50-200 metres) (Hayward, 2004). Although the predominance of *C. perforatus* over *C. temperata* represents a shallower environment than the mid-outer shelf setting *C. temperata* is commonly found in. A likely depth range for these samples is inner to mid shelf. This sample does not fully

correlate with the inner shelf environment, obtained from sedimentological and palaeontological interpretations in chapter 3. As this sample is the youngest stratigraphically it could be suggested that there was a change in environment.

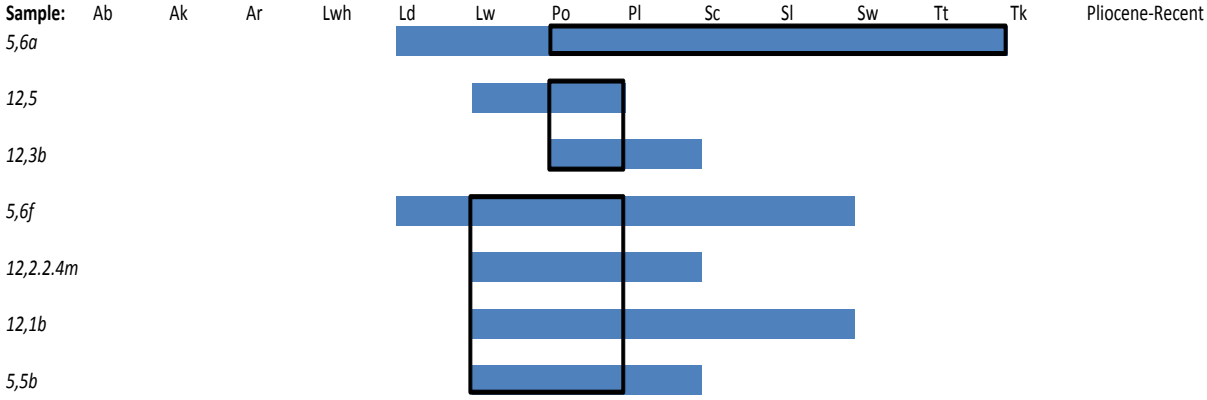

Table 4.11- Correlation of the age of foraminifera from the Pahau Siltstone Member. Location: Cascade Downs.

Observed age range of Pahau Siltstone Member:

The Pahau Siltstone Member biostratigraphy combines foraminiferal data from 7 samples (table 4.11). The youngest sample from this unit is 5,6a but this sample is not well constrained, with an age of Otaian to Tongaporutuan stage. Samples 12,5 and 12,3b being younger are constrained by the age of sample 12,3b and are Otaian stage (21.7-19 Ma). The oldest samples from Cascade Downs, samples 5,5b to 5.6f can be constrained to the Waitakian to Otaian stage (21.7-19 Ma).

Summary

In this chapter, ten samples from three units were used to provide age and palaeoenvironmental data. In a number of samples the preservation quality of specimens was poor, making it difficult to identify specimens down to species level, resulting in a poorly constrained age range. The age ranges from these Tertiary units were constrained to the Runangan for sample 14,2 from the Coal Creek Formation, Waitakian to Clifdenian for sample 11,3b and Waitakian to Otaian 11,3t of the Flaxdown Limestone and Waitakian to Tongaporutuan (table 4.11) for the Pahau Siltstone Member. Palaeoenvironments determined from environmental indicators in this chapter generally correlate with environments interpreted in chapter 3.

5. Diagenesis

5.1 Introduction

This chapter will outline the processes and theory of diagenesis and present the results of petrographic analysis of Mandamus-Pahau District rocks. There are a number of diagenetic processes occurring on carbonate sediments and rocks, these include: micritization, dissolution and cementation, compaction, dolomitization and the replacement of carbonate grains and matrix (Flugel, 2004). These diagenetic processes are controlled by a number of factors including mineralogy and chemistry of the carbonates, pore water chemistry, dissolution, rate of precipitation, pore space and grain size. The primary cements of the samples within this thesis consist of calcite with the following chapter covering carbonate diagenesis.

Dissolution

Dissolution occurs due to the undersaturation of carbonate in pore fluids, leading to dissolution of metastable carbonate grains and cements (Flugel, 2004). Dissolution is prominent in shallow meteoric environments, in deep burial or cold and deep sea environments where sea water is undersaturated with respect to calcite or aragonite (Flugel, 2004).

Neomorphism

Neomorphism refers to processes incorporated in replacement and recrystallisation that have led to a change in the mineralogy of a unit. Instead of just referring to change in crystal size neomorphism considers replacement textures (Tucker and Bathurst, 1990). One of the main forms of neomorphism is the replacement of fine grained limestones by coarser crystalline cement (Tucker and Bathurst, 1990). Calcitisation is an important neomorphic process by which aragonite is replaced by calcite (Tucker and Bathurst, 1990).

Cementation

Cementation is the filling of pore spaces with carbonates among other minerals. Alteration of original bioclasts or marine cements within carbonate samples is one of the most common processes leading to the isotopic change of a marine carbonate (Sharp, 2007). Cemented carbonates combine the unaltered original carbonate and a new cemented

carbonate. This cementation process can occur in primary or secondary pore spaces, due to the saturation of pore fluids with respect to the cemented mineral (Flugel, 2004). The precipitation of cement is controlled by factors including pore fluid composition, water energy, porosity of the sediment/rock, oversaturation or under saturation and Mg/Ca ratios influencing the growth of crystals (Flugel, 2004). Aragonite marine cements and aragonite bioclasts may be altered during burial. In carbonates it is likely the oldest cements occur in a marine setting in equilibrium with ocean water, although deep or cool-water carbonates may not contain marine cements (Sharp, 2007). Buiral cements are more likely to be stable low-Mg calcite that is less prone to recrystallisation at a later stage, therefore retaining the original isotopic signature (Sharp, 2007). Cements are therefore more likely to provide information on the genuine isotopic composition of the crystallisation environment at the time of creation i.e pore fluids in burial or seawater. However paragenesis is used to determine the origin of cements in order to determine the source of isotopic signatures.

Compaction and pressure solution

These processes occur mostly at depth with overburden of sediments increasing the temperature and pressure placed on the sediment. Compaction and pressure solution, can lead to stylolitization; a chemical process that occurs due to the overburden of sediments, increasing pressure and temperature conditions during burial (Flugel, 2004). Stylolitization leads to a decrease in unit volume, altering the characteristics of the unit's primary fabric. Chemical compaction seen in dissolution seams is often characterised by a zigzag pattern, varying due to solubility levels of the different components within the unit.

5. 2 Diagenetic Environments

Diagenetic environments are divided into surface or subsurface zones which are characterised by different diagenetic processes (Flugel, 2004). The criteria that characterise these environments include cement types and fabrics. The three main zones of diagenesis include: meteoric, marine and burial diagenesis (Flugel, 2004).

5.2.1 Meteoric diagenesis

Meteoric diagenesis is not just limited to shallow surface areas, due to the division of meteoric diagenesis into vadose (above the water table) and phreatic (below) environments (figure 5.1). The vadose zone (figure 5.1) is characterised by freshwater diagenesis, with the

concentration of water at grain contacts (Flugel, 2004). This zone consists of pores not only filled with water but also water vapour and air, with water held in place by capillary forces (Tucker and Bathurst, 1990). Cements created in this zone are generally low magnesium calcite, due to the low Mg/Ca ratio of pore waters (Tucker and Bathurst, 1990).

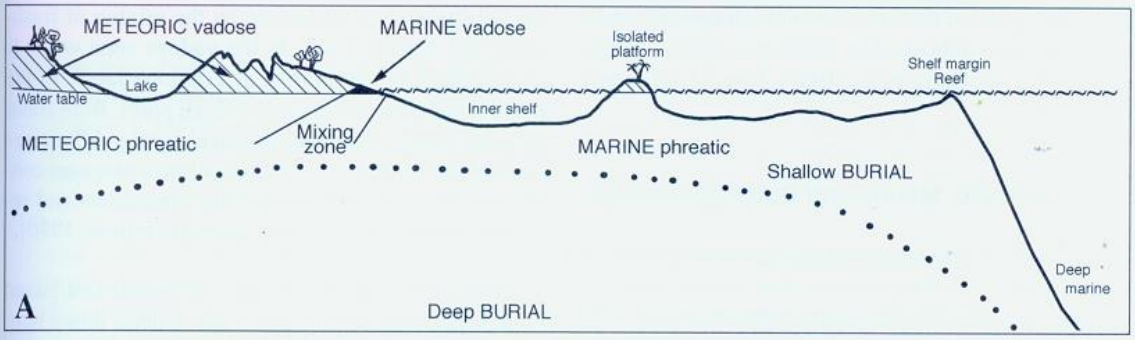

Diagenetic environment	Location	Pore Filling	Processes	~ Time needed
Meteoric vadose environment	Above water table, between land surface and meteoric phreatic zone	Pores filled with freshwater and/ or air	*Solution zone* (soil): Extensive solution; removal of aragonite; formation of vugs. *Precipitation zone* (near surface): Minor cementation	10^3 - 10^5 years
Meteoric phreatic environment	Below water table, may tend downwards 100s of meters	Pores filled with freshwater	*Solution zone* (e.g. sinkholes, caves): Solution; formation of molds and/or vugs. *Active zone* (upper part of meteoric phreatic environment): Dissolution of aragonite and Mg-calcite; rapid and diverse cementation; precipitation of calcite; creation of molds and vugs. *Stagnant zone* (deeper part and in arid climates): Little cementation; stabilization of aragonite and Mg-calcite	10^3 -10^5 up to 10^6 - 10^7 years
Marine phreatic environment	On the shallow or deep sea floor or just below	Pores filled with marine water	*Shallow-marine environment:* Waters oversaturated with respect to $CaCO_3$; rapid cementation by aragonite and Mg-calcite; diverse cement types. *Deep-marine and cold-water environments:* Waters undersaturated with respect to $CaCO_3$; strong dissolution of aragonite and calcite at two dissolution levels	10^1 - 10^4 years
Burial environment B	Subsurface beneath reach of surface-related processes, down to realm of low-grade metamorphism. May tend downwards 1000s of meters	Pores filled with brines of varying salinity, from brackish to highly saline	*Shallow burial* (first few meters fo tens of meters) and *deeper burial* (sediment overburden of hundreds to thousands of meters): Physical compaction; chemical compaction (pressure solution); cementation; porosity reduction	10^6 -10^8 years

Figure 5.1- Major diagenetic environments. A) Simplified environmental diagram, B) List of the major processes that occur in different diagenetic environments, including the location, pore filling and time (Flugel, 2004).

The phreatic zone (figure 5.1) consists of pores completely filled with water (Tucker and Bathurst, 1990). The extent of this zone depends on rainfall, hydrostatic head and permability of the surrounding sediments (Tucker and Bathurst, 1990). Clear equant spar is most common in the phreatic zone with syntaxial overgrowth occurring on echinoderm

material and other bioclasts (Tucker and Bathurst, 1990). Calcite spar is generally mostly non-ferroan in the early growth stages, whereas more stagnant zones produce ferroan and manganoan calcite (Tucker and Bathurst, 1990).

5.2.2 Marine Diagenesis

Diagenesis within the marine realm takes into consideration the phreatic environment, located on the shallow or deep sea-floor as well as beaches and tidal flats (Flugel, 2004). Marine carbonate diagenesis occurs in both areas of high energy with seawater being pumped through porous sediments. This form of diagenesis also occurs in less turbulent, protected areas of the marine realm, with less intensive processes such as local precipitation instead of cementation taking place (Tucker and Bathurst, 1990). Micritization can also occur in quieter regions in the marine environment, with micrite formation taking place around bioclasts (Tucker and Bathurst, 1990). Cements characteristic of shallow marine diagenesis include Mg-calcite and aragonitic cements (Choquette and James, 1990). The morphological characteristics of these cements include: micrite, fibrous to bladed rinds, blocky or equant crystals and epitaxial crystals (Choquette and James, 1990). These marine cements are generally precipitated from seawater in near isotopic equilibrium, therefore the isotopic composition depends on the seawater chemistry at the time of cementation (Tucker and Bathurst, 1990). If this isotopic signature is not altered during burial, a record of ancient seawater isotope chemistry may be obtained. The rate of carbonate supply as well as the precipitation of aragonite or high Mg-calcite control calcite mineralogy in the cement (Tucker and Bathurst, 1990).

5.2.3 Burial Diagenesis

Burial diagenesis is divided into two zones depending on depth; shallow burial and deep burial, although exact depths are not defined for these zones (figure 5.1)(Flugel, 2004). The shallow burial zone is from a few metres to tens of metres depth in the sedimentary profile (Flugel, 2004). This burial environment is affected by changes in pore water chemistry from the mixing zone (meteoric and marine water mixing), temperature and pressure controls (Flugel, 2004). Cementation in the shallow burial zone can occur in weakly derived marine waters that are generally only slightly reducing, if not oxic (Flugel, 2004).

Deep burial diagenesis occurs where pore water has become more saline and therefore acts in a reducing manner (Flugel, 2004). This reducing environment tends to mobilise redox sensitive elements, including Mn and Fe, incorporating them into calcite or saddle dolomite cements (Flugel, 2004). There are a number of processes that Flugel (2004) includes in the definition of the deeper burial environment, these include:

- *Compaction due to sediment overburden*, therefore reducing the thickness, porosity and permeability of sediments, leading to distortion of grains and fabrics.
- *Chemical compaction* (commonly occurring at several hundreds and thousands of metres or overburdens of 100-200 metres) has a similar effect on features as compaction, as well as producing stylolites and other pressure solution features.
- *Cementation* producing coarse calcite spar cements. These cements are generally enriched in Fe and Mn, commonly with calcite mosaics and dolomite.

5.3 Mineralogy

Diagenesis is change that occurs during lithification and post deposition, encompassing physical, chemical and biological processes (Flugel, 2004). The main minerals involved in carbonate diagenesis are aragonite and Mg-calcite, followed by low-Mg calcite and dolomite (Flugel, 2004). The mineralogical composition of carbonates controls the vulnerability of the rock to alteration during diagenesis. Sediments consisting of both high magnesian calcite and/or low magnesian calcite have a lower potential for diagenesis, whereas aragonitic sediments have a high dissolution potential (Flugel, 2004).

There are a number of impurities or trace elements that can be incorporated within calcite. Ferroan calcite occurs as cement, as well as filling cracks, replacing calcite matrices and aragonitic or magnesian calcite skeletons. Cements of ferroan calcite composition often occur as a function of late diagenesis and may indicate reducing conditions from deep burial (Flugel, 2004). Ferroan calcite is more likely to form in a deep burial setting in more reducing conditions as shallow settings favour oxidation (Flugel, 2004). Calcite that contains ferrous iron, named ferroan calcite, can be distinguished from non-ferroan calcites by staining with potassium ferricyanide (Flugel, 2004). This chapter reviews standard optical petrography, field observations and alizarin red-s staining for diagenetic analyses.

5.4 Results of Petrographic Analysis

A number of samples that were analysed in chapters 3 and 4 were stained with Alizarin red-S solution. In combination with petrographic and field observations, samples were analysed in terms of diagenetic processes and paragenesis involved in their deposition and alteration.

5.4.1 Coal Creek Formation

The Coal Creek Formation appears relatively unaffected by diagenesis in thin section samples. Carbonate cement is not visible in sample 3,12 from Cascade Downs, with the matrix consisting of mud and hydrothermally altered fibrous cements (Figure 5.2). Spar cements such as blocky calcite and microgranular burial cements. Spar cements can be seen in samples from Glens of Tekoa (5,2a and 4,10.3) (figure 3.3).

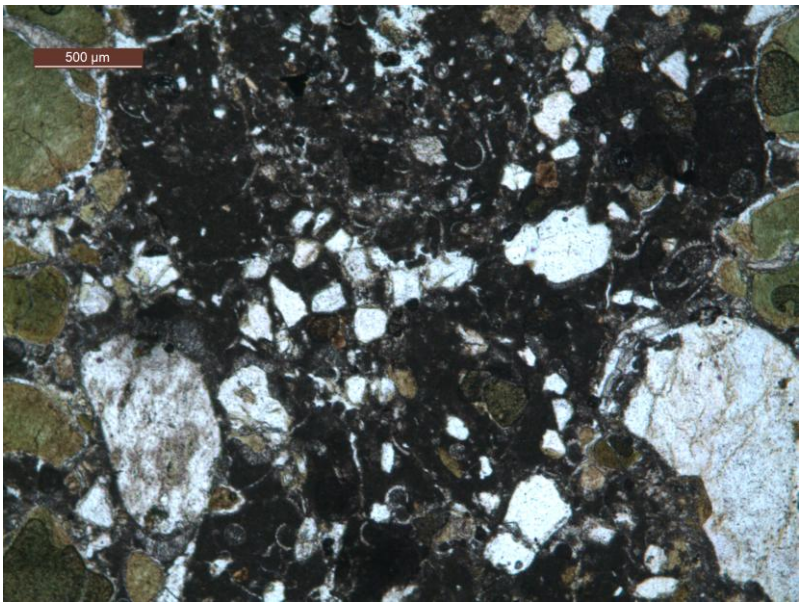

Figure 5.2- The Coal Creek Formation from Cascade Downs (sample: 3,12). The quartz grain in the bottom left shows fibrous cements on the top and bottom due to the inclusion of hydrothermal fluids.

Paragenesis of the Coal Creek Formation follows the order:

1. Deposition of glauconite, bioclasts, quartz and mud.
2. Burial of the unit.
3. Inclusion of hydrothermal fluids in pore spaces and the development of fibrous cements. Fibrous cements developed on the top and bottom of quartz and glauconite grains (figure 5.2).

4. the creation of blocky and microgranular calcite burial cement in samples 5,2a and 4,10.3

Interpretation

This unit has undergone burial diagenesis**.** It is likely the fibrous cements are the product of hydrothermal fluids. Hydrothermal fluids linked with the overlying Cookson Volcanic basalts may have been incorporated into the pore fluids of the Coal Creek Formation. The Coal Creek Formation varies in different locations. At the Glens of Tekoa the unit contains sparite cement, indicating it has undergone burial diagenesis.

5.4.2 Flaxdown Limestone Member

The Flaxdown Limestone Member contains the most evidence of diagenetic alteration**.** Burial diagenesis is visible in thin sections with differentiation between ferroan calcite and non-ferroan calcite cements. In petrographic slides Flaxdown Limestone samples consist of bioclasts surrounded by a thin film of fibrous marine cements and development of central blocky ferroan calcite cements (figure 5.3b and d)**.** Identified bioclasts within the Flaxdown Limestone are generally calcitic in origin in the Bryozoan and Algal-rich Grainstone Facies with coralline red algae, foraminifera, bryozoans and brachiopods occurring. Whereas the Molluscan-rich Grainstone facies consists of mostly aragonitic molluscs and low percentages of calcitic bioclasts such as bryozoan and foraminifera, making the unit more susceptible to alteration during diagenesis. Paragenesis of the Flaxdown limestone follows the order:

1. The deposition of bioclasts and matrix (figure 5.4a-d).
2. Creation of sparse marine cements.
3. Deep burial of the marine sediments (> 100m), leading to the formation of coarse, mosaic calcite, burial cements. These cements consist of ferroan calcite (figure 5.3b).
4. Stylotilisation is a prominent diagenetic feature due to chemical compaction and pressure solution at depth. Styolites are visible at the Glens of Tekoa site in the field area. These deep burial diagenetic features occur in bands 1.5cm to 2 cm in size and grade into weakly developed stylolite bands of 2 to 3 cm in size.

Interpretation

The development of stylolites is a large scale feature of pressure dissolution with minor features seen in petrographic analyses of the Flaxdown Limestone. These include compaction of sediments with deformation features visible in some bioclasts. Plastic deformation is seen with a number samples from the Bryozoan and Algal-rich Grainstone facies from the Glens of Tekoa in the form of squashed bioclasts. These compression structures are visible throughout thin sections of the Flaxdown Limestone.

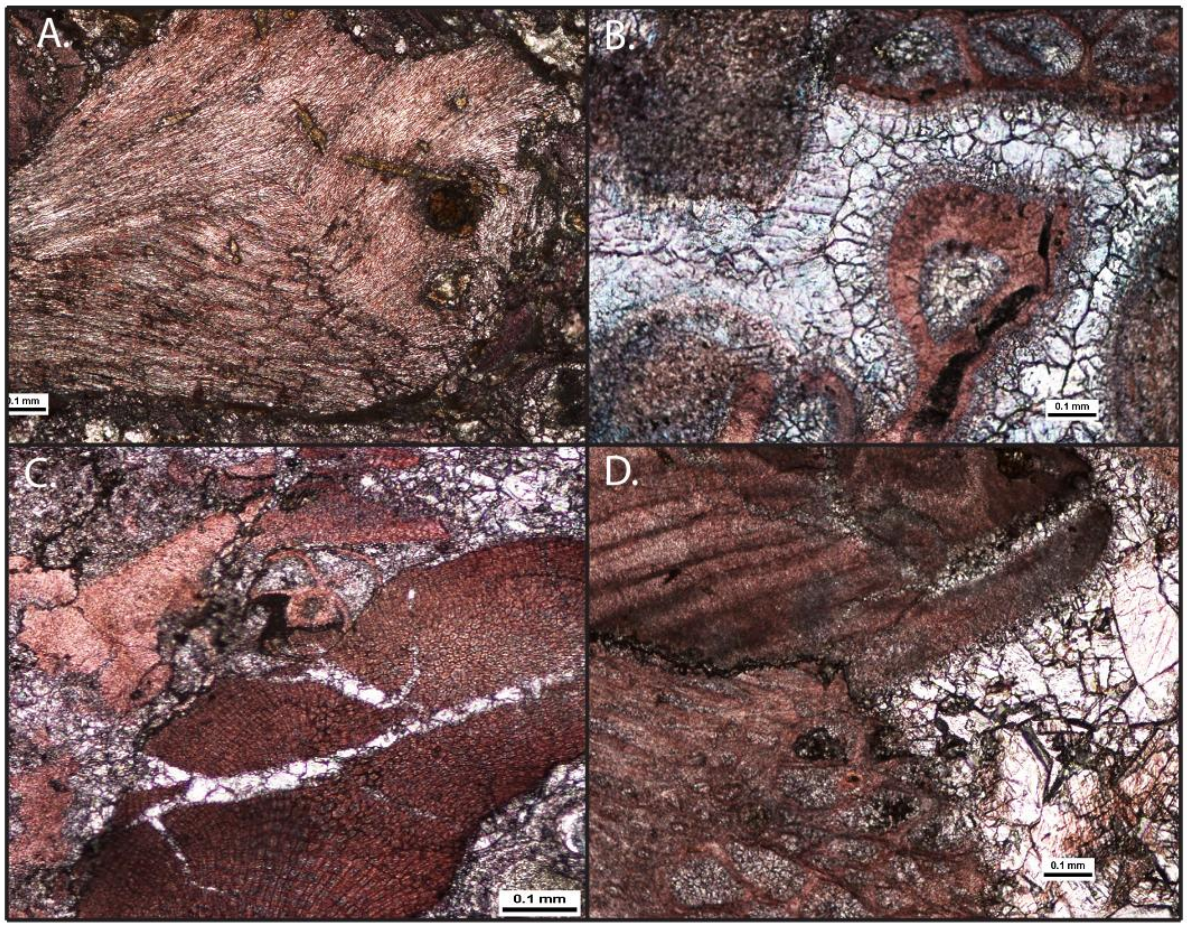

Figure 5.3- Variations of cements and minerals within the Flaxdown Limestone Member. A) Brachiopod, B) Ferroan calcite (blue tint) burial cement, C) Calcite cement within cracks in coralline red algae, D) Blocky cement alongside bioclasts.

Samples: **A**: 9,3 location: Pahau Downs **B:** 4,3 location: Glens of Tekoa **C:** 4,3 **D:** 14,12 location: Culverden back section.

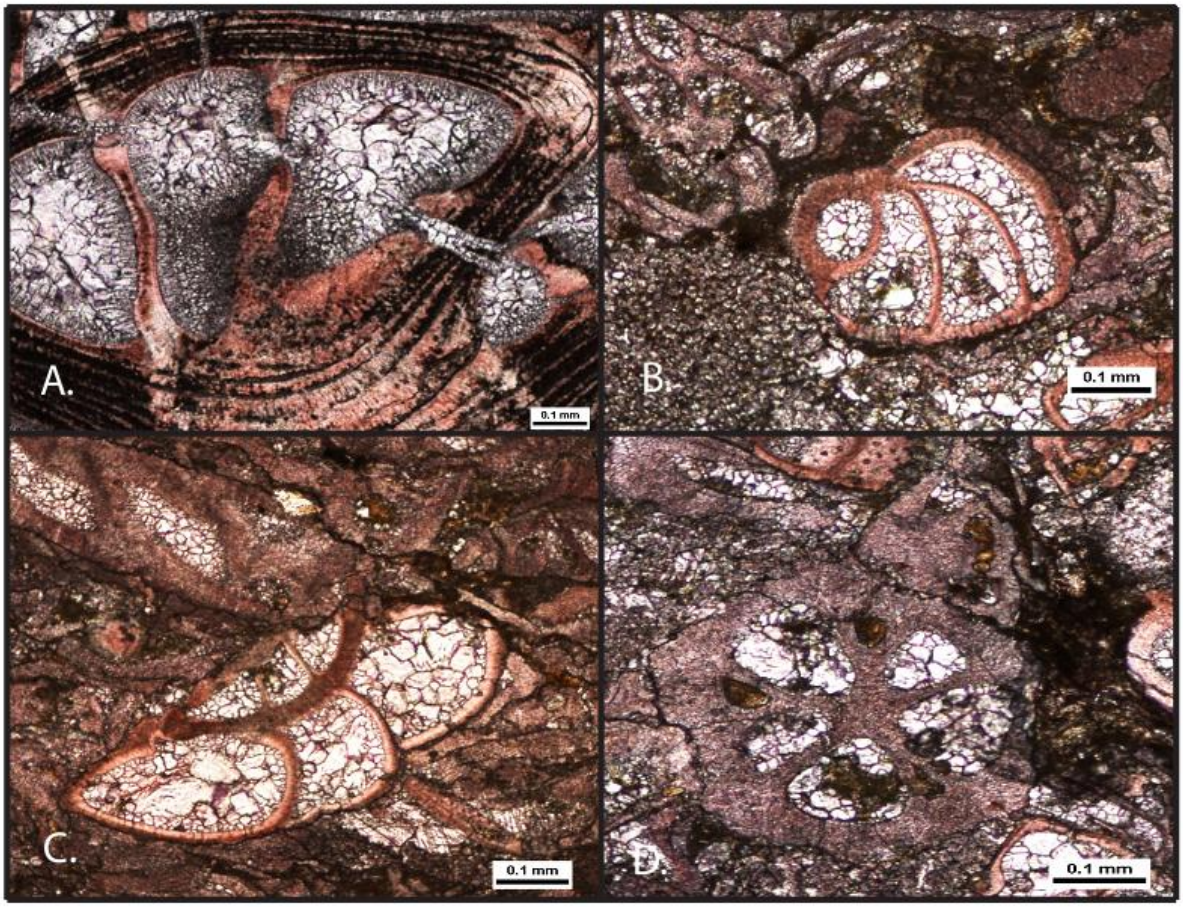

Figure 5.4- Stained bioclasts with diagenetic cements incorporated (Flaxdown Limestone Member). A) Benthic foraminifer with fibrous marine cements and blocky burial calcite, B and C) Benthic foraminifer with calcite cements, D) A bryozoan with ferroan calcite.

Samples: **A:** 4,9,12 location: Glens of Tekoa **B:** 9,3 location: Pahau Downs **C:** 9,3 **D:** 9,3

5.4.3 Pahau Siltstone Member

The Pahau Siltstone Member is the unit that is the least affected by diagenesis. It is likely that this unit has been affected by shallow burial diagenesis. Burial diagenesis is visible due to the development of blocky calcite cements in foraminiferal pore spaces. Carbonate cement is not visible in this sample with the matrix consisting of fine terrigenous mud. Although there is a lack of diagenetic features visible in petrographic samples of the Pahau Siltstone Member, other diagenetic features are visible in the field, such as concretionary horizons. Bioclasts are sparse in the Pahau Siltstone Member with the majority of bioclasts being aragonitic in nature (molluscs), especially in the Fossiliferous Sandstone facies. The

only calcitic bioclasts observed in this sample are foraminifera. Paragenesis of the Pahau Siltstone follows the order:

1. Reworking of glauconite and deposition with bioclasts and quartz in terrigenous mud.
2. Calcite dissolution and reprecipitation. Calcite cement has infilled pore spaces within bioclasts, mostly foraminifera. This is likely to have occurred during shallow burial (figure 5.5a, b).
3. Calcite precipitation is evident in this unit in the form of concretionary horizons. This precipitation has produced well lithified sections with the development of concretions. It is likely these concretions have formed due to the inclusion of calcite rich pore fluids linked with precipitation during diagenesis.

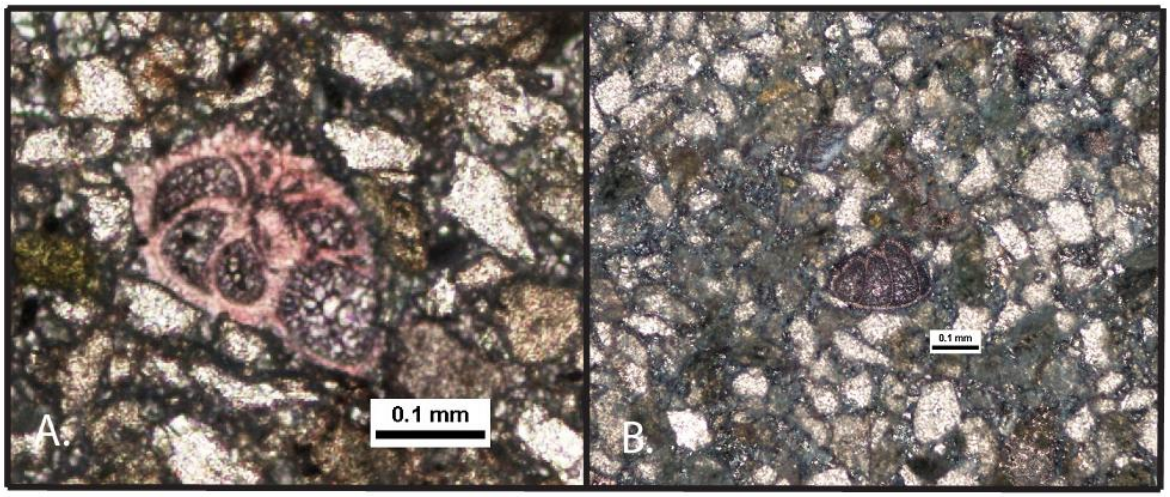

Figure 5.5- Foraminifera from the Pahau Siltstone Member, displaying calcite cementation within the foraminifera.

Samples: **A:** 12,4 location: Cascade Downs **B:** 12,4 location: Cascade Downs

Summary

Diagenetic alteration is evident in all of the Tertiary units from the Mandamus-Pahau District. Burial diagenesis is visible in the Coal Creek Formation, Flaxdown Limestone Member and Pahau Siltstone Member. These burial cements occur either as blocky equant calcite or microgranular calcite cement. Burial diagenetic cements occur around and within bioclasts, with ferroan calcite in the majority of Flaxdown Limestone samples. Other features of burial are visible in the Flaxdown Limestone, including stylolites, a feature

formed due to chemical compaction during burial. Both the Flaxdown Limestone and Pahau Siltstone contain molluscs which are aragonitic in nature. Interestingly these aragonitic bioclasts have been retained during burial diagenesis. The creation of these burial cements indicates that the isotopic signature retained in these samples will not show equilibrium with sea-water at the time of unit deposition.

6. Stable Isotope Analysis

6.1 Introduction

Thesis Application

Shelf sediments are well represented in New Zealand's sedimentary record, one excellent example of this is the Mandamus-Pahau District in North Canterbury which includes shelf units of Palaeocene through Miocene age. Climate change is reflected in global sedimentary and geochemical records, with variations appearing in both the Oligocene and Miocene isotope records due to the expansion of the Antarctic ice sheet. Oligocene and Miocene sediments that may record global cooling consist of the Flaxdown Limestone Member (Oligocene) and the Pahau Siltstone Member (Miocene).

This chapter presents a stable isotopic record of shelf carbonates from the Mandamus-Pahau sequence including whole rock and foraminiferal analyses. These data contrast the combined pelagic-benthic global isotope stratigraphy of the Zachos curves (2001). The North Canterbury records are compared to the global records to determine if similar patterns are present despite the different environments. Carbonate diagenesis is an issue in the North Canterbury sequence and is not unexpected as secondary processes proceed at a faster rate in shallower environments with coarser grainsizes than in deeper water systems (Veizer *et al.,* 1999).

Palaeoclimatology

Various geochemical techniques are used in the interpretation of sedimentary, environmental and diagenetic conditions. Carbonate oxygen and carbon stable isotopic compositions are useful proxies of palaeotemperatures when primary carbonate is available (Hudson, 1977; Nelson and Smith, 1996; Pufahl *et al.,* 2006). Stable isotopic composition depends on many factors, carbonate $\delta^{18}O$ values depend on the isotopic composition, salinity and temperature of its 'parent' fluid, whereas $\delta^{13}C$ carbonate values are sensitive to the source of CO_2 involved in carbonate precipitation (Nelson and Smith, 1996). Calcareous organisms are useful in stable isotopic analysis as if these organisms are well preserved, they may record secular trends that are helpful in the reconstruction of the isotopic composition

of past ocean water (figure 6.1)(Kump and Arthur, 1999). Thus $\delta^{18}O$ versus $\delta^{13}C$ in bivariate plots can facilitate interpretation of depositional or diagenetic environments, or both in addition to revealing stratigraphic patterns such as diagenetic susceptibility and unit specific isotopic signals (Nelson and Smith, 1996).

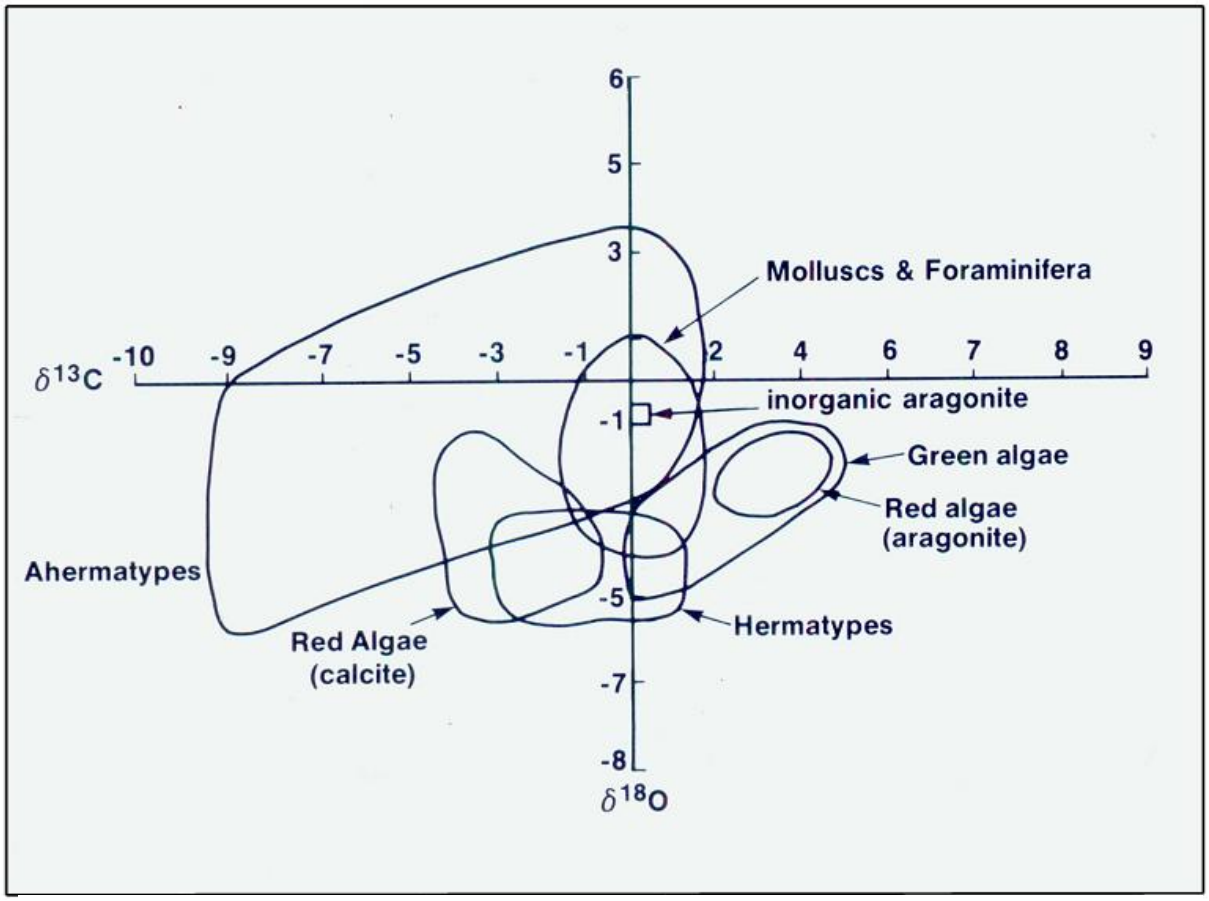

Figure 6.1- Isotopic composition of certain groups of calcareous organisms (Morse and Mackenzie, 1990).

Global Isotope Curve

Oxygen and carbon isotope ratios are important for environmental and diagenetic interpretations on both the local and global scale. The use of carbonate $\delta^{18}O$ and $\delta^{13}C$ in determining past environments and the processes acting on sediments is an important part of stable isotope geochemistry. $\delta^{18}O$ values are sensitive to both the composition and temperature of sea water, with more negative values generally associated with a decrease in salinity, and/or a rise in temperatures (Hudson, 1977; Nelson and Smith, 1996). $\delta^{13}C$ on the other hand records information on aqueous carbonate carbon sources, including sea water ($\delta^{13}C$ 0‰), the dissolution of marine shells ($\delta^{13}C$ 0‰), processes affecting soil

weathering ($\delta^{13}C$ ~−10‰) and other biogenic processes ($\delta^{13}C$ ~15 to -80‰) (Nelson and Smith, 1996). These oxygen and carbon proxies assume that the precipitation of carbonates occurred under isotopic equilibrium conditions, thus yielding values that reflect the environment and conditions of deposition.

The global deep-sea oxygen and carbon isotope curve created by Zachos *et al.,* (2001) provides a framework based on deep-sea foraminifera of the Cenozoic (figure 1.6). Foraminiferal information from more than 40 deep-ocean drilling sites was incorporated into a single global record. This oxygen isotope data has been used to outline changes in deep-ocean temperatures and land ice-volume (Zachos *et al.,* 2001). Deep-sea isotope records are generally considered to provide a more accurate representation of secular global stable isotope variation than shelf records. Accurate isotope records from deep-sea data are due to limited impact of diagenesis on these sediments. (Zachos *et al.,* 2001). Circulation of polar-derived waters can then be recorded in these $\delta^{18}O$ and $\delta^{13}C$ primary isotopic compositions and palaeoceanographic information can be interpreted. These polar derived waters also provide time-averaged data of sea-surface temperatures (SST) from regions of high latitudes (Zachos *et al.,* 2001). Carbon isotopes are also important in the global isotope curve, in that they provide insight into changes in the global carbon cycle and deep-ocean circulation patterns (Zachos *et al.,* 2001).

A major concern when interpreting stable isotope ratios is the fact that biological organisms may, or may not, precipitate carbonate in equilibrium with sea-water (figure 6.1) (Morse and Mackenzie, 1990). Depending on the location of organisms in the marine environment e.g planktic organisms in the water column or benthic bottom-dwelling organisms, isotope ratios may be significantly different. Taking the ecological distribution of foraminifera into consideration, planktic foraminifera record sea-surface temperatures, although it is not known exactly where in the water column this carbonate secretion occurs (Zachos *et al.,* 2001; Morse and Mackenzie, 1990). The deep bottom water carbonate $\delta^{18}O$ and $\delta^{13}C$ values recorded by benthic foraminifera may be altered by pore waters and overlying carbon dioxide pools (Zachos *et al.,* 2001; Morse and Mackenzie, 1990).

Oxygen and carbon isotope analysis based on marine carbonates is controlled by a certain number of rules according to Sharp (2007), these include:

1. The average $\delta^{13}C$ and $\delta^{18}O$ values of modern unaltered marine carbonates are ~0‰ (figure 6.1; 6.2). Carbonate with lower values than these are unlikely to be primary marine carbonates and instead can be related to a number of secondary processes.
2. The main source of carbon from marine limestone comes from dissolved bicarbonate. Average $\delta^{13}C$ values for bulk ocean water analyses are 0‰ with shallow oceans consisting of higher values of 1 to 2‰ due to the biological pump.

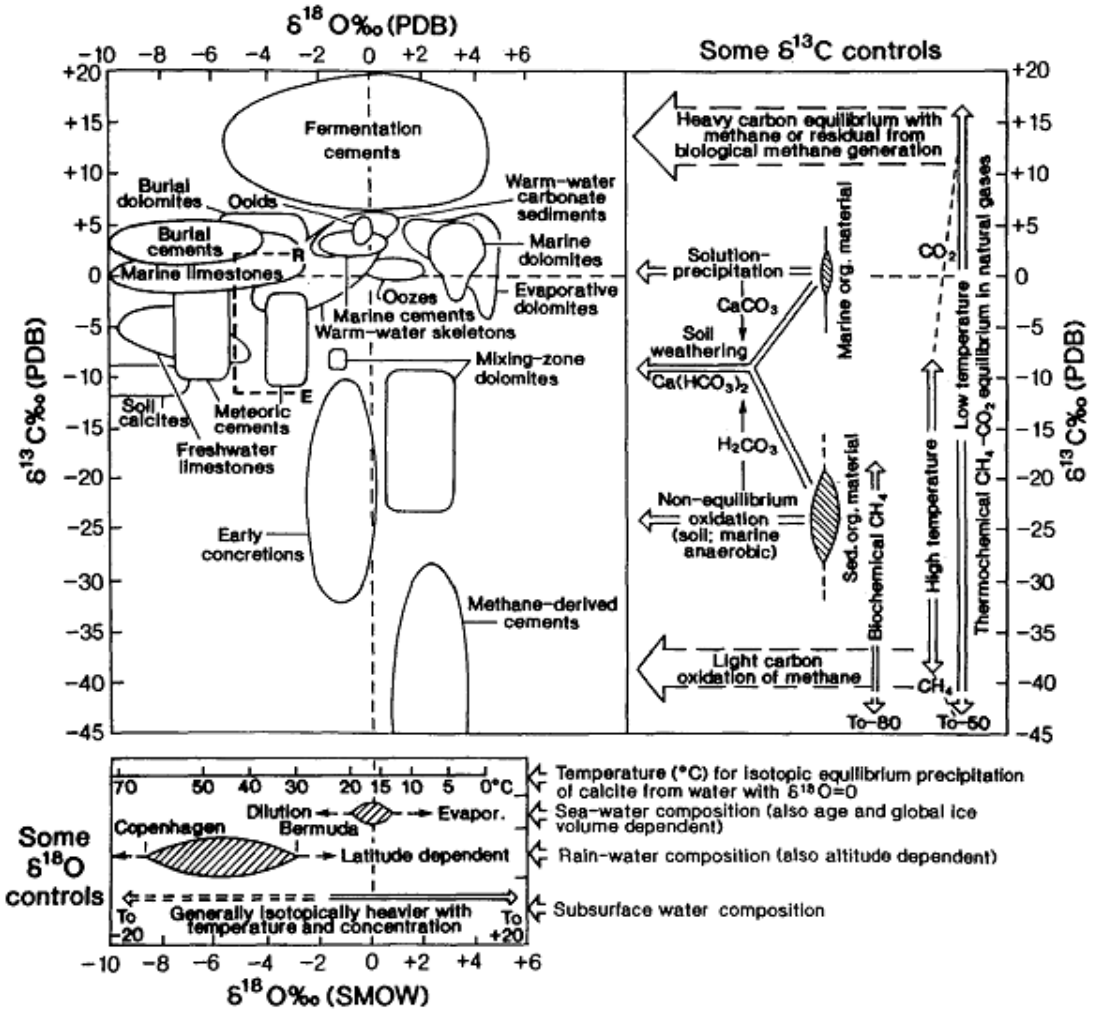

Figure 6.2- Distribution of carbon and oxygen isotopic compositions of carbonate sediments. (Nelson and Browne, 1996, modified from Hudson, 1977)

3. The $\delta^{18}O$ values of terrestrial carbonates are more negative than marine carbonates due to the formation of these units in equilibrium with meteoric derived waters. If dissolved inorganic carbon occurs from the dissolution of marine carbonates it is likely the $\delta^{13}C$

value will be close to zero. However dissolved inorganic carbon from the oxidation of organic matter produces much more negative $\delta^{13}C$ values in terrestrial carbonates than in marine carbonates.

4. Diagenesis effects carbonate stable isotopic compositions, most commonly manifesting as a shift in $\delta^{18}O$ towards more negative values. $\delta^{13}C$ values also generally become more negative during diagenesis, but this is often not as large as that seen in $\delta^{18}O$. This is due to the generally low amounts of dissolved carbon in diagenetic fluids.

All four of these factors must be considered when interpreting marine and terrestrial sedimentary isotopic compositions, particularly in uplifted shelf sequences such as the Mandamus-Pahau sequence. Stable isotopic data presented in this chapter are interpreted with an aim towards determining whether these local shelf sediments provide similar isotopic trends to the Zachos *et a.,l* (2001) global isotope curve.

6.2 Stable isotopic results

Figure 6.3 illustrates geochemical data from foraminifera and bulk rock samples of the Mandamus-Pahau field area, illustrating the distribution of this geochemical data within or outside expected carbonate ranges. The majority of data for these samples falls within either the expected range for marine or terrestrial carbonates with high altitude topography nearby, or burial diagenesis. The scattering of data points below the expected marine carbonate range indicates a possible increase in meteoric/burial diagenesis. The bulk of Flaxdown Limestone Member and Pahau Siltstone Member samples fall in the expected range for marine carbonates.

Many of the Coal Creek Formation samples fall within an expected range for burial diagenesis of marine rocks, and also coincide with terrestrial carbonate precipitates (including the interaction of meteoric fluids with decomposing terrestrial organic matter (figure 6.2). Although in figure 6.4 some samples fall outside both the expected marine and terrestrial carbonate range.

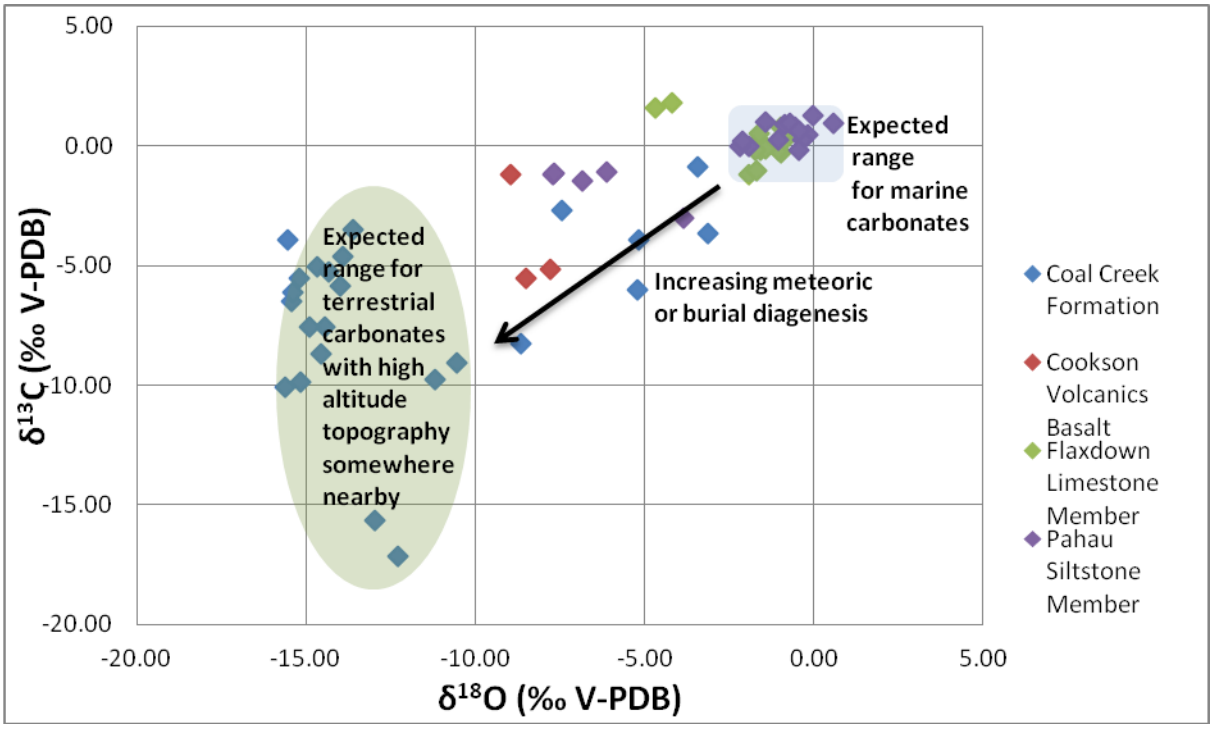

Figure 6.3- $\delta^{13}C$ and $\delta^{18}O$ of foraminifera and bulk rock samples from the Mandamus-Pahau District, North Canterbury. This figure illustrates the expected range for terrestrial and marine carbonates. Expected carbonate ranges from Sharp (2007).

6.2.1 Coal Creek Formation

The bulk of the Coal Creek Formation samples fall outside the expected range (close to 0‰) for marine carbonates. The samples from this unit range from $\delta^{18}O$ -1.07‰ to -15.64‰ and $\delta^{13}C$ -0.87‰ to -17.14‰. The majority of the samples from this unit plot in the expected range for terrestrial carbonates (~-5‰ and below). Although the data plots the unit within the terrestrial range previous chapters (3 and 4) have interpreted the depositional environment of the Coal Creek Formation as marine. Therefore these isotope values reflect alteration of marine values not terrestrial carbonate precipitates, and this record shows alteration of primary carbonate material. The Coal Creek samples have very few foraminifera preserved and isotopic signatures possibly record carbonate formed during burial diagenesis. Therefore the isotope record is suggestive of burial diagenesis not terrestrial carbonates or original sea water composition.

6.2.2 Flaxdown Limestone Member

The bulk of samples from the Flaxdown Limestone Member are located within the expected range for marine carbonates (close to 0‰). The samples from this unit range from $\delta^{18}O$

−0.92‰ to -4.69‰ and $\delta^{13}C$ 1.82‰ to -1.18‰. The samples that plot within the marine carbonate range do not record as much variation with $\delta^{18}O$ values from -0.92‰ to -1.93. There are two samples from the Flaxdown Limestone that plot quite far outside the expected marine range due to variations in $\delta^{18}O$ values. These $\delta^{18}O$ values of -4.19‰ and -4.69‰ are both from sample 9.1 from the Pahau Downs site (figure 6.3). If viewed in terms of diagenesis these two samples appear to have been altered to a greater extent by burial diagenesis, possibly being buried to a greater depth than the Culverden back section samples (-0.92‰ to -1.93‰).

6.2.3 Pahau Siltstone Member

The majority of samples from the Pahau Siltstone Member fall within the expected range for marine carbonates with values of close to 0‰ for both $\delta^{13}C$ and $\delta^{18}O$. The range of these samples are for $\delta^{18}O$ 0.59‰ to -7.71‰ and $\delta^{13}C$ 1.26‰ to -3.00‰. Oxygen values for the marine carbonates that plot within the expected range are $\delta^{18}O$ 0.59‰ to -2.17‰. There are two samples from the Pahau Siltstone that fall outside these values, these samples are 12,3a and 12,5 from Cascade Downs. These samples occur within well lithified sections of the Pahau Siltstone that have been affected by burial diagenetic precipitation altering these isotopic values.

6.3 Discussion

The main anomalies in this data set occur in the Coal Creek Formation. The location of the majority of samples from this unit within the expected range for terrestrial carbonates poses a number of problems due to the deposition of this unit in a marine setting. There are a number of possible reasons for such depleted $\delta^{13}C$ and $\delta^{18}O$ values in this unit. These are:

1. Burial diagenesis, with burial of the Coal Creek Formation at a temperature of >40°C to a depth of >500m (figure 6.7) (Nelson and Smith, 1996).
2. Burial diagenesis with fluid inclusions of meteoric nature (showing similar value to groundwater/fluid that has interacted with decomposing terrestrial organic matter).
3. Alteration of the unit at a faster rate due to lack of calcareous material.
4. Meteoric diagenesis of the unit (this is modelled in figure 6.4 with a meteoric water value of -10‰).

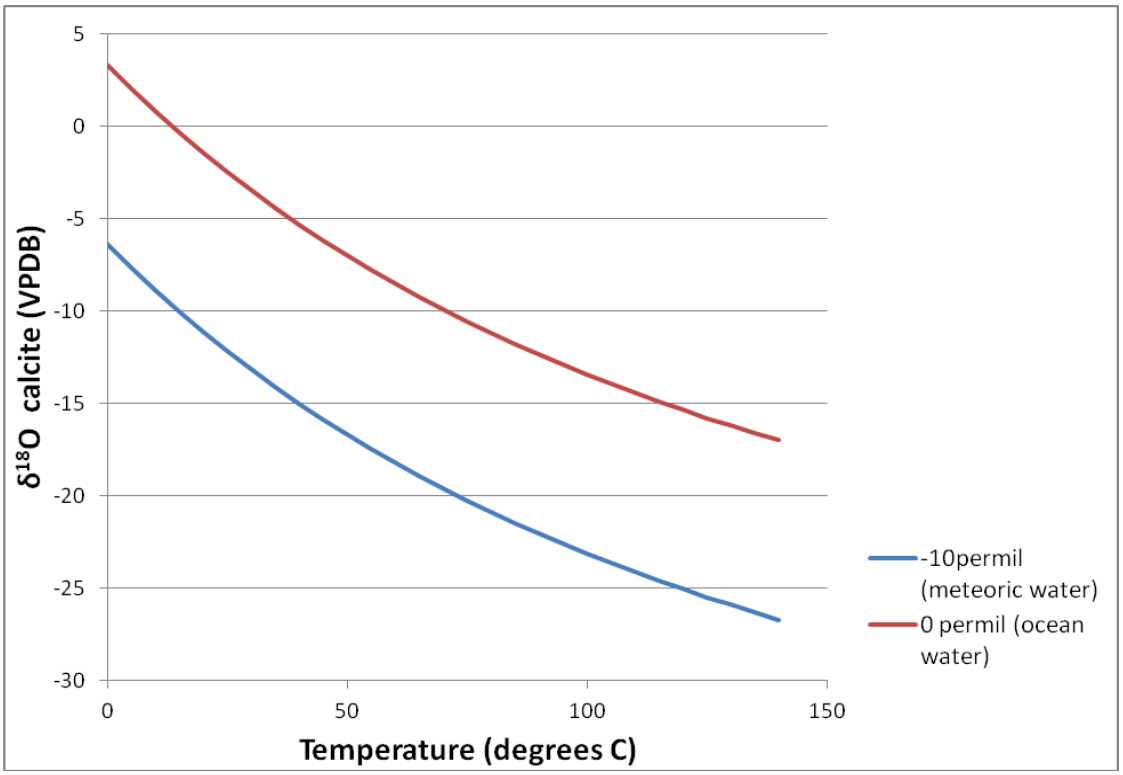

Figure 6.4- Calcite $\delta^{18}O$ isotope equilibrium fractionation model, of meteoric water (-10‰) and ocean water (0‰), with the space between these lines showing mixing of both.

Although these six ideas listed above provide a possible explanation for depleted $\delta^{13}C$ and $\delta^{18}O$ values, they do not reflect the petrography of samples from the unit. Petrographic studies of this unit support burial diagenesis. The majority of samples from the Coal Creek Formation contain burial cements. These cements are blocky Fe-calcite burial cements. The depleted $\delta^{13}C$ and $\delta^{18}O$ values seen in the Coal Creek Formation can be linked to the associated temperatures needed to create the burial cements present in these samples. Temperatures of anywhere from 40°C to >115°C may have influenced the creation of calcite cements within these samples. The location of these temperature lines on figure 6.5 is dependent on an ocean water $\delta^{18}O$ value of 0‰ (equation 6.1). Samples that have formed cements in the higher temperature ranges (>50°C) are likely to have been buried to depths of >500m to as deep as 1500m (Nelson and Smith, 1996). There are other factors that are not evident in petrographic studies but could influence the isotopic values of this unit. The relation of the depleted isotopic values to terrestrial carbonates could suggest alteration of the unit post burial diagenesis. Thus recording terrestrial values due to recent terrestrial weathering. The lack of calcareous material in this unit could have also led to a faster rate of alteration compared to other units.

$$\delta^{18}O_{cc} - \delta^{18}O_{H_2O} = [2.78 \times (10^6 / T(K)^2)] - 2.89$$

Equation 6.1- Calcite $\delta^{18}O$ (‰) for MAT at local water $\delta^{18}O$ of -10‰ (Kim&O'Neil, 1997)

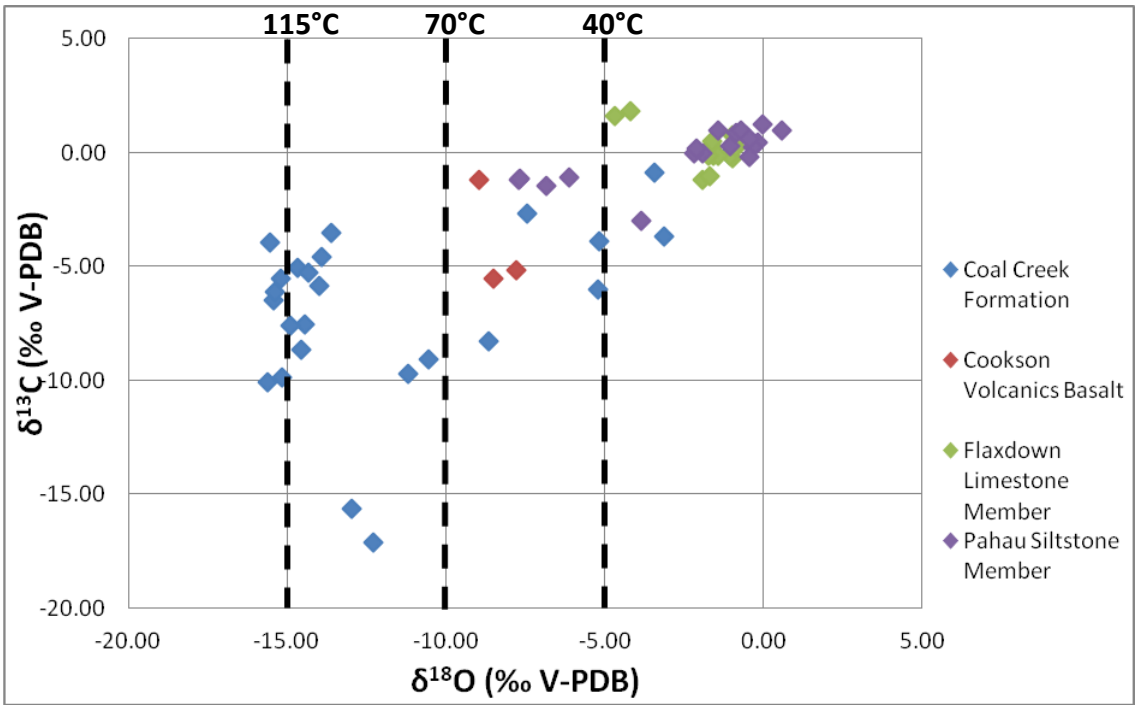

Figure 6.5- Graph illustrating temperatures under which burial diagenetic calcite formed. This is shown on a graph of $\delta^{13}C$ and $\delta^{18}O$ values of foraminifera and bulk rock sample from the Mandamus-Pahau District.

The location of the majority of Flaxdown Limestone Member samples within the expected range for marine carbonates suggests limited diagenetic alteration, yet petrographic samples provide evidence for burial diagenesis. All Flaxdown Limestone petrographic samples contain blocky Fe-calcite cement, indicative of burial cements. Evidence of burial diagenesis in this unit is not just limited to thin sections, but is also seen in the field. In the field this unit is typified by development of stylolites that suggest burial depths of at least a few hundred metres (Choquette and James, 1990). This diagenesis appears to have altered the majority of samples, but not to the extent of the Coal Creek Formation. This diagenesis has not altered the bulk of samples to a great extent as isotopically they are still recognisable as marine carbonates. One Flaxdown Limestone sample from the Pahau Downs site has depleted

isotopic values suggestive of burial diagenesis at higher temperatures/greater depth than the rest.

All but two samples from the Pahau Siltstone plot within the expected marine range. As with the Flaxdown Limestone the samples from this unit contain features of burial diagenesis. Burial diagenetic cements fill pore spaces in foraminifera. This burial cement is contained within foraminifera is a coarse mosaic form of blocky calcite (cannot be defined in terms of Fe-calcite). Two samples from this unit fall outside of the expected marine range (12,3a; 12,5). These two samples are from more lithified sections, suggesting the interaction of calcium carbonate rich fluids from dissolution, altering sections of the unit.

To calculate whether there was any change within samples at least two sets of data were analysed for most locations. The differences between bulk rock samples or foraminiferal and bulk rock samples were then calculated. This provided $\Delta\delta^{13}C$ ‰ (PDB) and $\Delta\delta^{18}O$‰ (PDB) for the majority of samples. This data is displayed in figure 6.6 showing that the majority of samples from the field sites fall within the range of 1‰ ($\delta^{13}C$ and $\delta^{18}O$). The Coal Creek Formation is the unit with the highest variation with half of the 10 samples collected falling outside of the 1‰ range. The Flaxdown Limestone samples all plot within the 1‰ (in a bivariate plot of $\Delta\delta^{13}C$ ‰ versus $\Delta\delta^{18}O$‰). The Pahau Siltstone Member shows similar correlation with only one sample falling outside of the 1‰ range. The correlation of these samples within 1‰ (PDB) may be due to a number of possible reasons:

1. Foraminifera are the dominant or possibly even sole source of carbonate in the majority of units. Therefore plotting foraminifera values against bulk rock data that is based on foraminifera will show little variation.
2. Foraminifera carbonate values are isotopically similar to secondary diagenetic cement or appear indistinct from primary carbonate values.

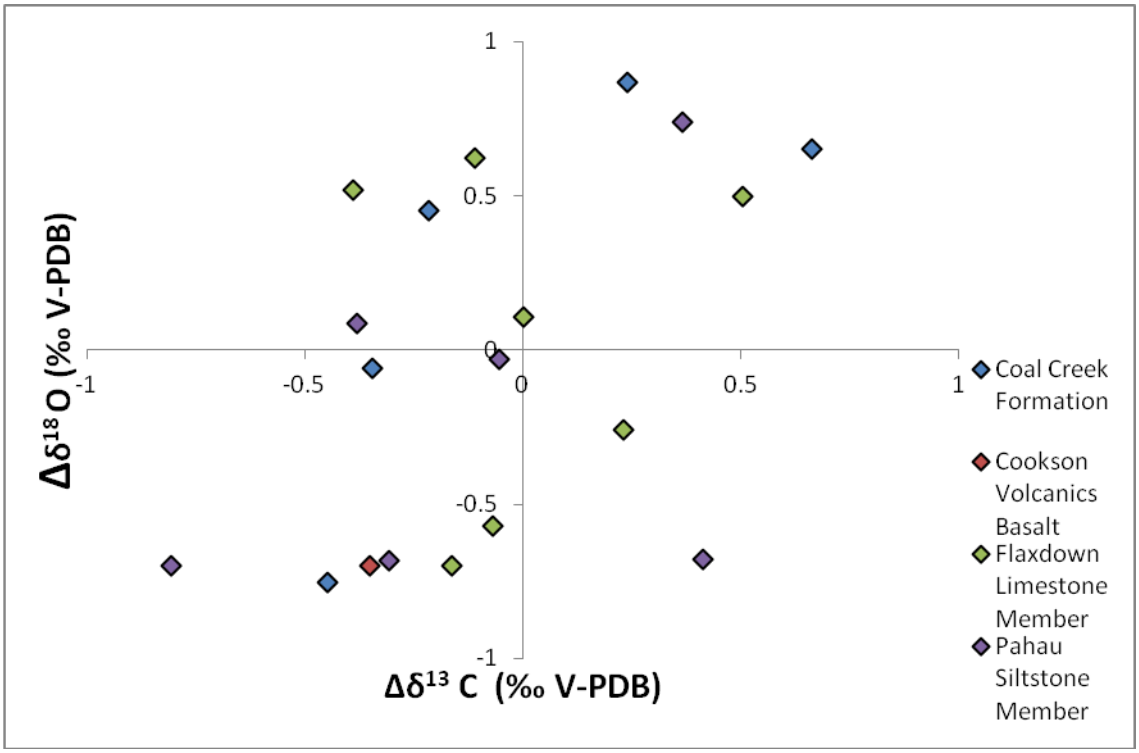

Figure 6.6- $\Delta\delta^{13}$ C and $\Delta\delta^{18}$O of bulk rock and foraminifera samples within 1-mol of Tertiary units of the Mandamus-Pahau District, North Canterbury.

6.4 Correlation to the global marine isotope curve

6.4.1 Oxygen

Oxygen values from foraminiferal data show variations of ~2‰ to ~4.5‰ from global marine isotope data. $\delta^{18}O$ values from Runangan samples of the Coal Creek Formation (from the Culverden back section) start at -3.44‰. Due to lack of foraminiferal samples through the Early to Mid Oligocene, the next sample is post-Marshall Paraconformity (therefore the excursion cannot be noted). The transition from the Late Eocene to the Late Oligocene shows a positive trend from $\delta^{18}O$ -3.44‰ to -1.58‰. This positive trend continues to the Oligocene/Miocene boundary where it peaks at -0.18‰. This peak appears to mirror the climatic conditions at the Oligocene/Miocene boundary and those recorded in the Zachos (2001) marine isotope record (figure 6.7). Correlation of these values to the marine isotope record can be linked to the occurrence of sea ice volume. This enrichment appears to reflect a small scale glaciation (figure 6.7). This cannot been seen in the sedimentary record (chapter 3) in the North Canterbury region and the Mandamus-Pahau District with shallowing to the west at this associated with uplift and erosion. As this data does not correlate it can be suggested that this peak reflects alteration during diagenesis, not original sea water composition. This peak is followed by a rapid depletion in $\delta^{18}O$ to -1.92‰ and −3.82‰. A positive trend back to -0.43‰ then occurs, suggesting alteration of sample 12,2, 2.4m (-3.82‰) due to a variation of ~4‰. This variation is out of the $\delta^{18}O$ ~2‰ range Pufahl *et al.,*(2006) observed between shelf and deep water sediments. Trends from the early Miocene into the Mid Miocene shows enrichment of $\delta^{18}O$ values from -2.17‰ (12,5) to −1.42‰ (5,6a) providing evidence for the development of continental glaciation in Antarctica, this enrichment of $\delta^{18}O$ is due to the uptake of $\delta^{16}O$ by ice sheets. If linked to development of continental ice sheets and sea level changes, this glaciation should be supported by a shallowing in the sedimentary record. Although biostratigraphic data shows the samples collected from Cascade Downs are unlikely to be younger than the Altonian-Clifdenian and therefore do not depict environmental change.

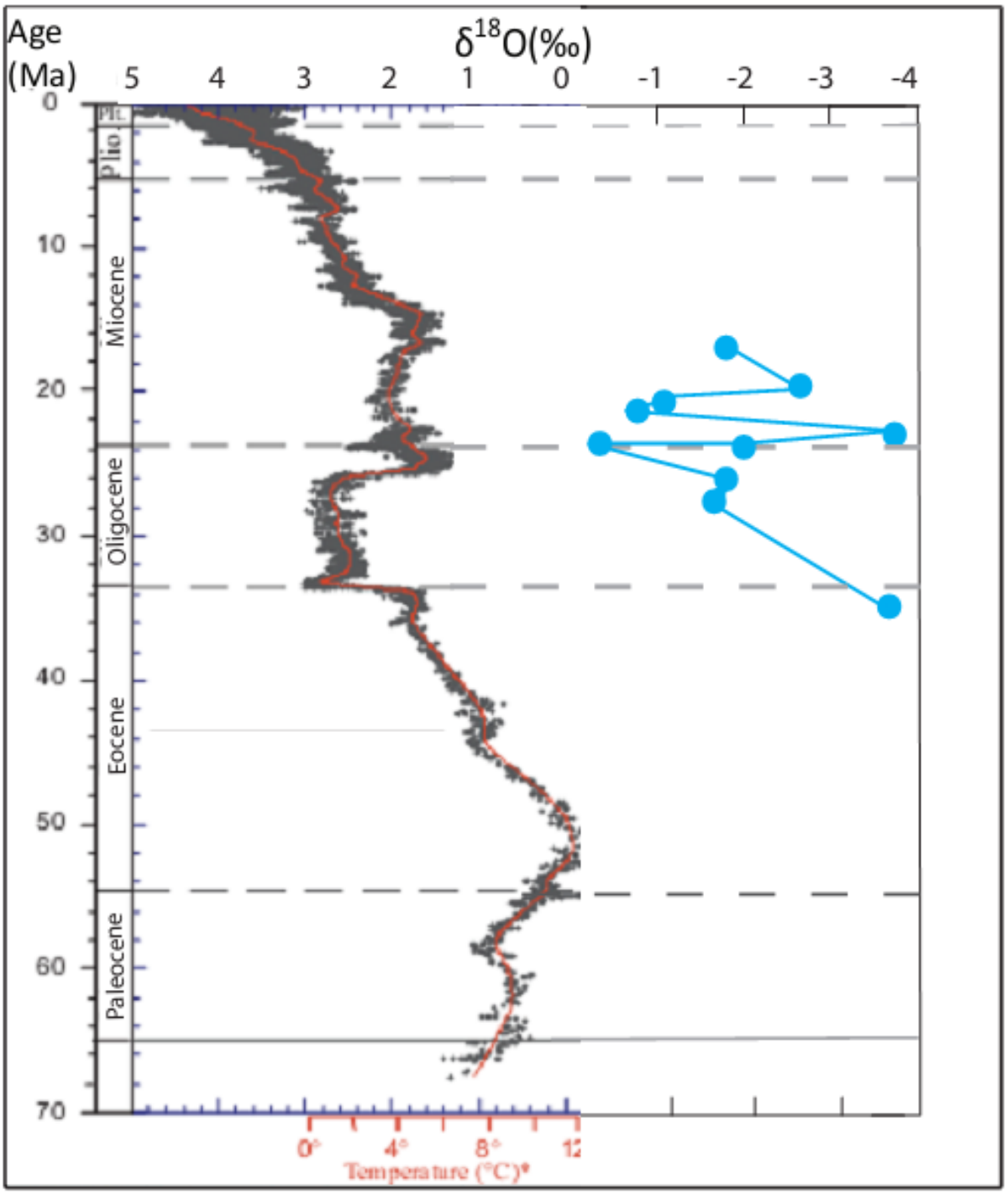

Figure 6.7- The Zachos (2001) deep-sea oxygen curve, with the Mandamus-Pahau District foraminifera samples $\delta^{18}O$ (‰ PDB) plotted beside (on the right hand side in blue). Modified from Zachos *et al.,* 2001.

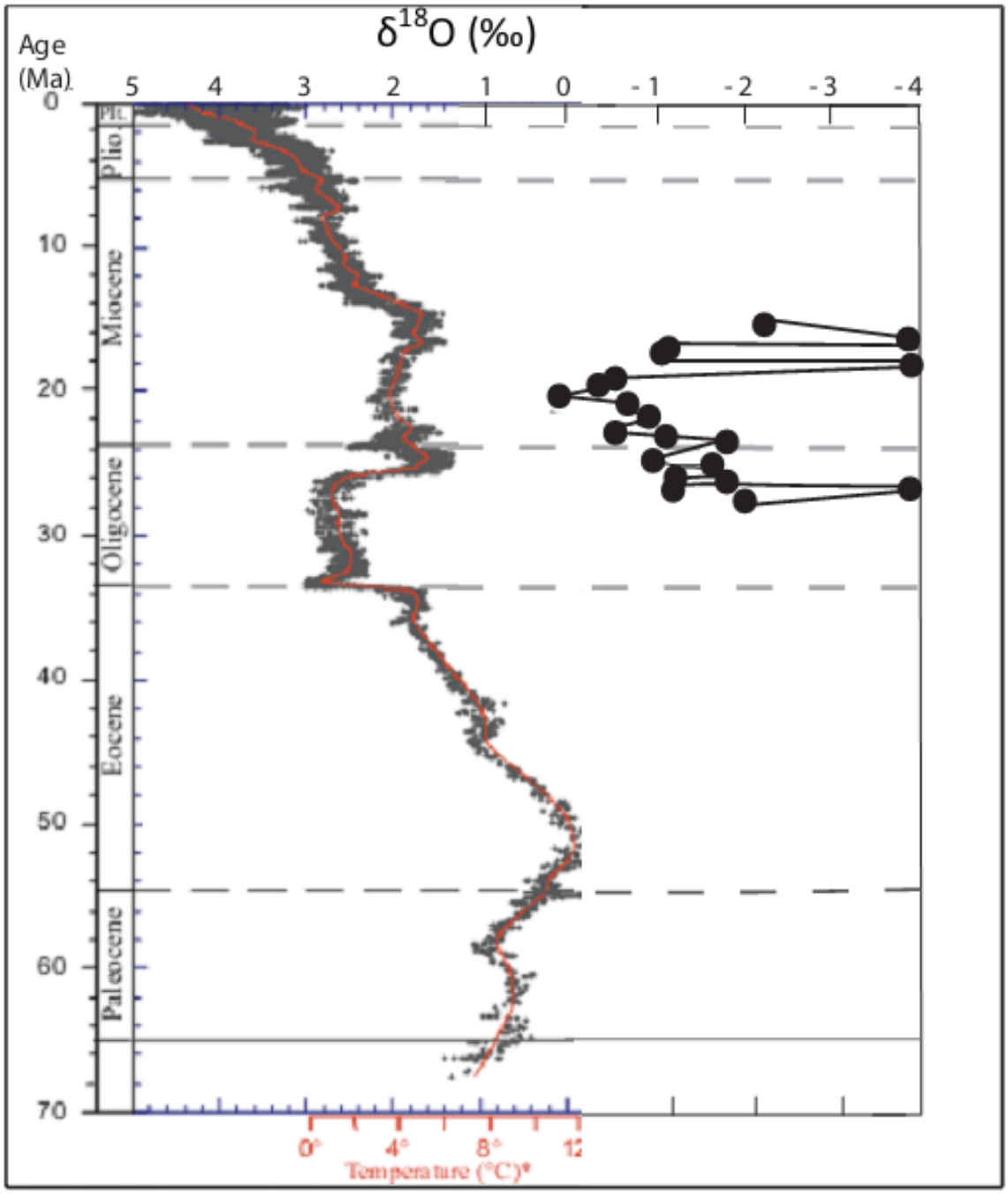

Figure 6.8- The Zachos (2001) deep-sea oxygen curve, with the Mandamus-Pahau District bulk rock samples $\delta^{18}O$ (‰ PDB) plotted beside (on the right hand side in black). Modified from Zachos *et al.,* 2001.

6.4.2 Carbon

Carbon isotope values show higher correlation to the $\delta^{13}C$ marine isotope record than $\delta^{18}O$ records. $\delta^{13}C$ isotope foraminifera show variations of ~0‰ to ~4‰ from global marine records (figure 6.9). The Runangan (Coal Creek Formation) marine $\delta^{13}C$ record on its own does not reflect variations in the global record, although it only varies from the global record by ~2‰. If foraminiferal data was obtained pre or post Runangan correlations may be drawn. This lack of data also limits the appearance of any excursions that may have been visible during or just after the Marshall Paraconformity. Post Marshall Paraconformity the late Oligocene Flaxdown (Culverden back section) Limestone values of -0.16‰ and 0.50‰ reflect the similar enrichment seen in the global curve. One sample (sample 11,3t) even plots in the same range as the Zachos curve, correlating with the global marine $\delta^{13}C$ values. This positive shift close to the Oligocene/Miocene boundary supports the influx of cold bottom waters, due the full circulation of the circum-Antarctic current (Kennett, 1977). This time period is associated with ACC development and the influence of currents from this circulation system affecting the east coasts continental shelf (Fulthorpe *et al.,* 1996). After the Oligocene/Miocene boundary a slight positive increase to 0.46‰ follows the enrichments in the global marine record, although samples 12,1b (from the fossiliferous facies) and 12,2,2.4m and 5,6f (quartz-rich facies) deviate from the global marine $\delta^{13}C$ values (figure 6.10). Sample 12,2,2.4m provides the most depleted $\delta^{13}C$ value with -3.00‰, it appears this sample may have been altered to a greater extent than the other Pahau Siltstone samples. Early to Mid Miocene $\delta^{13}C$ values following this spike return to values close to the global marine curve. The youngest sample (5,6a) from Cascade Downs supports a positive shift towards the Mid Miocene cooling linked with the termination of warm, saline water flow to the Southern Ocean (figure 6.9). As with the Oligocene/Miocene boundary bottom-water production in the Mid Miocene has been linked to burial of marine organic carbon (Pufahl *et al.,* 2006). Although as with the oxygen data, these samples may not depict the excursion at the Mid Miocene boundary.

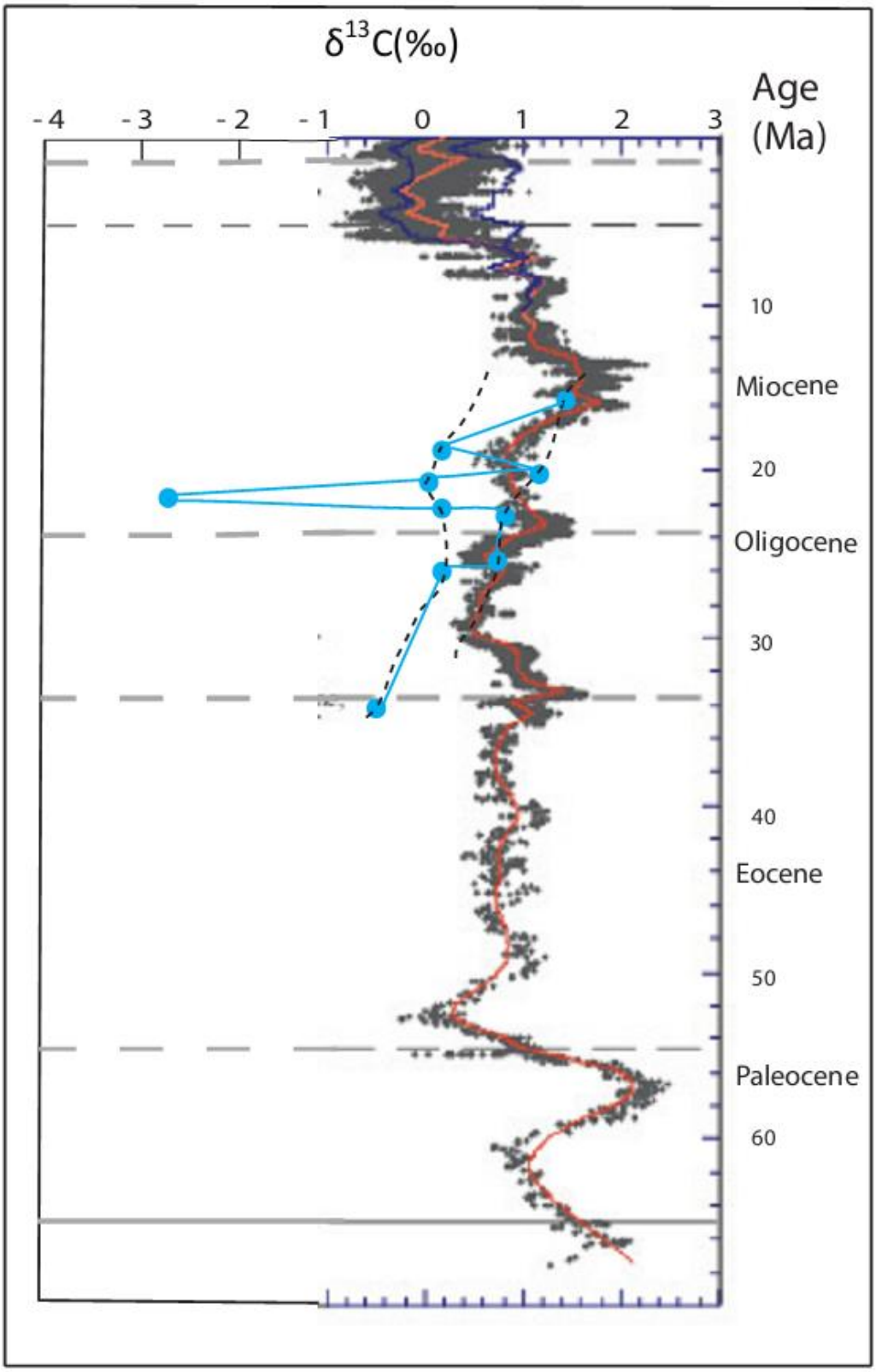

Figure 6.9- The Zachos (2001) deep-sea carbon curve, with the Mandamus-Pahau District foraminifera samples $\delta^{13}C$(‰ PDB) plotted beside (on the left hand side in blue, black dots represent possible trends). Modified from Zachos *et al.,*

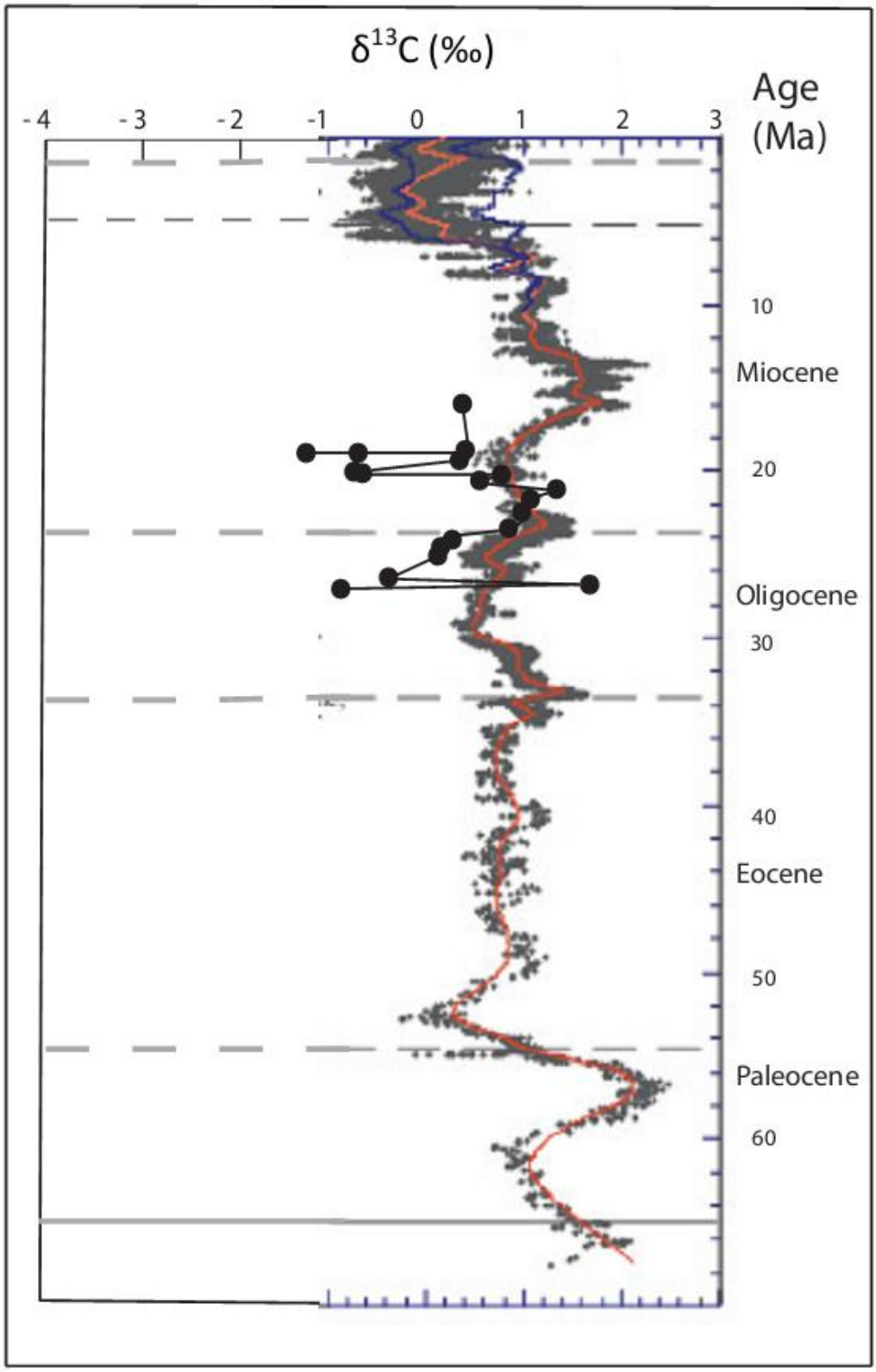

Figure 6.10- The Zachos (2001) deep-sea carbon curve, with the Mandamus-Pahau District bulk rock samples $\delta^{13}C$(‰ PDB) plotted beside (on the left hand side in black). Modified from Zachos *et al.,* 2001.

Summary

Global marine $\delta^{13}C$ and $\delta^{18}O$ records are not well reflected in Mandamus-Pahau District foraminiferal isotope data. Oxygen isotopic data does not record the Mid Miocene cooling as the original sea water values have been altered by burial diagenesis. The broad global shift in $\delta^{13}C$ from the Oligocene to Miocene can be seen in foraminiferal data. However some samples deviate due to burial diagenesis of this unit. These large variations in data could also be due to the unintended inclusion of cement within foraminiferal samples.

Bulk rock data can be seen in figures 6.8 and 6.10. When plotted against the deep marine curve this bulk rock data does not appear to show any correlations. Large deviations from the Zachos curve (2001) do not appear to show any correlation to lithofacies, grainsize or location of these samples. It is likely these bulk rock records are a result of unintended sampling of cements in the samples. Bulk rock sample cements are also more likely to contain bioclasts that are more prone to alteration during diagenesis, such as the inclusion of aragonitic shells in the Pahau Siltstone bulk rock samples.

7. Discussion

7.1 Palaeoenvironments

The data presented in chapters 3 and 4 is combined in this section to provide palaeoenvironmental interpretations. One of the main focuses of this project is to determine age and environmental data in order to interpret the geological history and depositional setting of North Canterbury rocks. The determination of palaeodepth using foraminiferal data focuses on foraminiferal assemblages, planktic/benthic ratios and benthic species diversity.

7.1.1 Coal Creek Formation

This unit is of Early Palaeocene to Late Eocene age and consists of the Cross-bedded Glauconite-rich Sandstone Facies and the Massive Glauconite-rich Sandstone Facies. This unit provides evidence for environmental change including sea level rise, typified by the transition from cross-bedded highly glauconitic sandstone to a quartzose, glauconite-rich sandstone containing phosphate nodules.

The cross-bedded facies consists of a medium to coarse sandstone with high glauconite content varying from ~15-20% at the base of beds grading gradually into ~2-3% glauconite and quartz rich beds. Trough cross-beds in this unit are indicative of an environment of high energy and sedimentation. Repetitive graded bedding displaying density settling of glauconite and quartz is attributed to the deposition of these minerals in an environment affected by rhythmic bedding, possibly associated with waning currents (Boggs, 2006). The deposition of high percentages of glauconite in this facies would normally be indicative of an environment with low sedimentation rates, yet the creation of trough cross-beds suggest otherwise. It is therefore likely that the glauconite that occurs in this facies is parauthochthonous and has been remobilised and reworked in to the cross-bedded facies due to current activity.

The cross-bedded facies that occurs in Coal Creek is replaced by glauconite and quartz-rich sandstone with interbeds of high glauconite content (~30%). Glauconite content varies from

~3-30% with quartz abundance remaining high throughout (44-45%). Rounding of the majority of quartz grains within this unit indicates reworking of these grains. Glauconite grains also appear to be rounded with remobilisation and reworking seen throughout this unit. Trace fossils occur throughout this quartz-rich facies with intense *Planolites* and more infrequent *Ophiomorphia* traces indicating soft sediments (MacEachern, 2010). Varying percentages of mud in this unit (3-20%) suggest changes in energy and environment throughout. An increase in water depth occurs between the deposition of cross-bedded facies and the youngest sample of the Coal Creek Formation, possibly due to sea-level rise in the Bortonian (Field and Browne, 1989).

Phosphate nodules consistently appear in the upper Coal Creek Formation at Glens of Tekoa and Cascade Downs. These phosphate nodules occur at Cascade Downs in glauconite-rich beds. The creation of phosphate nodules is linked to the upwelling of nutrient-rich ocean waters and low sedimentation rates (Prothero and Schwab, 1996). Trace fossils in phosphatised sections indicates current swept oxic bottom waters, with a dysoxic sediment profile.

Planktic foraminifera make up 28% of the fauna in this facies, with the most common species being *Globigerina linaperta* and *Globorotalia centralis*. Benthic foraminiferal species are dominated by *Cibicides parki, Cibicides maculatus, Cibicides notocenicus* and *Bolivina pupula. Cibicides sp* rely on organic matter and food from overlying water layers. The occurrence of low species diversity and the accumulation of organic matter for the formation of phosphate indicate a sediment profile that is possibly dysoxic with oxygenated waters above. The dominance of *Cibicides sp.* together with the 72%:28% benthic:planktic ratio indicates a mid to outer shelf environment (Hayward *et al.,* 1999).

Summary: Shallow inner shelf influenced by high energy (lower Coal Creek Formation) gradually deepening into mid-outer shelf with conditions leading to upwelling and the formation of phosphatised sections.

7.1.2 Cookson Volcanics Group

A period of non-deposition commonly known as the Marshall Paraconformity occurs between the final deposition of the Coal Creek Formation and the Cookson Volcanics Group. This hiatus in the Mid Oligocene is reflected in shelf successions from the eastern continental margin of New Zealand (Carter, 1985). The occurrence of the Marshall Paraconformity in the Mid-Late Oligocene (~32-28 Ma) was entirely non-depositional, possibly occurring due to lower sea-levels, cooling and increased current intensities. These climatic factors may have limited the deposition of carbonate units during this event (Fulthorpe *et al.,* 1996).

The Cookson Volcanic Group is of late Mid to Late Oligocene age (Duntroonian), and is typified by pillow basalts and volcaniclastic tuffaceous material interspersed with calcareous beds. The volcanic features seen in this unit are indicative of intraplate eruptive stage volcanism and reworking of tuffaceous material. Interbeds of tuff and calcareous material are 7-10cm thick and in places display sharp contacts representing pulses of tuff from a volcanic source to the east. Other sections at Glens of Tekoa appear to grade from volcaniclastic tuffaceous material into more calcareous beds, representing reworking of the volcanic material.

A lack of foraminiferal data for this lithofacies meant it was hard estimate an environmental interpretation. Environmental information of the Flaxdown Limestone Member above this volcanic unit constrains the possible environment in which these volcanic were deposited.

Summary: Mid shelf, eruptive basaltic processes.

7.1.3 Flaxdown Limestone Member

This Late Oligocene-Early Miocene unit consists of bryozoan, algal and molluscan-rich limestones. This unit's foraminiferal assemblage, macrofossils and petrography are important for environmental interpretation of this bioclastic grainstone. The occurrence of coralline algae indicates a shallow well-lit environment. A lack of high concentrations of carbonate mud throughout this unit moderate energy environment.

Fossil fauna within this unit indicate a mid shelf environment. This unit incorporates a number of facies that vary depending on the main indicator bioclasts. All facies contain bryozoans, although bryozoans are not always the most abundant bioclast type throughout the Flaxdown Limestone Member. Molluscan-rich sections within the Flaxdown Limestone (Culverden back section and Pahau Downs) show variations between grainstone and packstone beds. This variation in beds shows a change in energy (lower energy in packstone). Molluscan-rich beds in the Flaxdown Limestone Member occur in isolated sections. Bryozoan and coralline red algae commonly occur together in sections, with abundant bryozoan (~10-78%) and algae (~10-55%) bioclasts generally occurring in grainstone sections. Branching bryozoans are common occurring alongside dominant branching and rare encrusting coralline red algae. An optimum zone for both branching bryozoan and coralline red algae is to ~40-90m depth. This is due to the dependence of coralline red algae on light in combination with the lower energy settings dominated by branching bryozoans.

The high abundance of bryozoan and coralline red algae in association with common benthic foraminiferal species supports a shallow mid shelf environment. *Cibicides sp.* (>60%) is the dominant benthic genus in this unit with *Cibicides temperata and Cibicides perforatus* both occurring in high percentages. These two *Cibicides sp.* occur in combination with *Elphidium sp.* including *Elphidium advenum* (19%) and *Elphidium charlottense* (3%). In consideration of the lack of planktic foraminifera this assemblage indicates an environment where shallow water species thrive. A subtle change from dominance of *Cibicides perforatus* (stratigraphically higher) to *Cibicides temperata* at the top of this unit indicates the possibility of slight deepening throughout this unit. This deepening is also suggested by the lower abundance of *Elphidium sp.* A combination of the data discussed above indicates a mid shelf environment, with deepening towards the top of the Flaxdown Limestone Member.

Summary: Mid shelf in Bryozoan and Algal-rich Facies (40-90m, bryozoan and algal-rich sections), possibly slightly deeper in the Molluscan-rich facies due to the lack of coralline algae biolcasts: mid shelf.

7.1.4 Pahau Siltstone Member

This Early to Mid Miocene unit consists of fossiliferous and quartz-rich facies. Fossil assemblages provide important environmental indicators in this sandstone unit with benthic foraminifera making up 100% of bioclasts in some sections. Reoccurring benthic assemblages and indicator molluscs provide evidence for subtidal inner shelf environments. A lack of carbonate mud throughout this unit correlates with an absence of planktic foraminifera suggesting a near-shore moderate energy environment.

Quartz-rich beds with intermittent concretionary horizons are typical of this unit. Sections with concretionary horizons within fossiliferous beds are ~3.7m thick. Carbonate and glauconite (~4%) content is slightly higher in the concretions compared to the surrounding quartz-rich sandstone. The surrounding quartz-rich sandstone is well indurated but not to the extent of the concretionary horizons. Fossiliferous sections within the Pahau Siltstone Member contain molluscs representative of sheltered shallow-water environments. The molluscan species within this unit include *Glycymeris huttoni* and *Polinicies huttoni.* The occurrence of these two species in 1-10cm fossiliferous beds indicates shallow sheltered near-shore environments. Foraminiferal assemblages from these fossiliferous beds are defined by *Cibicides sp., Elphidium sp., Notorotalia spinosa* and *Zeaflorilus stachei. Notorotalia spinosa* and *Zeaflorilus stachei,* the most abundant taxa in this section, are generally found in abundance in the inner shelf. The combination of these two species with *E. crispum* limits the depositional environment to shallow subtidal (0-20m) (Hayward *et al.,* 1997).

The Pahau Siltstone Quartz-rich (42-86%) facies from Cascade Downs are more dominant than fossiliferous beds. Foraminiferal assemblages contain 100% benthic foraminifera and vary compared to those in the fossiliferous beds. *Cibicides sp.* occurs in higher abundance, with the most common species being *Cibicides perforatus, Cibicides novozelandicus* and *Cibicides temperata.* The occurrence of high *C. perforatus* percentages in combination with *C. novozelandicus* and *Z. stachei* indicates an inner shelf setting (Hornibrook *et al.,* 1989). This change in foraminiferal assemblages and lack of concentrated beds of fossiliferous material in these sections indicates a slight change in environment compared to the

Fossiliferous Sandstone facies. It is possible that phases of very slight deepening or small changes in energy have occurred. Shallowing or increases in energy may be associated with deposition of fossiliferous beds, winnowing of muds with a number of increases in energy as well as slight changes in depth occurring throughout this unit.

Summary: Inner shelf, sheltered subtidal.

7.2 Palaeogeography

The environments and units discussed in 7.1 are considered in this section in terms of stratigraphy and palaeogeography. These units were separated into suitable time frames in order to outline important processes that occurred throughout the Tertiary. This section breaks the formation of the Mandamus-Pahau Tertiary units into four time ranges from the Late Eocene to the mid Miocene. These are: late Runangan, late Whaingaroan-Duntroonian, Waitakain, Otaian.

7.2.1 Late Runangan 36.0-34.3Ma

At this time deposition of the Massive Glauconite-rich Sandstone Facies from the Coal Creek Formation was being deposited in the Mandamus-Pahau District. The Coal Creek Formation covers a long time span, but the only age determined from biostratigraphic data (in chapter 4) is restricted to the Runangan stage. Deposition in the Runangan is indicative of a rising sea level. Deepening is observed by the transition from shallow inner shelf (pre-Runangan) to mid-outer shelf facies. An increase in sedimentation or remobilisation of sediment is noted in this Massive Glauconite-rich Sandstone Facies with higher quartz content towards the upper Coal Creek Formation.

Contemporaneous to deposition of the Coal Creek sediments in a mid-outer shelf setting in were the micrites and deep water facies of the Amuri Limestone to the east (figure 7.1). The absence of Amuri Limestone in the Mandamus-Pahau District indicates a shallower environment than that of the Amuri Limestone. Sedimentation that was influencing the deposition of the Amuri Limestone changed slightly over this stage, with the production of a pelagic limestone, due to possible changes in circulation and reduced terrigenous influx (Fulthorpe *et al.,* 1996). The age of the Amuri Limestone appears to reflect continuing

marine transgression through the Late Eocene with the unit becoming younger from north to south in the North Canterbury Region (Field and Browne, 1989). Depositional environments of the Amuri Limestone also change from north to south with the unit shallowing towards the south.

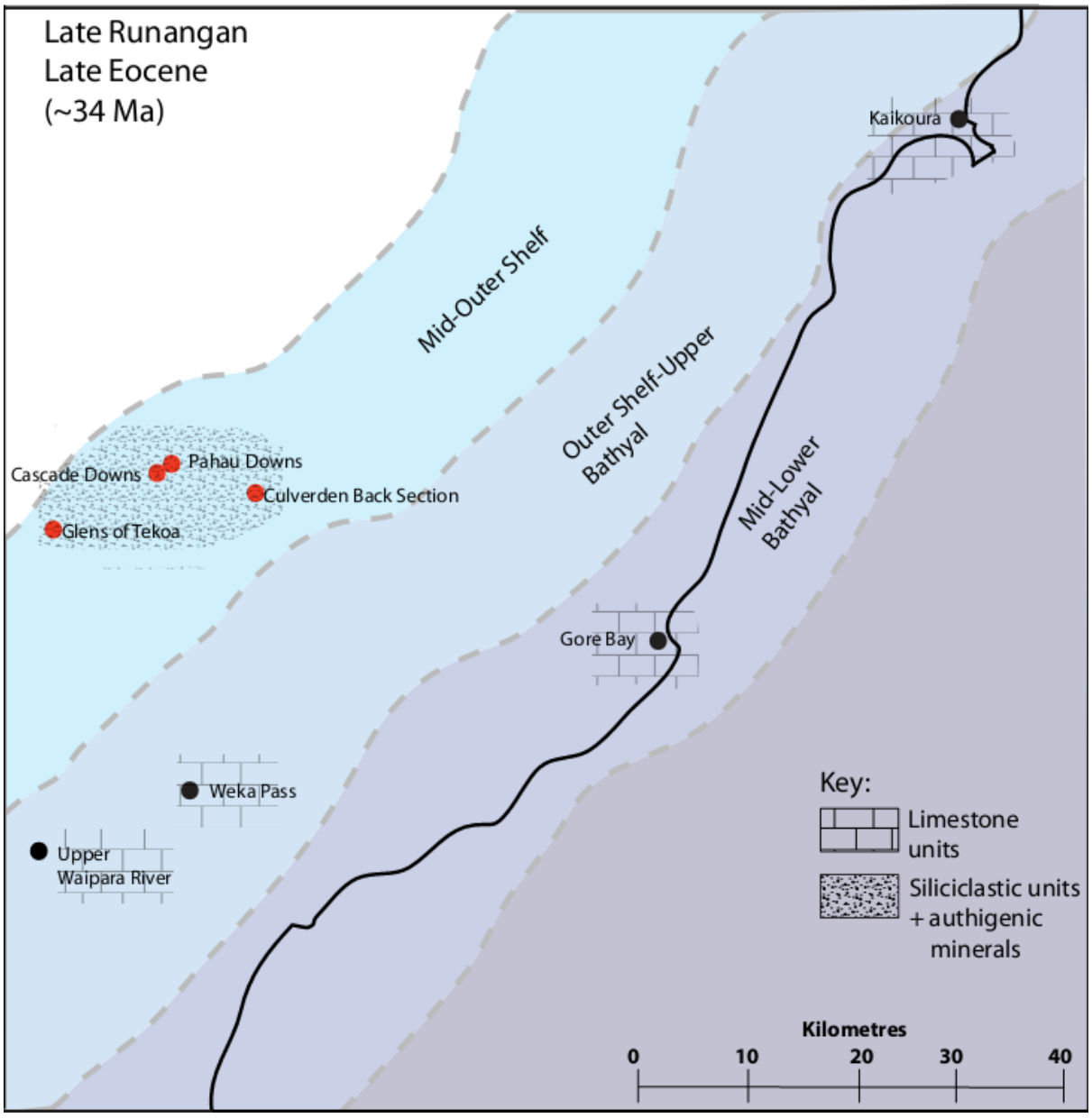

Figure 7.1- Suggested palaeogeography during the Late Runangan.

This stage appears to record continuing marine transgression and accumulation of carbonate rocks (Rattenbury *et al.,* 2006). Water depths at this time are inferred from sedimentological and biostratigraphic data.

7.2.2 Late Whaingaroan- Duntroonian ~27-25.2Ma

The Late Whaingaroan to Duntroonian was important in terms of depositional regime. The deposition of the Cookson Volcanics Group at this time represents regionally isolated deposition (figure 7.2). During this stage the majority of sites to the east of the Mandamus-Pahau District were experiencing non-deposition common during the Marshall Paraconformity. This hiatus occurred as a result of paleocirculation changes associated with the development of the ACC. An influx of cold water currents meant a lack of deposition on the New Zealand continental plateau.

The occurrence of pillow basalt and volcaniclastic tuff in the Mandamus-Pahau District throughout the Duntroonian indicates deposition possibly resumed in the more western sites before carbonate sedimentation began in the east in the Late Oligocene- Early Miocene. This period of non-deposition is not as well identified in the most western sites of this district, but it is inferred due to a break in sedimentation from the Late Eocene until the Mid-Late Oligocene. At Glens of Tekoa, Cascade Downs and the Culverden back section final deposition of the Coal Creek formation is inferred to occur in the Runangan. This is followed by a period of non-deposition until the Cookson Volcanic Group was deposited. This indicates a possible hiatus (non-depositional and erosional) of ~7 Ma.

There were stages of deposition to the east and south with sandstone units (Weka Pass) and bathyal pelagic and hemipelagic assemblages (Spy Glass Formation) accumulating. At this point in time the Weka Pass Sandstone was being deposited to the south at Weka Pass and in the Waipara River section. The Spy Glass Formation, which consists of mostly planktic foraminifera was accumulating at lower bathyal depths at Kaikoura and slightly shallower outer shelf to bathyal depths at Gore Bay, north of Motunau. The highly planktic foraminiferal component of this unit means it accumulated in a very deep water setting.
Volcanic activity inferred by the deposition of these facies is likely to have occurred due to the creation of underwater cones producing pulses of tuffaceous material and pillow basalts. These deposits are products of localised intraplate volcanism, with the source of this volcanism possibly located to the north east of the district. Water depths at this time can only be inferred from the overlying Late Oligocene- Early Miocene Flaxdown Limestone

Member. A similar depth for this unit is observed throughout the district with possible shallowing at the most eastern site (Glens of Tekoa). Therefore due to high coralline algae percentages the suggested paleodepth is mid shelf.

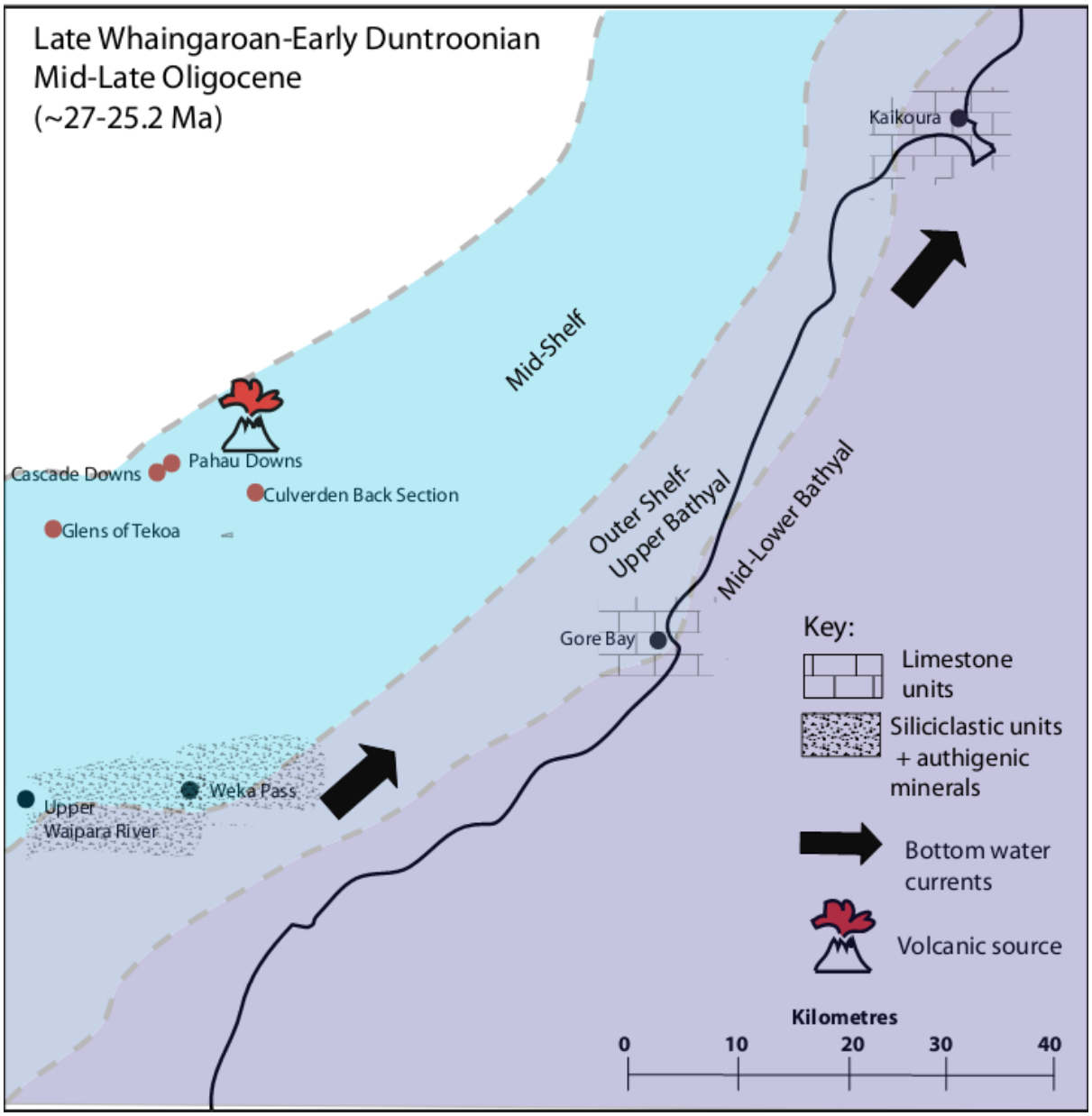

Figure 7.2- Suggested palaeogeography during the Late Whaingaroan- Early Duntroonian.

7.2.3 Early Waitakian ~25.2Ma

This stage marks the occurrence of widespread limestone deposition. At this time the Flaxdown Limestone Member from the Mandamu-Pahau District was being deposited. The occurrence of carbonate-rich sediments provides evidence of the return to normal sedimentation regime post-Marshall Paraconformity. The widespread development of shelf

carbonates illustrates the presence of a large shallow shelf. At this time it appears basins from the North Canterbury region were extending south leading to this broad carbonate shelf (Rattenbury *et al.,* 2006). Deposition of units from the late Oligocene sediments on a relatively sheltered shelf led to the production of clastic sands and a broad cover of carbonaceous units (Rattenbury *et al.,* 2006). To the south of the Mandamus-Pahau District the Weka Pass Stone was being deposited, with the Spy Glass Formation being deposited in an outer shelf to bathyal setting in Kaikoura and North Canterbury (Field and Browne, 1989). These units formed a blanket of carbonate deposition in the late Oligocene, either occurring interbedded with the Cookson Volcanics or unconformably on the Amuri Limestone (Rattenbury *et al.,* 2006).

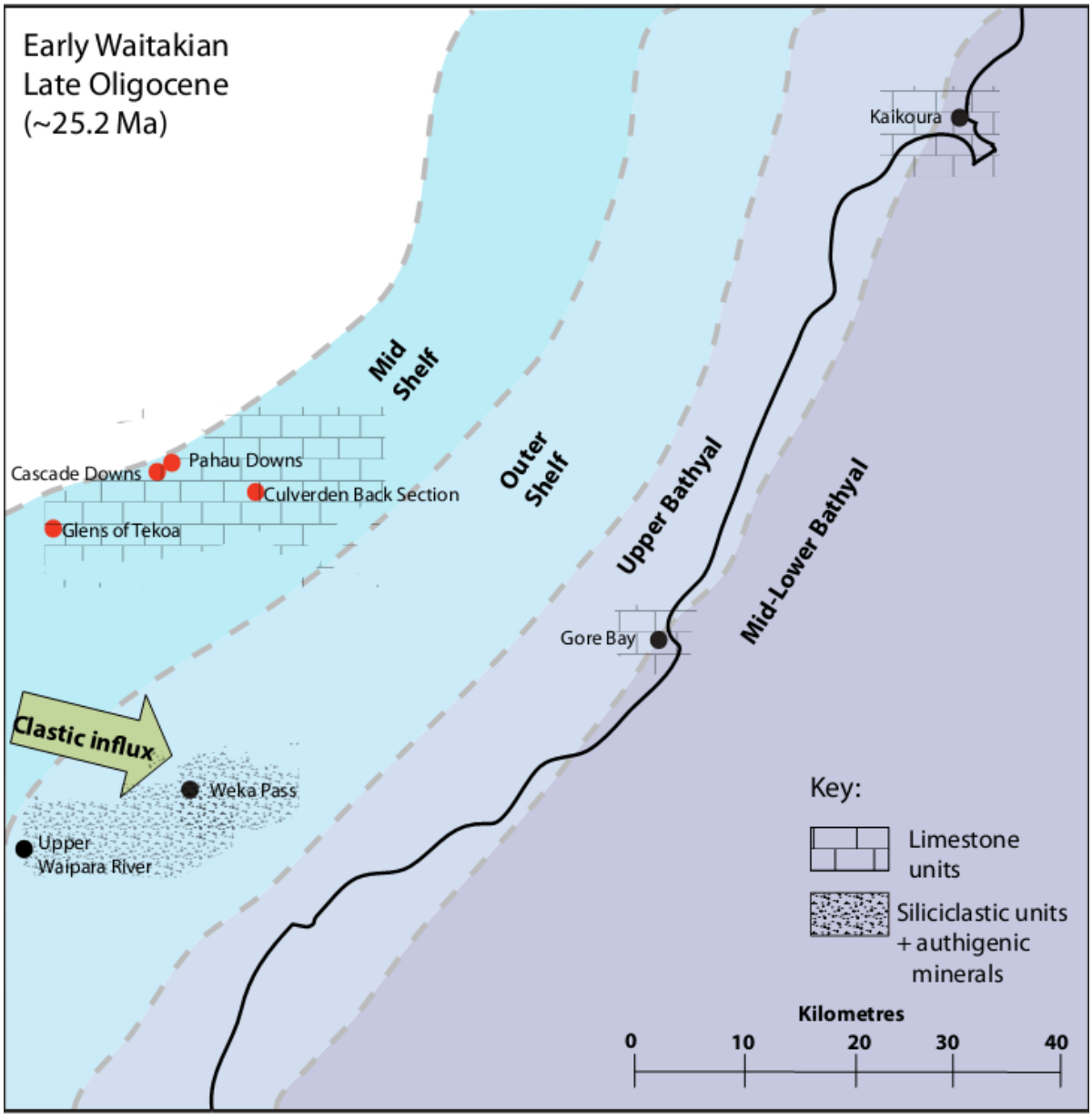

Figure 7.3- Suggested palaeogeography during the Early Waitakian.

The Flaxdown limestone does not appear to record changes in sea level or a change in tectonic regime, with units remaining relatively consistant grainstone facies. Facies changes are relative to fossil types that only suggest minor changes in sea level if any. The Flaxdown Limestone from the Mandamus-Pahau District records a similar depth throughout the Waitakian- Otaian: mid shelf, with deepening to the south and east.

7.2.4 Late Waitakian- Otaian ~ 21.7-19.0Ma

This stage is represented by the production of highly clastic sediments. This is seen in the deposition of the quartz-rich Pahau Siltstone Member.

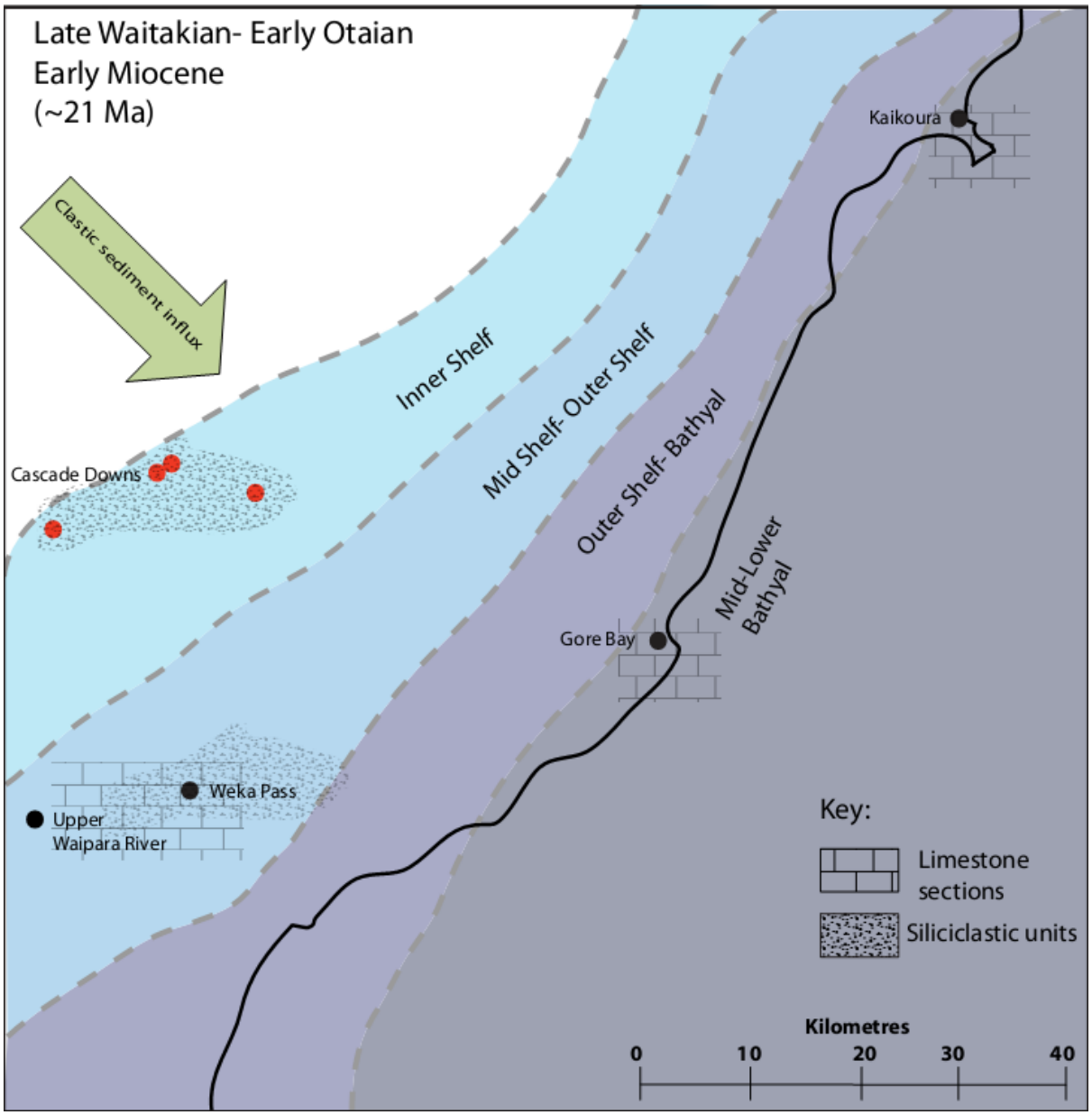

Figure 7.4- Suggested palaegeography during the Late Waitakian- Early Otaian.

The high siliciclastic content of this unit reflects a rapidly eroding source to the west. An increase in siliciclastic material is linked to the uplift in response to the inception of convergent tectonics developing along the Pacific-Australian plate boundary (Rattenbury *et al.,* 2006). Uplift and erosion associated with the Alpine Fault development increased the sediment input into the shallow shelf around the Canterbury region (Rattenbury *et al.,* 2006). This influx of siliclastic material is not seen to the same extent in more eastern regions in North Canterbury such as Kaikoura and Gore Bay. Irvine (2012) noted that, although siliciclastic input was influencing some North Canterbury sites in the Early Waitakian it was not until the Otaian-Altonian boundary that the influence of clastic sedimentation was seen across all North Canterbury sites.

At this time sedimentation in the Mandamus-Pahau Distirict is defined by siltstones and sandstones. Limestone units were not being deposited in the Mandamus-Pahau District at this time due to the large influxes of terrigenous material (figure 7.4). Continuing deposition of the Spy Glass Formation was occurring to the north-east in an outer shelf-bathyal setting (Field and Brown, 1989). This limestone deposition indicates limited siliciclastic input into these regions. The sites to the west were more affected by increased tectonic activity with shallowing due to uplift and an increase in terrigenous material. It is likely the sites to the east had not yet been affected by tectonic activity to the same extent of the western sites with siliciclastic input highest to the west, in shallow shelf regions (Irvine, 2012).

7.3 The Mandamus-Pahau District rocks versus the Global Isotope Curve

Analysis of stable isotopic data from both bulk rock and foraminiferal samples from the Mandamus-Pahau District (chapter 6) in combination with petrography, were used to determine diagenetic alteration of sediments from a Tertiary shelf setting. Comparison of stable isotope data to the global marine isotope curve in chapter 6 highlighted a number of problems and possible trends. In consideration to palaeogeography in section 7.2, sea level change over the Late Eocene to Mid-Miocene is minimal, whereas tectonic uplift and erosion were prominent.

In respect to the global marine isotope record the Coal Creek Formation samples collected from Glens of Tekoa, Cascade Downs and Culverden back section do not provide adequate data to draw any conclusions. Due to a lack of foraminifera within this unit the age of the majority of samples are only estimated and therefore this data could not be accurately applied alongside the Zachos (2001) deep-marine curve. Only one Coal Creek Formation sample provided foraminifera meaning this data cannot be used to analyse global marine trends. Whole bulk rock stable isotope samples were run as well as foraminiferal samples. The whole bulk rock samples collected from the Coal Creek Formation as well as lacking an age constraint are altered by diagenesis to the extent that they record highly depleted values. The effect of burial diagenesis on these samples means they do not record the original sea water composition, instead they reflect the burial diagenetic environment. Due to the limited data from the Eocene/Oligocene boundary trends can be implied, but it can be assumed that diagenesis would have obscured any isotopic record of this climate excursion. The only age determined from biostratigraphic data for the Coal Creek Formation is the Runangan. Post the Coal Creek Formation deposition does not resume until the Duntroonian (Late mid to Late Oligocene). This period of non-deposition due to the Marshall Paraconformity means the next carbon and oxygen values are from the Late Oligocene.

The Flaxdown Limestone and Pahau Siltstone Members provide a more promising correlation to the global marine isotope curve. An enrichment in both $\delta^{18}O$ and $\delta^{13}C$ at the Oligocene/Miocene boundary appears to record the Antarctic glaciations, yet this enrichment is not reflected in the sedimentological record. This boundary is marked by increased sediment input from a source to the west of the field area, indicating increased tectonic activity and erosion. An increase in silicilastic input onto the shallow shelf is represented by the quartz-rich inner shelf Pahau Siltstone. This slight shallowing in the west correlates with a low sea-level stand, due to the uptake of $\delta^{16}O$ by ice sheets, yet palaeogeography in 7.2 does not depict any large change in sea-level to the east, towards Gore Bay and Kaikoura. Therefore the shallowing present to the west at Cascade Downs is representative of increased erosion and tectonic uplift, due to a change in tectonic regimes along the Alpine Fault.

This stable isotope record from the Oligocene/Miocene does not correlate to the Zachos deep sea curve due to diagenetic alteration during burial. Unlike the Coal Creek Formation the Flaxdown Limestone contains visible characteristics of burial diagenesis. In the field pressure dissolution features indicative of burial to at least 200 metres were abundant, with 1.5cm to 2cm stylolite bands visible at the Glens of Tekoa site. In thin section minor features of compaction were apparent with plastic deformation breaking and compacting bioclasts within the limestone. Burial cements are also well recorded in the Flaxdown Limestone with the majority of samples consisting of blocky calc-sparite matrices. The Pahau Siltstone samples were also consistant with burial diagenesis, with blocky calcsparite cement filling pore spaces within bioclasts.

The final global cooling excursion considered in this thesis is the Mid Miocene cooling, linked to the development of the East Antarctic ice sheet. As with the Coal Creek Formation a lack of samples from this time period means only assumptions can be made about the isotopic record. In consideration to the age of the Pahau Siltstone with samples collected the youngest biostratigraphic age determined from samples was early Mid Miocene (only one Mid Miocene sample). Therefore a trend can only be inferred from the youngest Early Miocene sample to the one Mid Miocene sample. Enrichment in $\delta^{18}O$ is seen from the Early Miocene to Mid-Miocene. As with the Oligocene/Miocene boundary this record is obscured by sediment influx and uplift from the west, providing a false record of shallowing due to sea-level change. The isotopic values recorded by this Mid Miocene sample suggest alteration during burial diagenesis as is evident in the other units.

In this thesis a look at local shelf carbonate isotope records versus the global deep sea carbonate isotope record, shows that in the case of the Mandamus-Pahau rocks, burial diagenesis has altered the original sea-water isotopic signature. This limits the use of these shelf sediments in association with global climate excursions. The main reasons why shelf rocks are inadequate to record global climate excursions are grainsize and in this case a temperate to cool-water environment with dominant burial diagenesis. Grainsize is the major factor influencing diagenesis of shelf sediments as shelf sediments seen in this study mostly consist of grainstones with thin packstone layers throughout and Pahau sandstones.

The coarse grainsize of these units allows a higher flow of pore fluids through sediments than in deep-ocean units. Generally deep ocean units are micritic, finer grained sediments, with smaller pore spaces, therefore limiting pore fluid flow. Cool-water, temperate or warm-water environments are influenced by different carbonate processes and therefore are affected by differing levels/forms of diagenesis. The Coal Creek Formation was most likely deposited in a temperate carbonate environment in the Eocene, with a lack of carbonate material possibly linked to low productivity rates amongst calcareous organisms at the sea floor. The rest of the rocks from the Mandamus-Pahau District were deposited in a temperate to cool-water carbonate environment dominated by cement precipitation in a burial diagenetic environment, instead of precipitation at the sea floor, commonly seen in warm-water carbonate systems. These cements thus record burial pore-fluid characters, not sea-floor chemistry.

This thesis provides strong evidence for problematic global isotopic signatures in local shelf sediments due to grainsize and diagenesis, yet other studies have proved it is possible to reconstruct the global isotope curve from shelf sediment records (Pufahl, 2006). Shelf sediments containing fossil proxies less prone to diagenetic alteration such as brachiopods can be a reliable gauge of local and global environmental change. In these cases, although even with diagenetic overprinting occurring from diagenesis, global records can still be discerned.

8. Conclusion

The objective of this thesis was to analyse the preservation potential of shelf sediments from the North Canterbury region, in consideration to the Oligocene and Miocene climate driven excursions. The constraint of age and palaeoenvironments from the Tertiary rocks from the Mandamus-Pahau District allowed for the comparison of local shelf isotopic data to the global deep-sea marine curve created by Zachos (2001). From this thesis five main conclusions can be made:

1. The Marshall Paraconformity can be observed in the mid shelf, with this hiatus representing a ~3-4 Ma period of non-deposition in the Mandamus-Pahau District.

2. The initiation of a compressional regime along the Alpine Fault results in a transition from carbonate to siliciclastic sedimentation. This change in tectonics is recorded by an increased influx of siliciclastic material in the west. This increased sedimentation is not recorded in the deeper environments in the east until later.

3. The preservation potential of stable isotope records in these shelf rocks is limited due to grainsize, with the majority of the Flaxdown Limestone samples consisting of grainstones, allowing high pore fluid flow compared to fine grained deep-ocean sediments.

4. The low abundance of non-carbonate clasts within the Coal Creek Formation provided insufficient carbonate for pore-fluids to precipitate in cements. Whereas the high bioclastic content of the Flaxdown Limestone and Pahau Siltstone, allowed for dissolution of shells at the sea-floor and precipitation of cements during burial diagenesis.

5. These shallow shelf rocks do not appear to have recorded the isotopic sea-water composition at the time of deposition, instead the isotopic signatures recorded by

these rocks is suggestive of alteration during burial diagenesis. It can therefore be stated that the preservation potential of these shelf rocks does not allow for accurate correlations with the Zachos (2001) global deep-sea curve.

References:

Amorosi, A., 1997, Detecting compositional, spatial, and temporal attributes of glaucony: a tool for provenance research: Sedimentary geology v. 109(1): 135-153.

Andrews, P., 1963, Stratigraphic nomenclature of the Omihi and Waikari Formations, North Canterbury: New Zealand Journal of Geology and Geophysics v. 6:2, p. 228-256.

Andrews, P. B., 1968, Patterns of sedimentation during Early Otaian (Early Miocene) time in North Canterbury, New Zealand. New Zealand Journal of Geology and Geophysics v. 11(3), p. 711-752.

Boggs, S., 2006, Principles of Sedimentology and Stratigraphy. Pearson Education. Inc., Upper Saddle River, New Jersey.

Beu, A. G., and Maxwell, P.A., 1990, Cenozoic Mollusca of New Zealand: New Zealand Geological Survey Paleontological Bulletin, 58.

Carter, L., 2008, Water World. In Graham, I.J (Ed)., A Continent on the Move: New Zealand in the 21st Century. Hong Kong, Bookbuilders, p. 207-220.

Carter, R.M., and Norris, R.J., 1976, Cainozoic history of southern New Zealand: An accord between geological observations and plate-tectonic predictions: Earth and Planetary Science Letters, v. 31, p. 85-94.

Carter, R.M., 1985, The Mid-Oligocene Marshall Paraconformity, New Zealand: Coincidence with Global Eustatic Sea-Level Fall or Rise?: The Journal of Geology, v. 93, p. 359-371.

Carter, R. M., 2008, Climate Swings and Roundabouts. In Graham, I.J (Ed)., A Continent on the Move: New Zealand in the 21st Century. Hong Kong, Bookbuilders, p. 249-276.

Choquette, P.W., and James N.P., 1990. Limestone-The Burial Diagenetic Environment, In Morrow, D. W. and I. A. McIlreath (Eds), Diagenesis: Newfoundland, Geoscience Canada Reprint Series 4.

Cooper, A. F., 2008, Astride a Plate Boundary. In Graham, I.J (Ed)., A Continent on the Move: New Zealand in the 21st Century. Hong Kong, Bookbuilders, p. 47-72

Dickson, J. A. D., 1966, Carbonate identification and genesis as revealed by staining Journal of Sedimentary Research v. 36: 2, p. 491-505

Ennyu, A and Arthur, M.A., 2004, Early to Middle Miocene Paleoceanography in the Southern High Latitudes off Tasmania. In Exon, N.F., Kennett, J.P., Malone, M.J (Eds). The Cenozoic Southern Ocean Tectonics, Sedimentation and Climate change Between Australia and Antarctica, AGU, United States of America, p. 215-234

Field, B.D., Browne, G.H., and others., 1989, Cretaceous and cenozoic sedimentary basins and geological evolution of the Canterbury Region, South Island, New Zealand, Volume 2, New Zealand Geological Survey Basin Studies.

Flower, B.P., and Kennett, J.P., 1994, The middle Miocene climatic transition: East Antarctic ice sheet development, deep ocean circulation and global carbon cycling: Palaeogeography, Palaeoclimatology, Palaeoecology, v. 108, p. 537-555.

Flugel, E., 2004, Microfacies of carbonate rocks; analysis, interpretation and application: Federal Republic of Germany (DEU), Springer, Berlin, Federal Republic of Germany (DEU).

Fulthorpe, C.S., Carter, R.M., Miller, K.G., and Wilson, J., 1996, Marshall Paraconformity: a mid-Oligocene record of inception of the Antarctic circumpolar current and coeval glacio-eustatic lowstand?: Marine and Petroleum Geology, v. 13, p. 61-77.

Haq, B.U., Hardenbol, J., and Vail, P.R., 1987, Chronology of Fluctuating Sea Levels since the Triassic: Science, v. 235, p. 1156-1167.

Haast, J.von., 1871, On the Geology of the Amuri District, in the Provinces of Nelson and Marlborough: Report on Geological Exploration during 1870-1, p. 25-46.

Hayward, B. W., C. J. Hollis., Grenfell, H.R., 1997, Recent Elphidiidae (Foraminiferida) of the south-west Pacific and fossil Elphidiidae of New Zealand: Institute of Geological & Nuclear Sciences, Monograph 16, Lower Hutt, New Zealand.

Hayward, B. W.; Grenfell, H. R.; Reid, C. M.; Hayward, K. A., 1999, Recent New Zealand shallow-water benthic foraminifera: taxonomy, ecologic distribution, biogeography, and use in paleoenvironmental assessment: Institute of Geological & Nuclear Sciences Monograph 21, Lower Hutt, New Zealand.

Hayward, B.W., 2004, Foraminifera-based estimates of paleobathymetry using Modern Analogue Technique, and the subsidence history of the early Miocene Waitemata Basin: New Zealand Journal of Geology and Geophysics, v. 47, p. 749-767.

Hayward, B.W., Grenfell, H.R., Sabaa, A.T., Neil, H.L., and Buzas, M.A., 2010, Recent New Zealand deep-water benthic foraminifera: Taxonomy, ecologic distribution, biogeography, and use in paleoenvironmental assessment: Institute of Geological & Nuclear Sciences Monograph 26, Lower Hutt, New Zealand.

Hollis, C.J., Beu, A.G., Crampton, J.S., Crundwell, M.P., Morgans, H.E.G., Jones, J.I., and Boyes, A.F., 2010, Calibration of the New Zealand Cretaceous-Cenzoic Timescale to GTS2004, GNS Science Report, Volume 2010, p. 20.

Hornibrook, N.d.B., 1961, Tertiary foraminifera from Oamaru District, N.Z. : / Pt. 1. Systematics and distribution: Wellington, Dept. of Scientific and Industrial Research, New Zealand Geological Survey.

Hornibrook, N.d.B., Brazier, R.C., and Strong, C.P., 1989, Manual of New Zealand Permian to Pleistocene foraminiferal biostratigraphy, Volume 56: Lower Hutt, N.Z, New Zealand Geological Survey.

Hornibrook, N.d.B., 1996, New Zealand Eocene and Oligocene benthic foraminifera of the family Notorotaliidae: Institute of Geological & Nuclear Sciences Limited, Monograph 12, Lower Hutt, New Zealand.

Horton, T.W., Sjostrom, D.J., Abruzzese, M.J., Poage, M.A., Waldbauer, J.R., Hren, M.T., Wooden, J.L., and Chamberlain, C.P., 2004, Spatial and temporal variation of

Cenozoic surface elevation in the Great Basin and Sierra Nevada: American Journal of Science, v. 304, p. 862-888.

Hudson, J. D., 1977, Stable isotopes and limestone lithification: Journal of the Geological Society v. 133:6, p. 637-660.

Hutton, F.W., 1877, Report on the Geology of the North-east portion of the South Island, from Cook Straits to the Rakaia: Report on Geological Exploration during 1873-4, p. 27-58.

Irvine, J.R.M., 2012, Sedimentology, stratigraphy and palaeogeography of Oligocene to Miocene rocks of North Canterbury-Marlborough, Unpublished MSc thesis, Department of Geological Sciences, University of Canterbury Library database.

Jongens, R., Begg, J.G., Barrell, D.J.A., Forsyth, P.J., and Science, G.N.S., 2008, Geology of the Christchurch Area: Lower Hutt, N.Z, GNS Science.

Kennett, J. P., Houtz, R.E., Andrews, P.B., Edwards, A.R., Gostin, V.A., Hajós, M., Hampton, M., Jenkins, G.D., Margolis, V.S., Ovenshine, T.A and Perch-Nielsen, K., 1975, Cenozoic paleoceanography in the southwest Pacific Ocean, Antarctic glaciation, and the development of the Circum-Antarctic Current:Initial Reports of the Deep Sea Drilling Project 29: p. 1155-1169.

Kennett, J.P., 1977, Cenozoic evolution of Antarctic glaciation, the Circum-Antarctic Ocean, and their impact on global paleoceanography: Journal of Geophysical Research, v. 82.

Kim, S.T., and O'Neil, J.R., 1997, Equilibrium and nonequilibrium oxygen isotope effects in synthetic carbonates: Geochimica et Cosmochimica Acta, v. 61, p. 3461-3475.

King, P.R., 2008, Shifting Ground. In Graham, I.J (Ed)., A Continent on the Move: New Zealand in the 21st Century, Hong Kong, Bookbuilders, p. 123-140.

Kump, L.R., and Arthur, M.A., 1999, Interpreting carbon-isotope excursions; carbonates and organic matter: Chemical Geology, v. 161, p. 181-198.

Lever, H., 2007, Review of unconformities in the late Eocene to early Miocene successions of the South Island, New Zealand: Ages, correlations, and causes. New Zealand Journal of Geology and Geophysics v. 50: 3, p. 245-261.

Lu, H., and Fulthorpe, C.S., 2004, Controls on sequence stratigraphy of a middle Miocene–Holocene, current-swept, passive margin: Offshore Canterbury Basin, New Zealand: Geological Society of America Bulletin, v. 116, p. 1345-1366.

Lu, H., Fulthorpe, C.S., Mann, P., and Kominz, M.A., 2005, Miocene–Recent tectonic and climatic controls on sediment supply and sequence stratigraphy: Canterbury basin, New Zealand: Basin Research, v. 17, p. 311-328.

MacEachern, J.A., Pemberton, S.G., Gingras, M.K and Bann, K.L., 2010 Ichnology and Facies Models. In James, N.P and Dalrymple, R.W, (Eds)., Facies Models 4 : Geological Association of Canada, GEOtext: 6.

Mason, B., 1949, The Geology of Mandamus-Pahau district, North Canterbury: Transactions of the Royal Society of New Zealand, v. 77: 3, p. 403-428.

Moore, C. H., 1989, Carbonate diagenesis and porosity, Elsevier Science, Netherlands.

Morse, J. W. and Mackenzie, F. T., 1990, Geochemistry of sedimentary carbonates, Elsevier Science, Netherlands.

Murray, J.W., 1995, Microfossil indicators of ocean water masses, circulation and climate: Geological Society, London, Special Publications, v. 83, p. 245-264.

Nelson, C.S., and Cooke, P.J., 2001, History of oceanic front development in the New Zealand sector of the Southern Ocean during the Cenozoic - a synthesis: New Zealand Journal of Geology and Geophysics, v. 44, p. 535-553.

Nelson, C.S., and Smith, A.M., 1996, Stable oxygen and carbon isotope compositional fields for skeletal and diagenetic components in New Zealand Cenozoic nontropical carbonate sediments and limestones: A synthesis and review: New Zealand Journal of Geology and Geophysics, v. 39, p. 93-107.

Perrin, C., Bosence, D. W. J., and Rosen, B., 1995, Quantitative approaches to palaeozonation and palaeobathymetry of corals and coralline algae in Cenozoic reefs: Geological Society, London, Special Publications, v. 83: 1, p. 181-229.

Prothero, D.R., and Schwab, F., 1996, Sedimentary geology: an introduction to sedimentary rocks and stratigraphy, W.H. Freeman and Company.

Pufahl, P. K., James, N.P., Kyser, T.K., Lukasik, J.J., Bone, Y., 2006, Brachiopods in epeiric seas as monitors of secular changes in ocean chemistry: A Miocene example from the Murray Basin, South Australia: Journal of Sedimentary Research v. 76:6, p. 926-941.

Rattenbury, M.S., Townsend, D., and Johnston, M.R., 2006, Geology of the Kaikoura area; scale 1:250,000 geological map: Lower Hutt, New Zealand, Institute of Geological and Nuclear Sciences.

Selley, R. C., 2000, Applied Sedimentology(2nd Edition), Academic Press, USA.

Sevon, W., 1969, Stratigraphy and Sedimentology of the Tertiary rocks of the Mandamus-Dove River area, North Canterbury, New Zealand: New Zealand Journal of Geology and Geophysics v. 12:1, p.283-309.

Sharp, Z., 2007, Principles of stable isotope geochemistry: Pearson Education, Upper Saddle River, New Jersey.

Speight, R., 1918, Structural and Glacial Features of the Hurunui Valley: Transaction of the Royal Society of New Zealand, v. 50, p. 93-105.

Smith, A. M., 1995, Palaeoenvironmental interpretation using bryozoans: a review: Geological Society, London, Special Publications v. 83: 1, p. 231-243.

Tucker, M. E. and Bathurst, R.G.C. (Eds), 1990, Carbonate Diagenesis: Blackwell Scientific Publications, Great Britain.

van der Zwaan, G.J., Jorissen, F.J., and de Stigter, H.C., 1990, The depth dependency of planktonic/benthic foraminiferal ratios; constraints and applications: Marine Geology, v. 95, p. 1-16.

Veizer, J., Ala, D., Azmy, K., Bruckschen, P., Buhl, D., Bruhn, F., Carden, G.A.F., Diener,

A., Ebneth, S., Godderis, Y., Jasper, T., Korte, C., Pawellek, F., Podlaha, O.G., and Strauss, H., 1999, 87Sr/86Sr, d13C and d18O evolution of Phanerozoic seawater: Chemical Geology, v. 161, p. 59-88.

Wray, J. L., 1977, Calcareous algae, Elsevier Science, Netherlands, p. 45-77.

Wright, J. D. And Miller, K.J., 1993, Southern Ocean influences on late Eocene to Miocene deepwater circulation: Antarctic Research Series v. 60, p. 1-25.

Zachos, J., Pagani, M., Sloan, L., Thomas, E., and Billups, K., 2001, Trends, Rhythms, and Aberrations in Global Climate 65 Ma to Present: Science (Washington), v. 292, p. 686-693.

Zachos, J.C., and Kump, L.R., 2005, Carbon cycle feedbacks and the initiation of Antarctic glaciation in the earliest Oligocene: Global and Planetary Change, v. 47, p. 51-66.

Appendix:

Appendix A

Thin section counts

Coal Creek Formation

3,12
Grainsize: fine to medium sand
Sorting: Moderately sorted
Cement: Mud
Bioclasts (%) :
Forams: 100%
Nummulites
Globorotalia
Percentage estimations:
Quartz grains: 45%
Bioclasts: 5%
Glauconite: 30%
Matrix: 20%
99% planktic forams

5,2 a
Grainsize: Fine- medium sand
Sorting: Moderately sorted
Cement: Sparite
Bioclasts: None visible
Percentage estimations:
Quartz: 44%
Glauconite: 16%
Matrix: 40%

4,10
Grainsize: v. fine sand
Sorting: Moderatley sorted
Cement: 80% spar, 20% mud
Bioclasts: None visible
Percentage estimations:
Quartz: 65%
Glauconite: 5%
Biotite: 2%
Matrix: 28%

4,9 (1)
Grainsize: Coarse sand
Sorting: moderately sorted
Cement fabrics and type: sparite
Percentage estimations:
Quartz: 65%
Glauconite: 5%
Matrix: 30%
Bioclast : none visible

Basalt (Cookson Volcanics Group)

9,20 aka 9,6
Grainsize: Medium-Coarse grained
Textures: parallel textures, granular, porphyritic
Minerals: Plagioclase feldspar, pyroxene, olivine
Percentage estimations: plag: 65%, pyroxene: 15%, olivine: 20%
Extra/intraclasts:

14,11
Grainsize: Fine-medium grained
Textures: porphyritic in pyroxene, pilotaxitic texture, microlites in feldspar

Minerals: Olivine, calcite, pyroxene, plagioclase
Percentage estimations: Pyroxene: 40% Plagioclase: 60%
Extra/intraclasts:

Flaxdown Limestone Member

4,3
Dunham classification: Grainstone
Folk classification: Unsorted biosparite
Grainsize: Coarse spar
Sorting: Moderately- well sorted
Cement fabrics and type: Microcrystalline, sparite
Percentage estimations
Bioclasts: 40%
Matrix: 60%
Bioclasts:
Forams: 5%
Miliolina
Multichambered biserial (largest abundance)
Multichambered trochospiral
Multichambered planispiral
Bryozoans: 10%
Branching
Fenestrate
Mollusc fragments: 15%
Coralline red algae: 55%
Echinoderm fragments: 15%

4,5
Dunham classification: Grainstone
Folk classification: Unsorted biosparite
Grainsize: Coarse spar
Sorting: Moderately sorted
Cement fabrics and type: Granular, Sparite
Percentage estimations:
Bioclasts: 35%
Matrix: 65%
Bioclasts:
Forams: 15%
Nummulites
Multichambered biserial
Multichambered uniserial
Multichambered planispiral
Bryozoans: 65%
Branching
Fenestrate

4,4
Dunham classification: Grainstone
Folk classification: Unsorted biosparite
Grainsize: Coarse spar
Sorting: Moderately sorted
Cement fabrics and type: Equant spar
Percentage estimations:
Bioclasts: 35%
Matrix: 62%
Hematite: 3%
Bioclasts:
Forams: 0%
Multichambered biserial
Bryozoans: 78%
Fenestrate
Branching
Mollusc fragments: 2%
Echinoderm fragments: 5%
Coralline red algae: 15%

4,9 (12)
Dunham classification: Grainstone
Folk classification: Unsorted biosparite
Grainsize: Coarse spar
Sorting: Moderately sorted
Cement fabrics and type: Granular, sparite
Percentage estimations:
Bioclasts: 25%
Matrix: 75%
Bioclasts:
Forams: 3%
Multichambered trochospiral
Nummulites
Bryozoans: 55%
Branching
Fenestrate
Mollusc fragments: 2%
Echinoderm fragments: 2%
Coralline red algae: 38%

Echinoderm fragments: 5%
Mollusc fragments: 2%
Coralline red algae: 13%

9,3
Dunham classification: grainstone
Folk classification: Biosparite
Grainsize: Medium- coarse spar
Sorting: Moderately sorted
Cement fabrics and type: sparite
Extra:
volcanic minerals/clasts.
Glauconite/olivine
Percentage estimations:
Volcaniclastic material: 5%
Bioclasts: 80%
Matrix: 15%
Bioclasts :
Forams: 5%
Multichambered biserial
Multichambered planispiral
Multichambered trochospiral
Bryozoans: 68%
Branching
Fenestrate
Echinoderm fragments: 15%
Mollusc fragments: 2%
Coralline red algae: 10%

10,1 (10)
Very close contact to cookson volcanics, sitting right on top of cookson. (straight flat beds on one another step straight from volcanic to limestone with small volcanic clasts.
Dunham classification: Packstone
Folk classification: Unsorted biosparite *sections of mud possibly tuff (30%)
Grainsize: Medium-coarse spar
Sorting: poorly sorted
Cement fabrics and type: Microcrystalline and granular, sparite
Extra: volcanic minerals (Biotite, orthoclase, olivine, plagioclase), quartz grains.
Percentage estimations:
Extra/intraclasts: 20%
Bioclasts: 20%
Matrix: 60%
Bioclasts:
Forams: 20%

Multichambered trochospiral
Multichambered planispiral
Nummulites
Barnacles: 12%
Brachiopods: 3%
Mollusc fragments: 60%
Echinoderm fragments: 5%

11,4
Dunham classification: Grainstone
Folk classification: Unsorted biosparite
Cement fabrics and type: Sparite
Extra: Lithics and Volcanic minerals (Biotite, olivine) Hematite
Percentage estimations:
Volcaniclastic material: 2%
Hematite: 10%
Bioclasts: 75%
Matrix: 13%
Bioclasts:
Forams: 10%
Multichambered trochospiral
Bryozoans: 67%
Branching
Fenestrate
Echinoderm fragments: 5%
Coralline red algae: 28%

14,12
Dunham classification: Grainstone
Folk classification: Unsorted Biosparite
Cement fabrics and type: Granular sparite
Extra: Volcanic minerals, hematite
Percentage estimations:
Hematite: 2%
Bioclasts: 88%
Sparite: 10%
Bioclasts:
Barnacles: 7%
Bivalve shell fragments: 78%
Forams: 5%
Multichambered biserial
Bryozoans: 10%
Fenestrate
Branching

11,3 mid
Dunham classification: Grainstone
Folk classification: Unsorted biosparite
Grainsize: Coarse spar
Sorting: Moderately sorted
Cement fabrics and type: Unsorted biosparite
Extra: Quartz
Percentage estimations:
Quartz: 2%
Bioclasts: 75%
Matrix: 23%
Bioclast:
Bryozoans: 73%
Fenestrate
Branching
Forams: 3%
Nummulites
Biserial (majority)
Multichambered trochospiral
Echinoderm fragments: 1%
Mollusc fragments: 1%
Coralline red algae: 22%

14,3b
Dunham classification: Packstone
Folk classification: Unsorted biosparite
Grainsize: Coarse
Sorting: Poorly-moderately sorted
Cement fabrics and type: Granular sparite (80% matrix) mud (20% matrix)
Extra: Hematite
Percentage estimations:
Hematite: 15%
Bioclasts: 70%
Matrix: 15%
Bioclast:
Mollusc fragments: 5%
Forams: 20%
Multichambered biserial
Multichambered trochospiral
Nummulites
Bryozoans: 70%
Branching
Fenestrate
Echinoderm spines/plates: 5%

Pahau Siltstone Member

5,5a
Grainsize: v.fine – fine sand
Sorting: Moderately sorted
Cement: Lime Mud
Percentage estimations:
Quartz grains: 86%
Bioclasts: 2%
Glauconite: 2%
Matrix: 10%
Bioclasts:
Forams: 98%
Multichambered planispiral
Multichambered uniserial
Bivalve fragments: 2%

12.2.2.4m
Grainsize: v. fine sandto fine sand
Sorting: Well sorted
Cement fabrics and type: Lime Mud
Percentage estimations:
Quartz grains: 42%
Glauconite: 2%
Bioclasts: 1%
Matrix: 55 %
Bioclast:
Forams: 100%
Multichambered planispiral
Multichambered trochospiral

5,6g
Grainsize: v. fine to fine sand
Sorting: Well sorted
Cement fabrics and type: Lime Mud
Percentage estimations:
Glauconite: 2%
Quartz grains: 47%
Bioclasts: 1%
Matrix: 50%
Bioclast :
Forams: 100%

12,4
Grainsize: v. fine sand to fine sand
Sorting: Moderately sorted
Cement: Lime Mud
Extra/intraclasts: Glauconite
Percentage estimations:
Quartz grains: 78%
Bioclasts: 6%
Glauconite: 4%
Matrix: 12%
Bioclasts:
Mollusc fragments: 55%
Forams: 45%
Multichambered planispiral
Multichambered trochospiral
Multichambered uniserial

Appendix B

All samples used for biostratigraphy with foraminiferal species and their abundance.

Sample 14,2	
Benthics	
Cibicides parki	29
Cibicides maculatus	15
Cibicides vortex	1
Cibicides notocenicus	2
Cibicides molestus	2
Cyclammina incisa	1
Anomalinoides fasciatus	1
Dentalina subcostata	1
Bulimina pupla	2
Bolivinopsis cubensis	1
Hoeglundina elegans	2
Cibicides sp.	1
Bulimina sp.	1
Nodosaria sp.	1
Lenticulina sp.	1
Planktics	
Globigerina linaperta	17
Globorotalia centralis	11
Unknown benthics	11
Total	100

Sample 5,5b	
Benthics	
Cibicides perforatus	16
Notorotalia spinosa	75
Bolivina semitruncata	1
Anomalinoides parvumbilia	5
Lenticulina sp.	1
Unknown benthics	2
Total	100

Sample 11,3b	
Benthics	
Cibicides notocenicus	3
Cibicides perforatus	37
Cibicides vortex	1
Cibicides temperata	23
Elphidium advenum	21
Elphidium charlottense	3
Lenticulina (juvenille)	1
Globocassidulina cuneata	5
Cibicides sp.	3
Unknown benthics	3
Total	100

Sample 11,3t	
Benthics	
Cibicides temperata	62
Cibicides vortex	2
Cibicides notocenicus	4
Cibicides perforatus	17
Elphidium advenum	9
Anomalinoides fasciatus	1
Unknown benthics	5
Total	100

Sample 5,6a	
Cibicides temperata	35
Cibicides perforatus	43
Cibicides molestus	6
Cibicides novozelandicus	1
Anomalinoides parvumbilia	1
Siphotextularia	2
Anomalinoides	4
Unknown benthics	8
Total	100

Sample 5,6f	
Benthics	
Cibicides temperata	12
Cibicides novozelandicus	23
Cibicides vortex	13
Cibicides perforatus	3
Zeaflorilus stachei	15
Cancris lateralis	1
Nonionella novozelandica	3
Bolivina finlayi	7
Cibicides sp.	7
Lenticulina sp.	14
Unknown benthics	3
Total	100

Sample 12,3b	
Benthics	
Cibicides novozelandicus	1
Cibicides perforatus	12
Notorotalia spinosa	39
Zeaflorilus stachei	15
Anomalinoides parvumbilia	3
Gavelinopsis pukeuriensis	5
Elphidium crispum	3
Elphidium advenum	6
Lenticulina cultratus	1
Lagenoglandulina annulata	1
Bolivina finlayi	6
Cibicides sp.	4
Unknown benthics	4
Total	100

Sample 12,1b	
Benthics	
Cibicides perforatus	4
Cibicides novozelandicus	6
Elphidium crispum	32
Zeaflorilus stachei	4
Elphidium sp.	4
Cibicides sp.	17
Unknown benthics	40
Total	100

Sample 12,5	
Benthics	
Cibicides perforatus	9
Cibicides temperata	1
Notorotalia spinosa	11
Zeaflorilus stachei	68
Planulina renzi	2
Gavelinopsis pukeuriensis	1
Bulimina senta	2
Bulimina pupula	2
Glandulina symmertica	4
Total	100

S***ample 12.2.2.4m***	
Benthics	
Cibicides perforatus	77
Cibicides novozelandicus	2
Notorotalia spinosa	5
Zeaflorilus stachei	5
Nonionella novozelandica	3
Discorotalia tenuissima	1
Bolivina finlayi	1
Cibicides sp.	5
Unknown benthics	1
Total	100

Appendix C

Raw geochemistry data ($\delta^{18}O$ and $\delta^{13}C$) in stratigraphic order.

Sample Unit	Sample number	δ13C (‰ V-PDB)	δ18O (‰ V-PDB)	δ18O (‰ V-SMOW)
Coal Creek Formation	13.13	-9.87	-15.19	15.26
	13.13	-10.08	-15.64	14.82
	7.1.pom	-3.95	-15.56	14.90
	7.1.pom	-3.52	-13.64	16.76
	7.1.01	-5.05	-14.68	15.75
	7.1.01	-4.60	-13.93	16.48
	5.2a	-17.14	-12.29	18.07
	5.2.a	-15.65	-12.98	17.40
	4.10.6	-6.02	-5.20	24.95
	4.10.6	-0.06	-1.07	28.96
	4.10.5	-8.28	-8.65	21.61
	4.10.4	-3.67	-3.12	26.96
	4.10.4	-3.91	-5.18	24.96
	4.10.3	-2.70	-7.45	22.76
	5.1B	-9.08	-10.55	19.76
	5.1.b	-9.74	-11.20	19.13
	5.1d	-6.49	-15.44	15.01
	5.1.d	-6.14	-15.38	15.07
	5.1.d	-5.84	-14.01	16.41
	5.1e	-7.55	-14.45	15.97
	5.1.e	-8.68	-14.58	15.85
	5.1.e	-7.59	-14.92	15.52
	14.2.foram	-0.87	-3.44	26.65
Flaxdown Limestone Member	4.9.1	-5.29	-14.34	16.09
	4.9.1	-5.53	-15.21	15.24
	9.2	-1.20	-8.98	21.28
	14.11	-5.51	-8.50	21.75
	14.11	-5.16	-7.80	22.43
	14.3.b	-1.18	-1.93	28.12
	14.3B	-1.02	-1.68	28.37
	9.1	1.82	-4.19	25.93
	9.1	1.59	-4.69	25.45
	9.3	0.78	-0.98	29.04
	9.3	0.28	-1.60	28.44
	11.3.b	-0.27	-0.96	29.06
	11.3b	-0.16	-1.06	28.96
	11.3.B.foram	-0.16	-1.58	28.46
	11.3.M	-0.14	-1.44	28.60
	11.3M	0.25	-0.87	29.15
	11.3.T	-0.16	-1.75	28.30
	11.3T	0.44	-0.92	29.10
	11.3.T.foram	0.50	-1.63	28.41

Pahau Siltstone Member	5.5b	0.79	-0.57	29.44
	5.5.b	0.87	-0.86	29.16
	5.5.b foram	0.46	-0.18	29.82
	12.1.b foram	-0.02	-1.92	28.13
	12.2	0.96	-0.70	29.31
	12.2	1.26	-0.02	29.98
	12.2.2.4m.foram	-3.00	-3.86	26.25
	5.6g	0.24	-0.34	29.66
	5.6.g	0.63	-0.43	29.57
	5.6.f.foram	-0.17	-0.43	29.58
	12.3a	-1.20	-7.71	22.51
	12.3.a	-1.15	-7.68	22.54
	12.3.b.foram	0.96	0.59	30.56
	5.6.d	0.26	-1.06	28.96
	12.5	-1.11	-6.11	24.07
	12.5	-1.48	-6.85	23.35
	12.5.foram	-0.03	-2.17	27.89
	5.6.a	0.17	-2.12	27.93
	5.6.a.foram	0.98	-1.42	28.61

Appendix D

Geological Maps of field sites (see figure 3.18 for key).

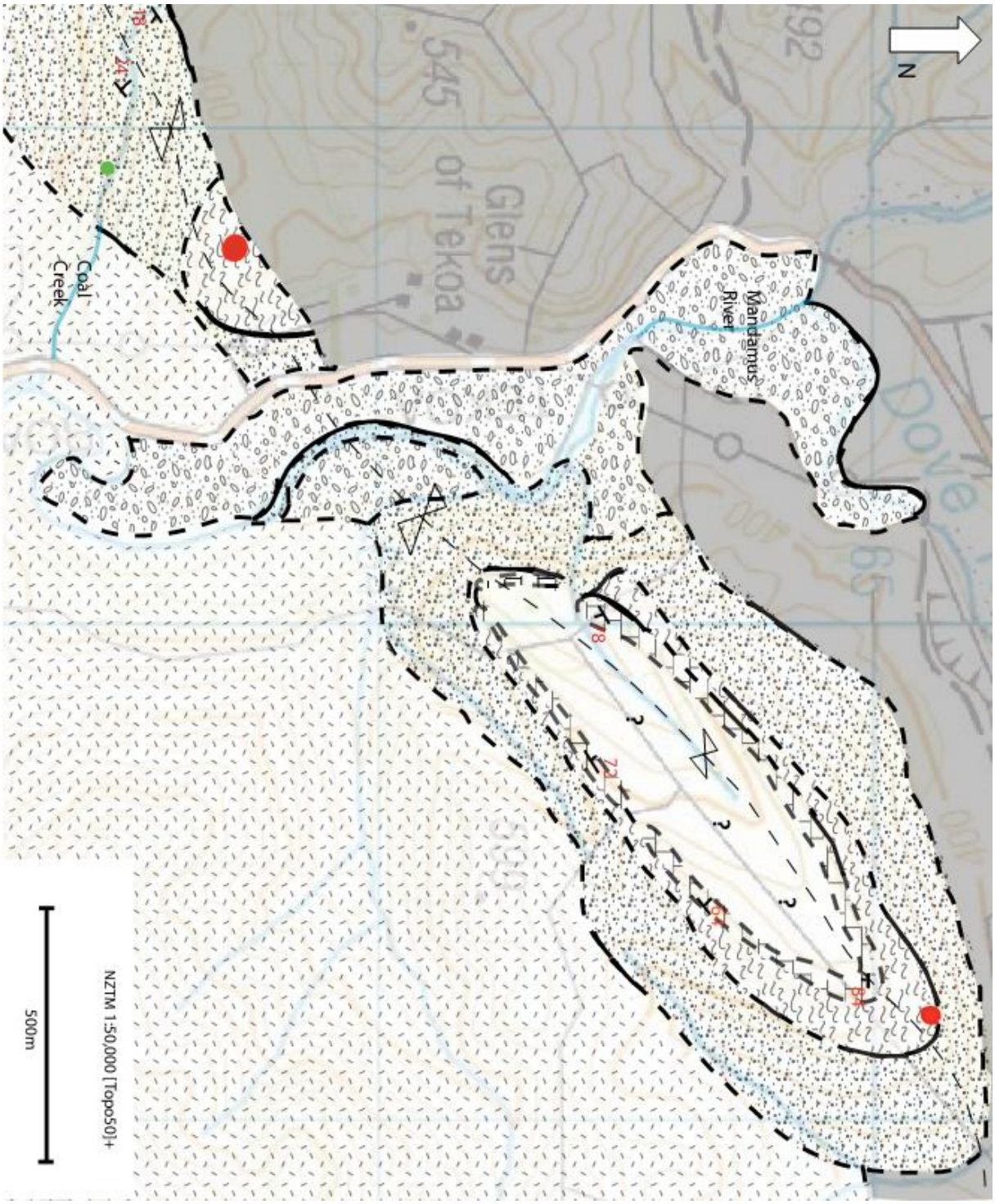

Geological map of the Glens of Tekoa field area (Mandamus-Dove River area) North Canterbury, New Zealand. Map compiled from field work and Google Earth, 2012.

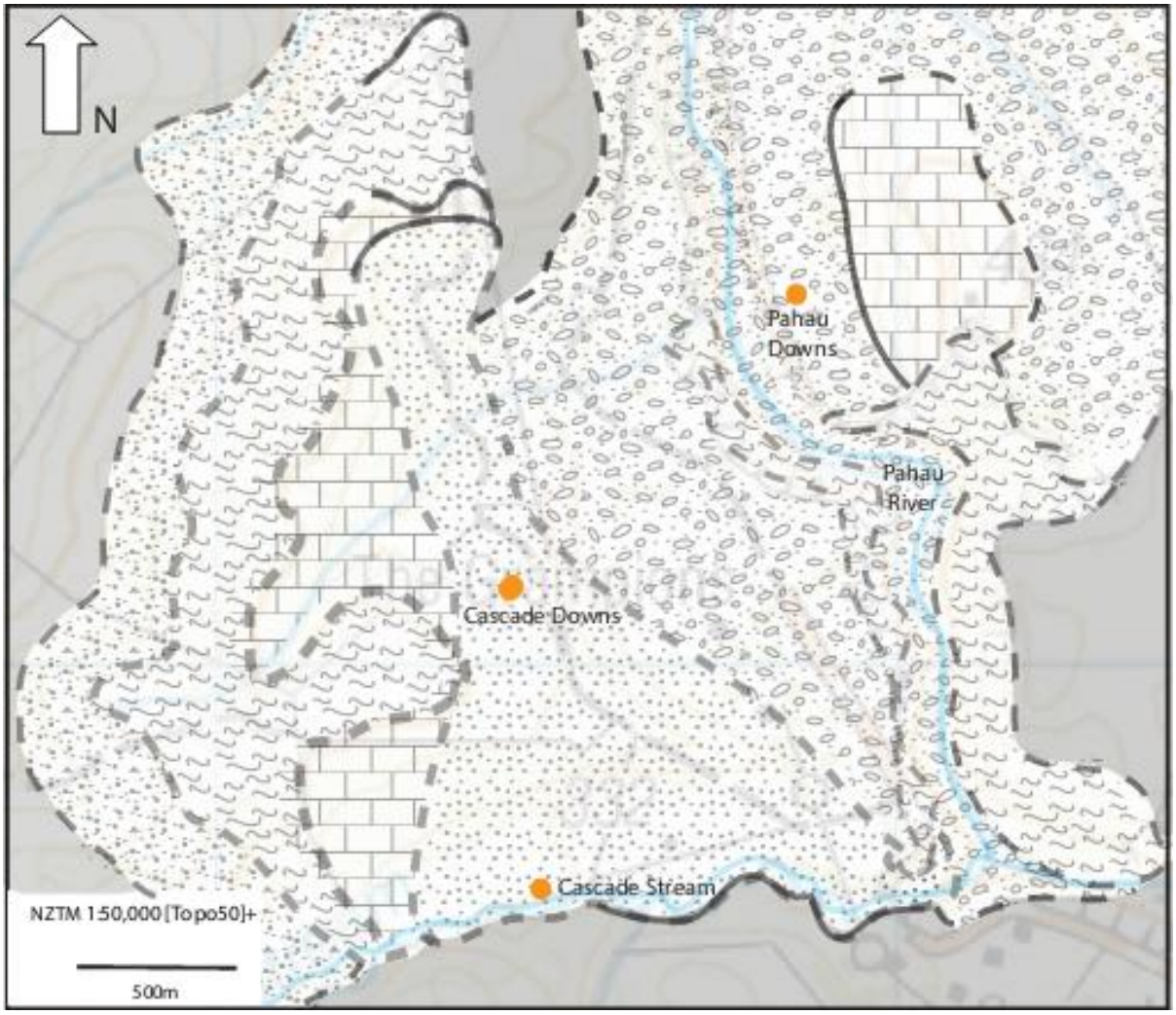

Geological map of Cascade Downs and Pahau Downs field areas, North Canterbury, New Zealand. Map compiled from field work and Google Earth, 2012. (See figure 3.18 for key).

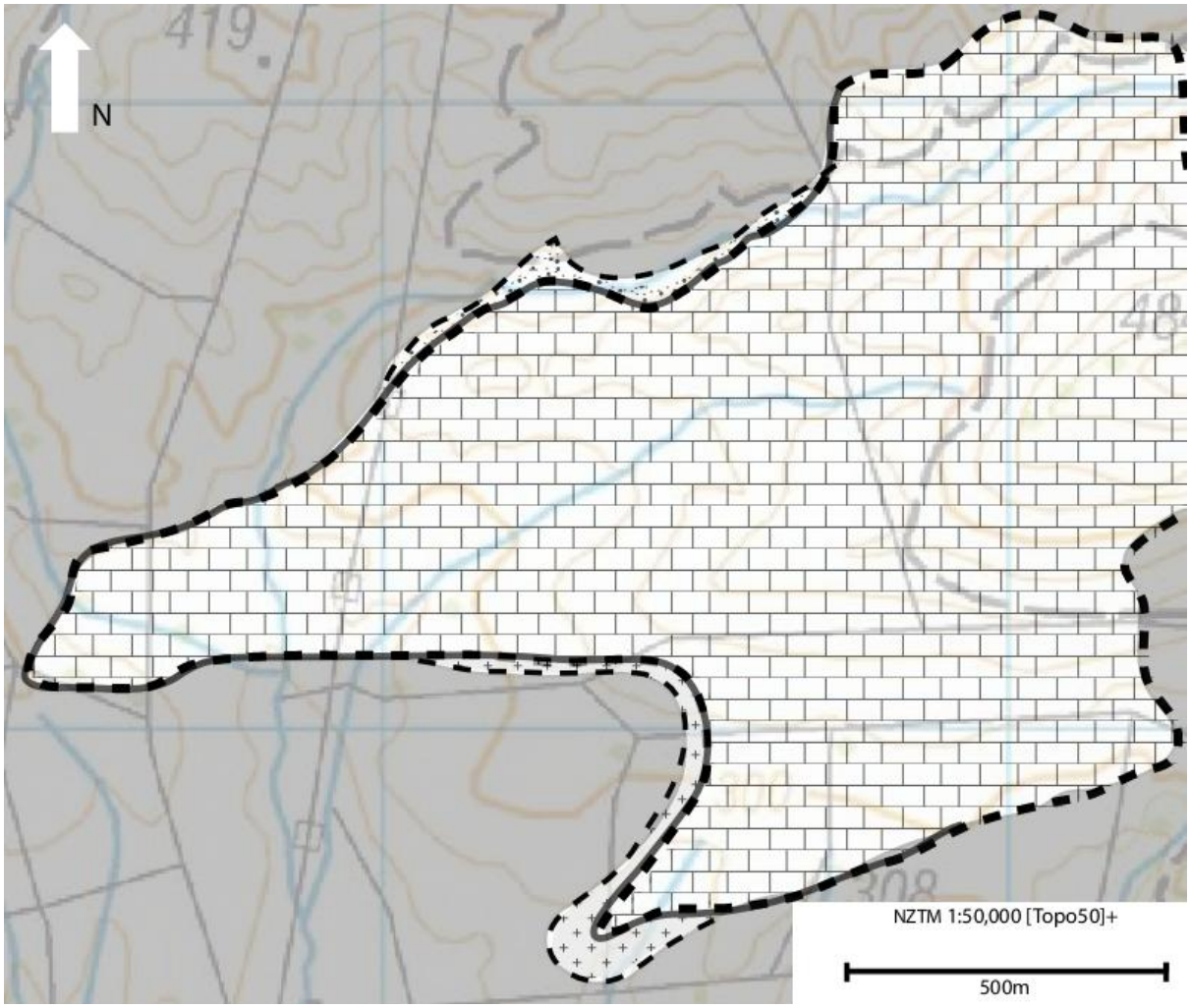

Geological map of Cascade Downs and Pahau Downs field areas, North Canterbury, New Zealand. Map compiled from field work and Google Earth, 2012.

Appendix E

UoC Rock Catalogue numbers for this thesis.

Field and thesis sample numbers	UoC Catalogue numbers
3,12	19686
4,3 middle	19687
4,3 top	19688
4,4 5.4 m	19689
4,5 top 3.8	19690
4,9 1	19691
4,9 12	19692
4,10 3	19693
4,10 1	19694
4,10 5	19695
5,1 a	19696
5,1 b	19697
5,1 d	19698
5,1 e	19699
5,2 a	19700
5,2 b	19701
5,5a	19702
5,5 b	19703
5,6 d	19704
5,6 f	19705
5,6 g	19706
7,1 j	19707
7,1 M1	19708
7,1 M2	19709
7,1 P 0M	19710
7,1 4M	19711
7,1 O1	19712
7,1 O2	19713
9,1	19714
9,3	19715
9,6 (9,20)	19716
10,1 2.5m	19717
10,1 3.5m	19718
11,3m	19719
11,3 a	19720
11,3 bottom	19721
11,3 top	19722
11,4	19723
12,1 b	19724
12,2 2.4m	19725
12,3 a	19726
12,3 b	19727
12,4	19728
12,5	19729
13,12	19730
13,13	19731
13,15	19732
13,16	19733
13,18	19734
14,1	19735
14,2	19736
14,3 bottom a	19737
14,11	19738
14,12 top b	19739
5,6a	19740